EXPLORING DNA-MEDIATED CHARGE TRANSPORT WITH FAST RADICAL TRAPS

Thesis by

Joseph C. Genereux

In Partial Fulfillment of the Requirements

for the Degree of

Doctor of Philosophy in Chemistry

California Institute of Technology

Pasadena, California

2010

(Defended November 16, 2009)

ACKNOWLEDGEMENTS

When I arrived at Caltech, I had little understanding of the research endeavor, and thought of DNA more as a code than as a molecule. In Professor Jackie Barton's group I have learned how to think like a chemist, how to identify significant questions, and just as importantly how to design the experiments and controls that can answer those questions. Jackie has taught me how to create and how to communicate science.

My thesis committee members, Professor Ahmed Zewail, Harry Gray, and Rudy Marcus, have provided insightful suggestions and I appreciate the time that they have taken to help me in my academic development. Mo Renta is a fearsome advocate for us and shields us from much of the drudgery of academic paperwork and regulations. Many teachers and professors played important roles in instilling me with a love of science and chemistry, particularly Tom Roper, Professor Ahamindra Jain, Professor Paul Rablen, and my undergraduate advisor Professor Bob Pasternack.

Dr. Kate Augustyn and Dr. Amie Boal generously invited me to collaborate with them, and I am extremely grateful for these productive opportunities. Amie, in particular, provided me with materials, training and insight related to several different projects, and will one day be a terrific advisor to graduate students of her own! Pam Sontz, Dr. Fangwei Shao, and Professor Ben Elias were also welcome collaborators, with whom I've had many stimulating discussions.

Professor Eddie Merino is a source of both guidance and friendship. I appreciate the assistance and advice of many other postdoctoral fellows in the group over the past few years, including Professors Valerie Pierre, Marisa Buzzeo, Mi Hee Lim, and Maria

DeRosa, and Dr. Jason Slinker, as well as Professor Eric Stemp. Dr. Brian Zeglis, Dr. Paul Lee and Hang Song generously shared metallocomplexes, materials, advice, and good humor. Wendy Mercer was a good friend and labmate, and trained me in how to run attractive gels. Eric Olmon offered many valuable insights. Anna Folinsky provided materials and mentoring to me as a fellow teaching assistant. Being in the Barton group is a privilege; people freely share data and ideas, and I'll miss the exciting scientific discussions with the entire group. I have also had the privilege of collaborating with two smart, productive undergraduates: Molly Davis and Stephanie Wuerth.

My family have all been constant cheerleaders, supporting me through the travails of graduate school. My brothers Scott and Michael, my sister Debbie, and my mother and father have always given me unconditional love and unflagging support. My fiancée, Dr. Cindy Puckett has been my constant partner. She has critiqued the first draft of each of my manuscripts and presentations, and kept my spirits up when things were difficult. Every day is a richer one for sharing it with her.

ABSTRACT

The π-stack of double stranded DNA is a competent bridge for mediating charge transport (CT), both by single-step (coherent) and multi-step (hopping) mechanisms. The yield of long-range single-step CT from photoexcited 2-aminopurine, a fluorescent analogue of adenine, to guanine across adenine tracts has a shallow, periodic distance - measure total CT yield to the DNA bases, herein we employ the fast radical traps N_2-cyclopropylguanine (^{CP}G), N_6-cyclopropyladenine (^{CP}A), and N_4-cyclopropylcytosine (^{CP}C), which are energetically similar to the unmodified bases, but undergo rapid decomposition upon oxidation or reduction. We find that decomposition of ^{CP}G by a photoexcited rhodium intercalator across an adenine tract has a similar periodic distance dependence to the quenching of 2-aminopurine by guanine, and the same temperature dependence as well. In contrast, decomposition of ^{CP}G by photoexcited 2-aminopurine is monotonic with respect to adenine tract length, and also competes with back electron transfer. Eliminating back electron transfer by separating 2-aminopurine from the adenine tract with three high-potential inosine bases restores the non-monotonic distance dependence. We also determined decomposition of ^{CP}A along adenine tracts by photoexcited rhodium, and found the CT yield to be distance-independent, demonstrating that the periodicity associated with guanine oxidation is with respect to adenine tract length, not donor-acceptor separation. This length-dependent periodicity, and the associated temperature dependence, support a model of conformational gating in the formation of CT-active domains along the DNA.

DNA-mediated electrochemistry is facile in self-assembled monolayers on electrodes, and redox-active dyes are reduced through the DNA π-stack at potentials far lower than those of the individual bases. Since cytosine is the most readily reduced base, we incorporated ^{CP}C into DNA monolayers to assay for bridge occupation, and ^{CP}C decomposition was not observed.

To explore the relative contributions of single-step and multi-step mechanisms to CT yield across adenine tracts, we compared quantum yields previously collected from 2-aminopurine fluorescence quenching experiments to those from ^{CP}G decomposition. We find that for seven or eight intervening adenines, single-step CT accounts for the entire CT yield, while for four to six adenines, multi-step CT is the dominant mechanism. We interrupted multi-step CT by substituting ^{CP}A for an adenine on the bridge, and found the total CT yield across five or six intervening adenines is lowered to the single-step CT yield. Blocking coherent CT by replacing the terminal guanine with redox-inactive inosine does not affect ^{CP}A decomposition on the bridge. These results imply that single-step and multi-step CT processes are not in direct competition for these assemblies, consistent with the model of conformationally gated CT-active states.

TABLE OF CONTENTS

LIST OF FIGURES AND TABLES

Chapter 1:
Mechanisms for DNA Charge Transport[†]

[†] adapted from Genereux, J.C.; Barton, J.K. *Chem. Rev.* **2009**, *in press.*

1.1. INTRODUCTION

DNA charge transport (CT) chemistry has received considerable attention by scientific researchers over the past 15 years since the first provocative publication on long-range CT in a DNA assembly.[1,2] This interest, shared by physicists, chemists and biologists, reflects the potential of DNA CT to provide a sensitive route for signaling, whether in the construction of nanoscale biosensors or as an enzymatic tool to detect damage in the genome. Research into DNA CT chemistry began as a quest to determine whether the DNA double helix, a macromolecular assembly in solution with π-stacked base pairs, might share conductive characteristics with π-stacked solids. Physicists carried out sophisticated experiments to measure the conductivity of DNA samples, but the means to connect discrete DNA assemblies into the devices to gauge conductivity varied, as did the conditions under which conductivities were determined. Chemists constructed DNA assemblies to measure hole and electron transport in solution using a variety of hole and electron donors. Here, too, DNA CT was seen to depend upon the connections, or coupling, between donors and the DNA base-pair stack. Importantly, these experiments have resolved the debate over whether DNA CT is possible. Moreover these studies have shown that DNA CT, irrespective of the oxidant or reductant used to initiate the chemistry, can occur over long molecular distances but can be exquisitely sensitive to perturbations in the base-pair stack.

Here we review some of the critical characteristics of DNA charge transport chemistry, taking examples from a range of systems, and consider these characteristics in the context of their mechanistic implications. This chapter is not intended to be

exhaustive but instead to be illustrative. For instance, we describe studies involving measurements in solution using pendant photooxidants to inject holes, conductivity studies with covalently modified assemblies, and electrochemical studies on DNA-modified electrodes. We do not focus in detail on the differences amongst these constructs but instead on their similarities. It is the similarity among these various systems that allows us to consider different mechanisms to describe DNA CT. Thus we review also the various mechanisms for DNA CT that have been put forth and attempt to reconcile these mechanistic proposals with the many disparate measurements of DNA CT. Certainly the debate among researchers has shifted from "is DNA CT possible?" to "how does it work?" This chapter explores this latter question in detail.

1.2. Properties of Long-Range Charge Transport in DNA

Among the most interesting characteristics of charge transport in DNA is the long distance over which it occurs (**Figure 1.1**).[3-6] Nevertheless, there are some DNA systems that do not mediate charge over long distances. How DNA CT occurs depends upon coupling and the structure and dynamics of the DNA assembly. The chemistry and photophysics of the photoexcited acridine (Acr^{*+}) containing systems, which mediate CT over only a few base pairs, have been particularly well-characterized in this regard.[7,8] It is important to note that the same physical laws apply to all CT processes.[9] The essential distinctions are with respect to the relative roles which different mechanisms play, and it is in this respect that long-range CT, with effective coupling to the base-pair stack, differs from short-range CT, with poor coupling. Here we focus on long-range CT, where

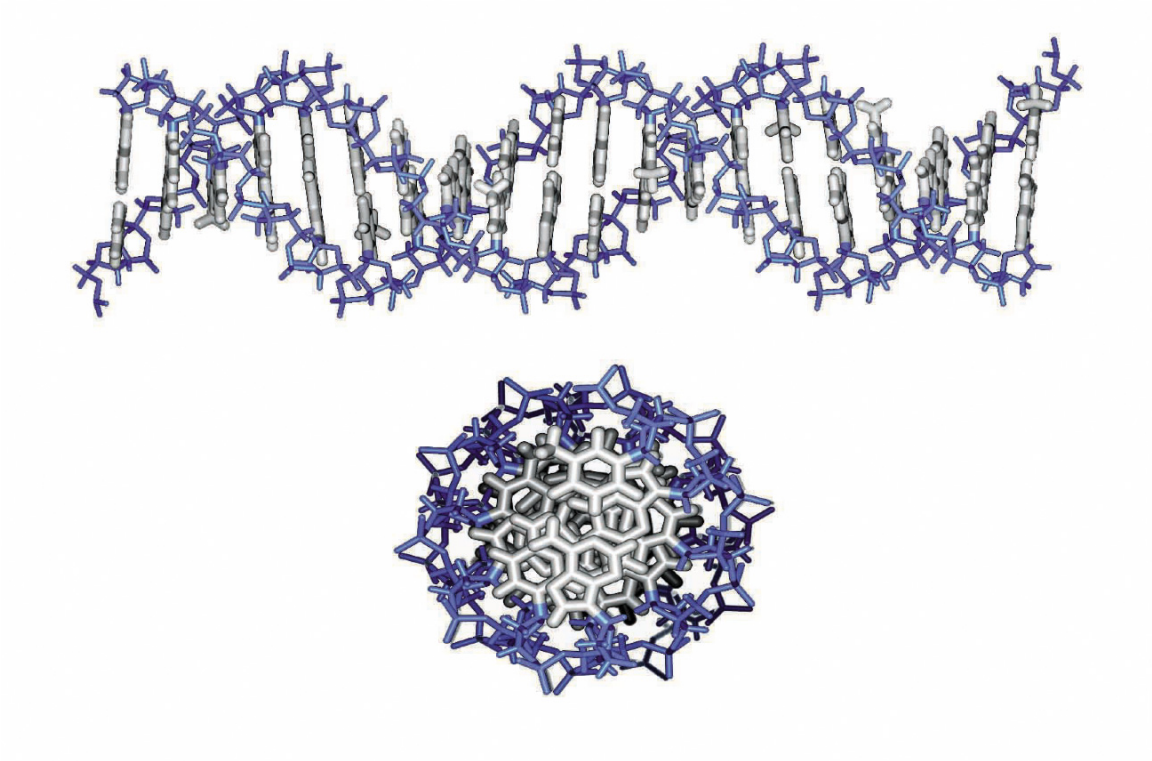

Figure 1.1. Transverse and longitudinal perspectives of DNA. The sugar phosphate backbone envelops the hydrophobic base pairs. The planar base pairs form a one-dimensional π-stack down the center of the DNA, insulated by the backbone.

transport is through the base pair stack, and discuss short-range systems only to the necessary extent to clarify the distinctions between the two regimes.

1.2.1. COUPLING TO THE DNA

It is notable that initial measurements of DNA-mediated charge transport for both photooxidation experiments[10] and device experiments[11] found rates and conductivities spanning several orders of magnitude over comparable distances, depending on the experimental conditions. This foreshadowed the same observation in scanning tunneling microscopy (STM) measurements of conductivity through other molecular bridges,[12] and, ultimately, was for the same reason. For short molecular bridges, it has been established both experimentally[12] and theoretically[13] that the coupling between the bridge and the donor (or acceptor) can dominate the observed conductivity. Similarly, when DNA is the bridge, the coupling can have a dramatic effect on both charge transport rates and yields **(Figure 1.2)**.[14-18] Characteristically, conductivity measurements that have not provided covalent contact between the DNA and the device yield a spectrum of behavior: from insulating to superconductive.[11,19-23]

In the case of DNA, the essential coupling is into the π-stack of the bases. This is a marked challenge, as DNA is essentially "insulated", with sugars and phosphates flanking the periphery of the bases.[24] This insulation, in part, explains why early experiments on dry DNA found insulating behavior, in contrast to that observed with conducting organic polymers. A series of well-conjugated charge donors and acceptors are now employed by various groups,[25,26] including metallointercalators, organic

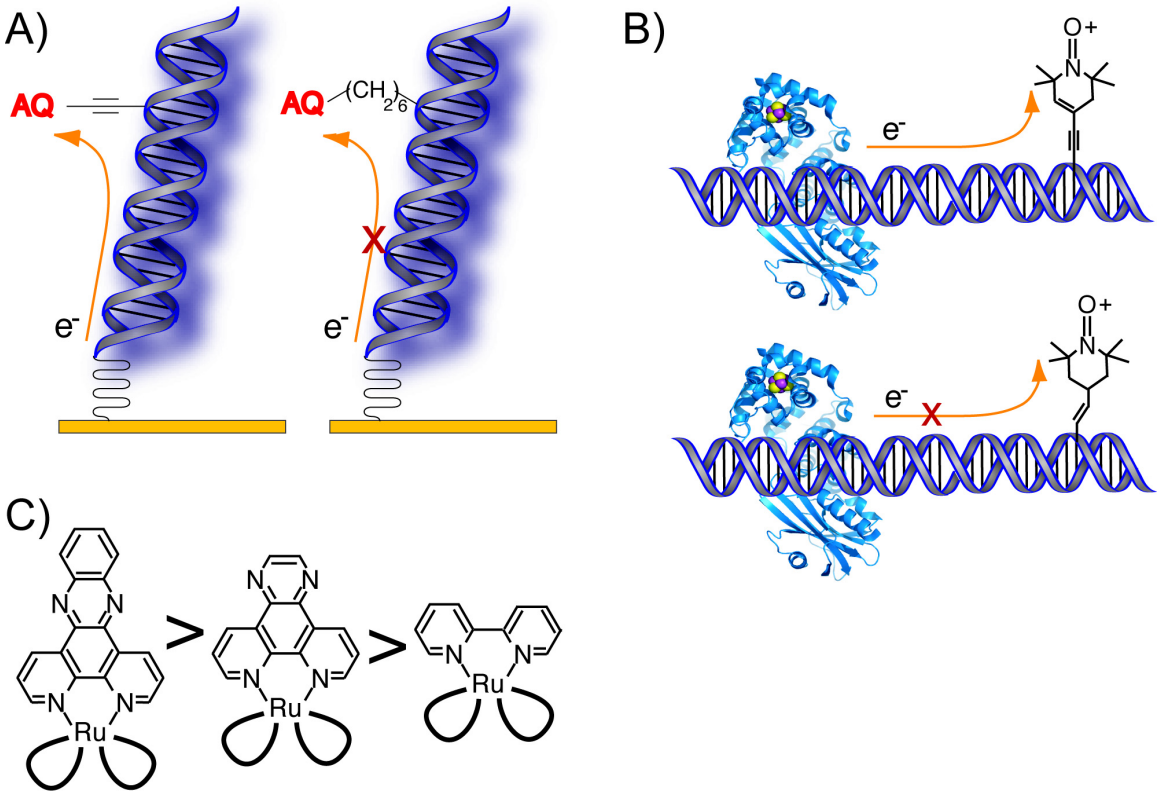

Figure 1.2. DNA-mediated CT requires electronic coupling to the base pair stack. (A) Electrochemical reduction of an electronically well-coupled anthraquinone (AQ) is facile, while that of a poorly coupled AQ is suppressed.[18] (B) MutY competently reduces an oxidized nitroxide spin label that is well coupled to thymidine, but not the nitroxide conjugated through the partially unsaturated linker.[160] (C) For a series of polypyridyl $Ru^{III}(bpy)_2L$ ground state oxidants, the yield of oxidative damage to DNA scales with the size and planarity of the intercalating ligand.[15]

intercalators, organic end-cappers, and modified bases. In several cases, direct comparison has been made between similar photooxidant pairs that differ primarily in their ability to couple well with the base stack. These examples include the adenine analogues ethenoadenine and 2-aminopurine (Ap),[14] two different coupling strategies for ethidium bromide,[27] and, most notably, a series of intercalating ruthenium analogues with decreasing planarity in the intercalating ligand.[15] As an extreme case, for two ruthenium complexes that are unable to intercalate, and that are attached on opposite ends of a short DNA duplex *via* terminal phosphate modification, the CT rate was found to be ~10^{-6} s^{-1};[28] this is what would be expected for the rate were the metal complexes connected solely through their σ tethers. Similarly, electrochemiluminescence studies find the same rates for DNA-mediated CT between a DNA-modified gold electrode and tethered $Ru(bpy)_3^{2+}$ as are observed through solely the tether itself.[29] In electrochemical studies of methylene blue covalently attached to a DNA duplex, effective transport is found only when the methylene blue is stacked in the helix, not under high salt conditions, where the dye, although still linked by a σ-bonded tether, is unstacked.[30] Indeed, electrochemical measurements on DNA films generally have been shown to be rate-limited by tether linking the DNA to the electrode surface[31]. In each case, it is clear that the coupling between the donor/acceptor pair and the bridge is dominating the measurement, and that the bridge is the π-stack of DNA.

1.2.2 Global Structural Integrity

The structure of DNA is central to its extraordinary effectiveness as the genetic template for the cell. This relationship between structure and function is underscored by the extent of the biological function that was first predicted in the landmark papers that reported the proper three-dimensional structure.[32,33] Hence, it is not surprising that DNA-mediated CT is also substantially affected by the global structure of a DNA sample. This is clear when considering the results of conductivity measurements on single or few DNA strands that have been performed in recent years. Various measurements from 1996 to the present have found DNA conductivities covering several orders of magnitude. Furthermore, conductivity has been found to be dependent on sequence, hydration, length, temperature, and hybridization in some experiments, while independent of each of those in others. Ultimately, the vast differences in observations can be largely reconciled by comparing the sample preparation methodologies of the individual studies.[11] Conditions that cause global DNA conformational changes or damage can both increase or decrease the observed conductivity. In one extreme case, it was found that imaging conditions commonly used prior to conductance measurements lead to a morphological change in the structure of the DNA, that is itself correlated with increased conductivity.[20]

Among experiments that examine undamaged DNA, a profound difference is always observed between single-stranded and double-stranded DNA: single-stranded DNA does not mediate CT over long distances. This has been observed by direct conductivity studies,[34] photooxidation,[35] transient absorption,[36] electrochemical AFM,[37,38] STM,[39] electrogenerated chemiluminescence,[29] and electrochemical experiments in DNA

monolayers.[40] The caveat in interpreting studies on single-stranded DNA is, however, that its structure and, importantly, stacking are heterogeneous and extremely dependent on sequence.

DNA, stabilized by a variety of hydrophobic and hydrophilic interactions and evolved for an aqueous environment, undergoes gross structural changes as a result of moving from a hydrated to a dehydrated environment.[41] Critically, these changes are to the *equilibrium* conformation of DNA; the effects of dehydration on DNA dynamics are not well understood. Highly bound waters play a major role in the dynamics that gate molecular recognition and other biochemical interactions between macromolecules.[42]

Regrettably, the first and many recent measurements of DNA conductivity were performed under vacuum. Vacuum is ideal for conductivity measurements due to the suppression of voltage leak and the associated background current. Even experiments performed in the presence of water frequently deposit the DNA under vacuum conditions. Similar to the previous case of poorly coupled versus well-coupled systems, there is wide disparity between the conductivities observed under conditions of low humidity. Recently, progress has been made in understanding the role of humidity in many of the poorly coupled systems.[43] Even without strong coupling into the DNA base stack, water adsorbed on the DNA and in DNA bundles can mediate ionic conduction. The amount of adsorbed water will depend strongly on humidity, and also on the adsorption environment of the DNA. This helps explain why many systems in which coupling to DNA was poor were still observed to conduct.[19,23,44]

Not surprisingly, experiments that have preserved the DNA in its native conformation, with leads covalently coupled to the bridge, have shown remarkably similar (and substantial) conductivities (**Figure 1.3**).[34,37,44,45] The conductivity measured by Xu et al. across a dodecanucleotide with terminal propylthiol-Au contacts (> 40 Å) is comparable (6×10^{-4} G_0, where G_0 is the quantum unit of conductance) to that found across the much smaller benzenedimethanethiol (~10 Å) under the same experimental conditions,[47] though this comparison is complicated by the possibility that DNA accommodates internal stretching during the measurement rather than extruding gold from the molecular junction, as is postulated for benzenedimethanethiol.

As is the case with water, ionic strength can dictate the conformation of DNA. High ionic strength drives the transition from B-form to the more extended Z-form of DNA. Poor base stacking, associated with this condensed structure, leads to less efficient DNA-mediated CT.[48] Conversely, sufficiently low ionic strength leads to strand dehybridization, which also suppresses CT.

Beyond issues of ionic strength, there is conflicting evidence as to whether the identity of the counterion affects CT. Some calculations have shown that counterion identity does not affect the electric field inside the DNA,[49] while others have found that movement of a single sodium has profound effects on base energies.[50] Similarly contrasting results have been observed in experimental work.[51-54] For solvent-exposed donors and acceptors, an ion-pair can form between dye and counter-ion that itself profoundly affects CT rate and yield.[55]

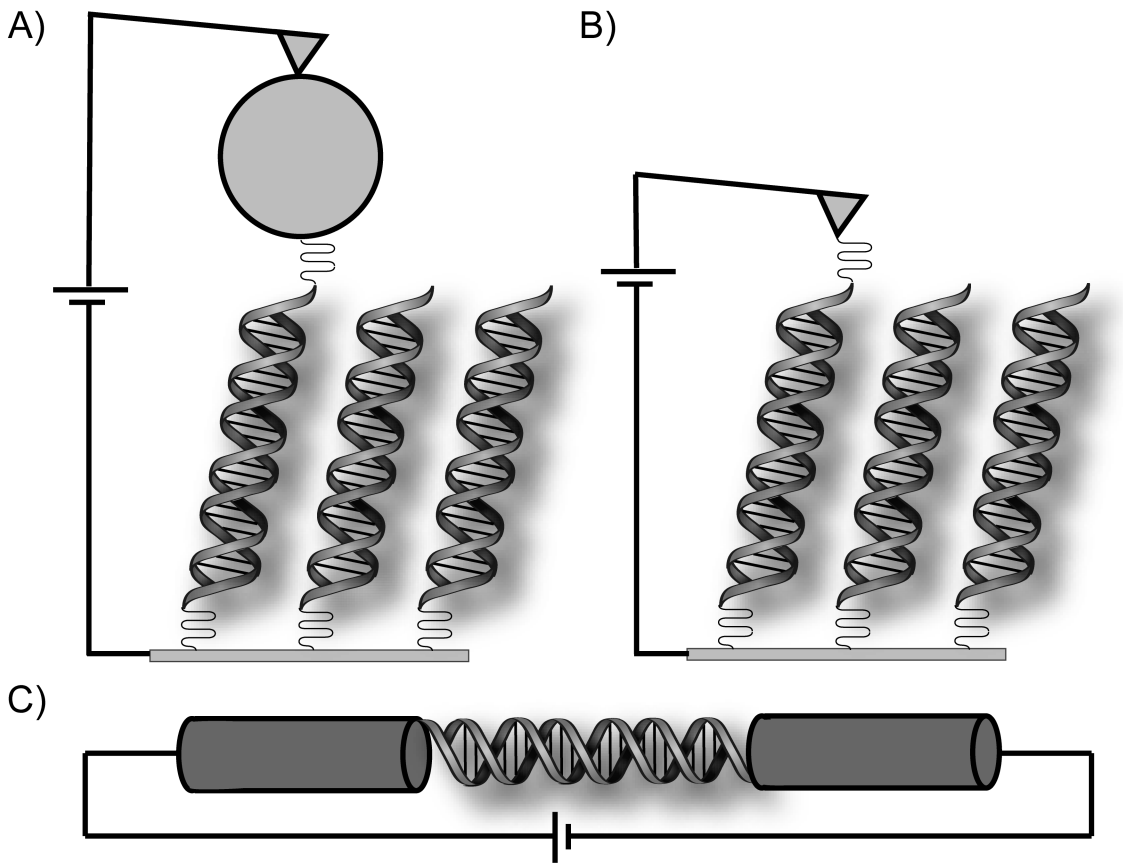

Figure 1.3. Devices for measurement of single molecule DNA conductivity through molecular contacts. In each case, currents between 10 and 100 nA are obtained for modest source-drain and gating voltages. A) A gold nanoparticle allows strong coupling between the EC-AFM tip and an individual 26mer DNA molecule on a gold electrode.[37] B) The gold STM tip is slowly brought in contact with thiol-modified DNA (8mer), allowing a histogram of conductance over many different orientations.[45] C) A single 15mer DNA is covalently attached across a gap between single-walled carbon nanotubes.[34]

More chemically controlled experiments elucidate the structural basis of environmental effects. RNA/DNA hybrids and double stranded RNAs adopt the A-form while alternating purine-pyrimidine sequences under certain conditions adopt Z-form structures. Both conformations support DNA charge transport, though Z-form is an inferior bridge relative to A-form and B-form for electrochemical,[48] but not photooxidation assays.[56] Not surprisingly, the competence for mediating CT has been shown to follow the extent of base stacking, both in solution studies with Ap as the photooxidant[57] and in electrochemical experiments monitoring the efficiency of reducing an intercalated redox probe.[48] Again, different coupling of the redox probes into these different conformations means that they cannot be quantitatively compared.

Perhaps most interesting is the comparison of rates of intrastrand versus interstrand base-base CT in DNA assemblies modified with Ap.[14,35,57] Here for the B-conformation, intrastrand CT is found to be three orders of magnitude faster than interstrand CT, consistent with the fact that stacking in the B-conformation is exclusively intrastrand; CT across strands requires CT across a hydrogen bond. However, in the A-form there is a mix of interstrand and intrastrand stacking down the helix, and here we observe that rates of intrastrand and interstrand CT are comparable.

1.2.3. Local Structural Integrity

A variety of studies have found similar effects of disrupting the base stack locally. The assays include electrochemical experiments in both films[30,58,59] and devices,[34] and solution experiments using time-resolved fluorescence,[60] irreversible trapping of

chemical product[61] and transient absorption measurements.[62] The presence of mismatches lowers both the rate and yield of DNA-mediated CT, and the extent of this attenuation scales with the base pair lifetime.[63] Abasic sites[64] and destabilizing lesions[65] also interfere with CT through DNA films.

Regarding those experiments that utilize product trapping, however, it is important to note that the results are convoluted with two effective clocks. The first is the rate of back electron transfer (BET), if it occurs.[66] The second is the rate of product trapping.[66-69] A disruption of the π-stack will only be observable in product trapping experiments if it is sufficient to disrupt equilibration of the radical cation on the time scale of BET and product trapping.[70] Towards this end, guanine damage assays have recently been replaced by assays for fast decomposition of a radical trap. *N*-cyclopropylguanosine (^{CP}G),[71,72] *N*-cyclopropyladenosine (^{CP}A),[17,73,74] and *N*-cyclopropylcytidine (^{CP}C)[75,76] are synthetically accessible, cause minimal perturbation to the DNA-duplex, and undergo irreversible picosecond ring-opening upon oxidation or reduction.

Not all modifications of DNA suppress long-range CT. A dephosphorylation nick to the backbone, despite causing substantial change to local ion density, does not have a measurable effect.[77,78] Furthermore, some modifications can enhance CT. Most notably, DNA with adenines replaced by the lower-potential base deazaadenine or the better-stacking benzodeazaadenine improves the rate and yield of DNA-mediated CT.[79-81]

In addition to global changes in structural integrity, subtle modulations to structure can also have profound effects on the rates and yields of DNA-mediated CT.

DNA-mediated CT is attenuated by the presence of mismatches, even though mismatched base pairs cause only minor distortions to the structure of DNA.[82,83] Nevertheless, mismatch discrimination has been observed in charge transport through DNA films,[58,59,84] single molecule devices,[34,85] and photooxidation systems.[35,61] This attenuation is identical for oxidative and reductive CT,[86] implying mechanistic similarity. Importantly, the extent of mismatch discrimination corresponds to the base-pair lifetime associated with the specific mismatch.[63] In the extreme case, an abasic site completely suppresses CT.[64,87,88] Subtle lesions, such as the oxidative guanine products O_6-methyl-guanine and 8-oxoguanine, attenuate CT.[65] It should be noted that although 8-oxoguanine terminates DNA-mediated CT as a thermodynamic and kinetic trap at high driving force,[89,90] this and other damaged base products also attenuate CT even under driving forces incompetent for direct oxidation. This property of DNA-mediated CT has led to the development of a new class of DNA-detection devices,[91,92] and might be relevant to damage detection in the cell.[93]

Local changes to structure can also be induced. Inside the cell, proteins can bend, twist, and dehybridize DNA, and some can extrude bases as well. Not surprisingly, many of these binding events have severe effects on DNA-mediated CT. Monitoring DNA-mediated electrochemistry to SoxR, a transcription factor that initiates the oxidative stress response in *E. coli*, is consistent with the prediction that the oxidized form twists DNA to initiate transcription,[94] as has since been validated by a recent crystal structure.[95] CT is also inhibited by the sequence-specific binding of TATA-binding protein (TBP),[58,96] which bends DNA. One particularly informative experiment involved the methylase

M.*Hha*I, which extrudes a cytidine within its recognition sequence, replacing it with glutamine. DNA with the *Hha*I recognition site shows attenuated CT in the presence of the protein. The Q237W mutant, in which the intercalating glutamine is replaced with the aromatic ligand tryptophan, however, barely affects CT compared to the absence of protein.[58,97] Importantly, proteins that do not distort the DNA π-stack, such as antennapedia homeodomain protein or unactivated R.*Pvu*II, do not attenuate DNA-mediated CT.[97] Indeed, the rigidification associated with R.*Pvu*II binding increased CT through the dynamically flexible TATA binding site. An interesting exception is the case of R.*BamH*I, a restriction endonuclease which does not bend the DNA π-stack, but contains an asparagine guanidinium that hydrogen bonds to a guanine in its cognate site. It has been shown that R.*BamH*I attenuates DNA CT to guanines both within and beyond its binding site, presumably due to electrostatic modulation of the intervening DNA *via* the hydrogen bonding interactions.[98]

Protein binding can also affect the fate of radicals in DNA.[99-101] Guanine radical has been shown to crosslink to histones and short peptides. In one case,[102] excitation of an anthraquinone (AQ)-DNA conjugate bound to a reconstituted nucleosome particle led to DNA-protein crosslinks; experiments with a different photooxidant with facile back electron transfer found no such effect.[103] Since it is clear that migration can occur over long distances in both isolated nuclei[104] and mitochondria,[105] this might not be a fast pathway for radical quenching; the time scale of protein-DNA crosslinking in the presence of guanine radical is similar to that for guanine radical decomposition to 8-oxoguanine.[106] These crosslinks are reversible under the processing conditions used to

convert base damage to strand cleavage, and hence are likely hidden in typical gel analysis experiments. Furthermore, protein cross-links can be formed as a secondary product after radical degradation in DNA to 8-oxoguanine.[107] Recently, it has been shown that a protein that disrupts the π-stack, Hbb of *Borrelia burgdorferi*, affects the conversion of radical damage to interstrand crosslinks.[108]

DNA CT is sensitive to even more subtle deviations in stacking integrity. The strongest stacking interactions occur between consecutive purines, as has been shown both experimentally and computationally. Extended purine-pyrimidine runs correspond to the minimal extent of base-stacking, while purine-purine runs, particularly adenine tracts, correspond to the maximal extent for DNA containing natural nucleotides. This relationship is borne out in the sequence dependence of CT.[51,109-111] Note that in photoactivated studies of electron transport, runs of pyrimidines, which are more easily reduced, are the preferred sequences.[112] Likely here too, the decreased flexibility of homopurine-homopyrimidine sequences plays a role.

1.2.4. CONFORMATIONAL GATING

The rate and efficiency of charge transfer is centrally related to the structure of the individual pathway(s) that mediates CT between the donor and acceptor. Over long distances, however, it is inevitable that fluctuations will be induced at nonzero temperature, such that the equilibrium structure only reflects an average over the ensemble. If these fluctuations are sufficiently large, and slower than CT for the equilibrium conformation, then CT no longer is properly described by a unitary rate

constant, but will instead proceed with a complicated time-dependence that convolutes the conformational dynamics with the CT rates of the different conformations.[113] To avoid this, the best-performing molecular wires are chosen for, among other properties, rigid homogeneous conformations.[114] For example, the conduction of certain oligophenyleneethynylenes can be substantially enhanced by the presence of bulky side-groups that limit the conjugation-breaking rotation around the acetylene bonds.[115,116]

It is not surprising that DNA, which even as a relatively short 15-mer contains several hundred atoms, exhibits substantial conformational flexibility. Interestingly, the effect of conformational gating in DNA is generally to *increase* CT rather than to decrease it. Duplexes frozen in glass show no attenuation in CT between the photooxidant Ap and neighboring guanine hole acceptor (**Figure 1.4**).[117] The insertion of a single adenine, however, between donor and acceptor completely suppresses CT. The temperature-dependence of CT between Ap^* and G for varying bridge length has been studied by both femtosecond transient absorption spectroscopy[35] and steady-state fluorescence quenching measurements.[54] The temperature-dependence has also been measured for CT between tethered, photoexcited $[Rh(phi)_2(bpy')]^{3+}$ and ^{CP}G.[68] For all bridges, CT efficiency increases with temperature, and the temperature dependence is greater with increasing bridge length.

Although thermal activation on its own does not imply a mechanism, the sequence dependence establishes a strong relationship between bridge structure and the activated process. The temperature dependence of the electronic contribution to the rate should be the same irrespective of increasing bridge length. The temperature dependence

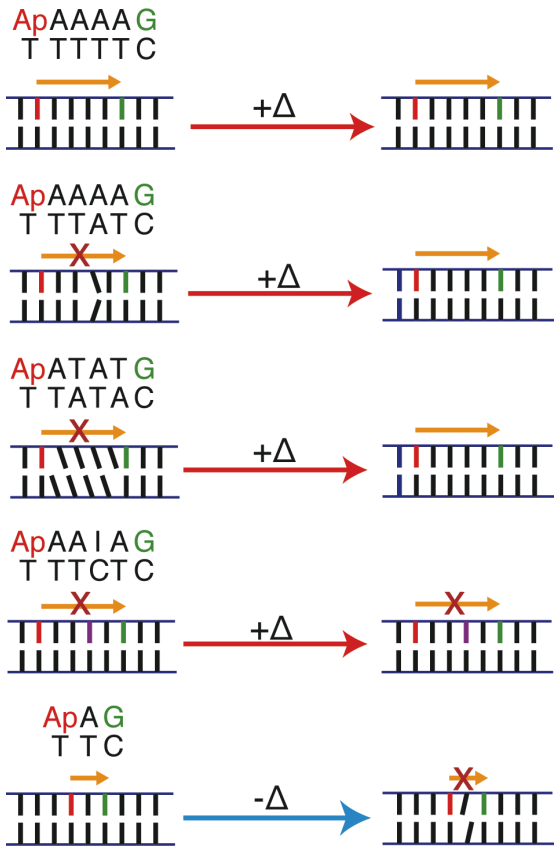

Figure 1.4. The sequence and temperature dependence of single-step oxidation of guanine by photoexcited 2-aminopurine (Ap) in DNA.[35,54,117] CT yield in well-matched $Ap(A)_4G$ increases with temperature (+Δ), up to duplex melting. Two perturbations that disturb CT due to poor stacking dynamics, an A-A mismatch and the sequence ATAT, attenuate CT at room temperature but are comparable to the A_4 sequence at higher temperature, while CT through a perturbation that disturbs CT due to an electronic barrier, AAIA, is only partially recovered at high temperature. This argues that the CT activation is related to the flexibility of the bridge. At low temperature (77K), an intervening adenine eliminates CT from Ap to G, implying that the equilibrium conformation is not the CT active conformation.

of the nuclear contribution, due to bridge-length dependences on driving force and reorganization energy (see below), can naturally be bridge-length dependent, but should disappear for distances above 10 to 15 Å,[118] which are exceeded here. Conformational gating to reach a CT-active state, however, is expected to lead to increased CT with temperature, and for this increase to be greater when more bridge units are required to align, i.e., for longer bridges.

Interestingly, this increase in the rate with respect to increasing temperature is even more profound when the bridge is poorly stacked ATAT,[54] or contains an AA mismatch,[35] consistent with the model whereby these sequences disrupt DNA due to poor dynamic stacking (**Figure 1.4**). When the bridge is AAIA, which stacks well but attenuates CT from Ap^* due to the inosine potential barrier, the increase in CT with respect to temperature is only modest. These experiments strongly suggest that the equilibrium conformation of DNA is not the active conformation for long-distance CT, but that conformational gating allows the formation of CT-active states. This is in direct contrast to the usual role dynamic disorder plays in molecular wires, where distortion from the equilibrium conformation decreases coupling and transport.[119]

There are two different implications of conformational gating. In one sense, reorientation of the photooxidant with respect to the DNA to form a CT-active conformation can be rate-limiting. Alternatively, formation of a CT-active state in the DNA itself can be the rate-limiting step for CT. Both senses are represented by the case of ethidium bromide. Ethidium bromide (Et^+) is competent for DNA-mediated oxidation and reduction of deazaguanine (^ZG) and $[Rh(phi)_2(bpy')]^{3+}$ respectively.[27,60,120,121]

Femtosecond transient absorption and fluorescence up-conversion spectroscopy of Et^+ site-selectively intercalated in DNA found that the Et^+ oxidized ^ZG with two rate constants.[120] One (5 ps) corresponds to Et^+ that is already present in a CT-active conformation. The other (75 ps) corresponds to the gating of Et^+ to reach a CT-active conformation with respect to the DNA. This is the first sense of conformational gating. As the distance between Et^+ and ^ZG increases, the rate of each component is unaffected, but the amplitudes monotonically decrease, suggesting that the increase in distance lowers the yields by virtue of changing the population of CT-active states, rather than by affecting the inherent rates of CT through the DNA. This represents the second sense of conformational gating.

To further test this model, a new method of conjugating Et^+ to DNA as a rigid base-pair surrogate was developed (**Figure 1.5**).[27] For the Et^+ separated from the hole acceptor, ^ZG, by a single base pair, the rate is similar to that for CT from the intercalated Et^+. This rate drops four orders of magnitude if another adenine is inserted between the Et^+ and ^ZG. Beyond a distance of two base pairs, the rate is constant. The authors interpreted this system as one that held the Et^+ rigidly in a CT-inactive state. The rate-limiting step is injection, which for a poorly coupled donor exhibits a steep distance dependence. At sufficient donor-acceptor separation, re-orientation of the donor is competitive with the slow CT from poorly coupled Et^+. Now the apparent distance-dependence is flat, for the same reason as for the intercalating Et^+.

A similar explanation might serve for the slow rate of charge injection into stilbene-capped hairpins where several AT base pairs separate the photoexcited stilbene

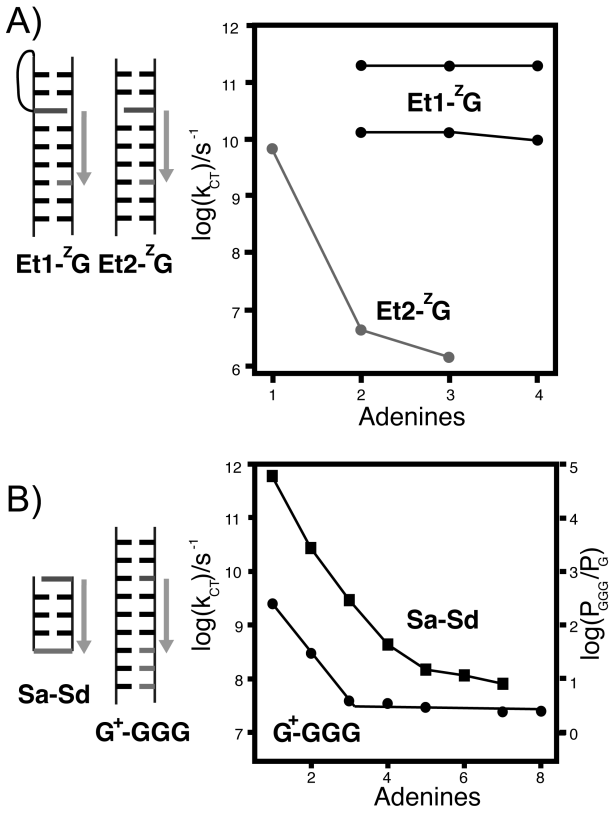

Figure 1.5. (A) The rate of coherent deazaguanine (^{Z}G) oxidation by ethidium bromide is the same over short distances for both the flexible linkage **(Et1**, black, both CT rates shown) and the rigid linkage **(Et2**, gray).[27] For two intervening nucleotides, a sharp drop in rate is observed for the rigid Et^{+}, but the rate is unaffected for the flexible Et^{+}. (B) This steep drop in rate over short distances is consistent with that observed for oxidation of guanine by a photoinduced sugar radical (circles),[207] and CT between hairpin capping stilbenes (squares, photooxidation of **Sd** by **Sa**),[125] and has been attributed to a crossover between coherent superexchange and incoherent hopping. In the latter case, comparison of injection and hole arrival rates supports superexchange for one or two intervening base pairs, and hopping for three or more base pairs between the stilbenes. Adapted from References 27, 207, and 125.

hole donor from a guanine hole acceptor. Stilbene-4,4'-dicarboxamide incorporated as a bridging and capping element in short AT containing hairpins (Sa-AT) has an extended nanosecond lifetime and hence higher fluorescence quantum yield versus the free dye, but a single GC pair close to the stilbene dramatically decreases the fluorescence intensity, via CT quenching.[122,123] The robust fluorescence in the absence of guanine was taken as evidence for a lack of CT between stilbene and adenine, despite the presence of several low-yield picosecond decay components. Eventually, these components were assigned to CT between the excited stilbene and adenine.[124,125] The charge-separated state can either undergo recombination, or, in the presence of distal guanine or a lower energy stilbene-4,4'-diether (Sd), the hole migrates to the acceptor leading to CT quenching.[126] It was argued that the recombination recovers the excited state, and that hence charge injection in the Sa-AT constructs only minimally quenches fluorescence.[124] This is distinct from exciplex emission, as the emission spectrum is similar to the unconjugated fluorophore. The stilbene radical anion is solvent exposed, and the motions of DNA, associated counterions, and bound water allow rapid relaxation of dyes,[127] so it is unlikely that recombination-induced emission would be of the same energy as radiation from the initial excited state. An alternate explanation is that this fast injection is limited to a small population that is in a CT-active conformation. The remaining population fluoresces normally in the absence of nearby guanine. In that context, the slow, strongly distance-dependent direct charge transfer from excited stilbene to guanine can be interpreted in the context of a donor that is not in a CT-active state with respect to the π-stack.[122]

1.2.5. BACK ELECTRON TRANSFER

Inevitably, photo-induced charge separation events are followed by charge recombination, also termed back electron transfer (BET). After all, if charge recombination is thermodynamically unfavorable, then charge separation is thermodynamically favorable and will not require photoexcitation. The effect of BET varies by the nature of the assay. Assays for the presence of the charge separated state, such as the slow oxidation of guanine cation radical, will generate yields that are convoluted with BET processes. In two extreme cases, thionine[128] and Ap,[73] which are competent for efficient charge separation, are not competent for the formation of permanent guanine oxidation products.

The case of the two excited electronic states of AQ offers a nice comparison of photooxidation with fast and slow BET. Irradiation of DNA-conjugated AQ at 350 nm promotes it to the singlet excited state, which relaxes to the triplet state. Both states are competent for direct oxidation of all four bases in DNA, but only the triplet radical anion reduces oxygen to superoxide. The singlet radical anion undergoes rapid BET, regenerating the initial state, while the charge injected by the triplet radical anion is persistent, and can equilibrate along the DNA on a longer time scale.[129,130] This scheme explains the incompetence of AQ to oxidatively repair cyclobutane thymine dimer;[131,132] repair can only proceed from the singlet state.

Experiments that rely on slow product trapping at guanine need BET to provide the fundamental clock that allows discrimination of CT attenuation.[66] Hence, although the results will be qualitatively diagnostic, the quantitative accuracy will only hold

relative to the BET rate for that system. For example, a single negatively charged phosphate group near the intercalation site of a tethered rhodium photooxidant changes the observed ratio of damage between a distal and proximal GG site by an order of magnitude, indicating that the distal/proximal damage ratio is not solely determined by the intervening bridge.[52]

Short-range CT is particularly subject to BET, as the recombination has a steeper distance dependence than separation, most likely due to greater separation in donor-bridge-acceptor energies, as discussed in **Section 1.3.2**.[122] This was first exploited in guanine damage systems using AQ as the donor, but has since been systematically studied in Acr^{+}-phenothiazine (Ptz) and napthalimide (NI)-Ptz systems.[133-136] In the former, suppressing BET allowed the extension of a canonical short-range CT system into one that exhibited persistent CT separation over a long range![136]

1.2.6 Injection and Migration Effects

Even among well-coupled donors and acceptors, substantial variations in CT yields and rates have been observed. The fastest observed rates (subnanosecond) over long-distances are for the $Ru^{II*/III}/Rh^{III/II}$ pair[1,137] and for the oxidation of ^{Z}G by Et^{+*} [120] and the reduction of Rh^{III} by Et^{+*}.[121] Oxidation of guanine by Ap^{*},[138] excited stilbene,[122] or even by guanine radical after initial oxidation by photoexcited stilbene,[139,140] is substantially slower. To first order, this trend reflects the relative stacking of donors and acceptors with the DNA duplex.

In addition, some of these results may be reconciled in the context of considering the effect of electrostatics on hole migration.[113] This effect was directly demonstrated by a study with Rh^{III*} as the photooxidant wherein the position of a terminal phosphate was varied.[52] In this experiment, comparative damage at GG sites proximal and distal to the Rh intercalation site was determined. Since the decomposition of the guanine cation radical is slow, and the DNA between the GG sites was short and undamaged, the final yield reflects both the relative extent of BET and the potentials at the GG sites. When a phosphate anion is added to the end opposite to the rhodium, there is a small increase in damage distribution towards the distal site. An extra phosphate anion on the same end as the rhodium, however, leads to a several-fold change in relative damage. For one sequence, relative damage at the proximal site increases from 16% to 56%. This argues that local charge can have a strong effect, both on the rate of BET and on the rate of migration. For AQ, which irreversibly injects a cation due to rapid oxygen quenching of the triplet AQ radical anion, this effect is not present,[141] consistent with a lack of BET,[66] although given the low amount of distal damage in these constructs, it is not clear whether a subtle change would be detectable.[142] Importantly, in biological systems the initial oxidation product is generally a guanine cation radical, without an anion radical also being localized on the DNA. Hence, coulombic attraction will not inhibit transport away from the injection site, as is the case for Ap^{*} and $Ap(-H)^{\bullet}$, stilbene, AQ, and other neutral photosensitizers.

1.2.7 ENERGETICS

The natural nucleosides of DNA are resistant to mild oxidation and reduction and the radical cations and anions undergo secondary chemical reactions on the microsecond time scale. Hence, the reversible potentials are not trivial to acquire.[143] Approaches for determining the nucleoside potentials fall into four categories: computational, electrochemical, pulse radiolysis, and photooxidation studies (**Table 1.1**). A common conclusion from all of these studies is that the oxidation potentials increase in the order G<A<C~T.

Electrochemical measurements of base potentials are limited to organic solvents, generally acetonitrile, DMSO, or DMF, due to the relative facile oxidation of water versus the four bases. Considering the hydrophobic interior of DNA, potentials determined under these conditions may be more relevant to DNA than potentials determined in aqueous solution. To date, reversible electrochemistry has not been achieved. Irreversible oxidation potentials of all four nucleosides have been measured, which should be close to the standard potential.[144] The values for dG are similar in acetonitrile and DMSO,[145] but substantially more positive and more negative values have been found in chloroform[145] and DMF,[146] respectively. In chloroform, it was found that the presence of dC, which allows the possibility of proton-coupled electron transfer (PCET), lowers the oxidation peak of guanine by 340 mV.[145]

The closest that electrochemical experiments have come to measuring the oxidation of guanine in its natural context in DNA are the electrocatalytic experiments using mediators on indium tin oxide.[147] That $[Ru(bpy)_3]^{3+}$ ($E^{1/2}$ ~ 1.3 V; all potentials

Table 1.1. Experimental and Calculated Oxidation Potentials of Nucleotides

Method	Solvent	Nucleotide Oxidation Potential (vs. NHE)				Reference
		dG	dA	dC	dT	
pulse radiolysis	aqueous	1.29 V	1.42 V	1.6 V	1.7 V	272
electrochemistry	MeCN	1.49 V	1.96 V	2.14 V	2.11 V	144
electrochemistry	DMSO	1.44 V				145
	$CHCl_3$	1.62 V				
	$CHCl_3$ + dC	1.28 V				
time-resolved quenching	aqueous	0.97 V	1.2 V			174
electrochemistry	DMF	1.52 V				146
DFT	organic	1.88 V	2.01 V	2.18 V	2.25 V	273
	organic + dC	1.48 V				
	organic + dT		1.81 V			
pulse radiolysis	aqueous, DNA	1.22 V				149

herein are vs. NHE) is a facile mediator for electrocatalytic oxidation of DNA indicates a comparable potential for guanine.[148] Analysis of oxidation rate using a variety of metal complex mediators of different potentials supports this value. Notably, sufficiently high ionic strength was used in these experiments to deconvolute the potential from the affinity of the metal complex. This result was later validated by pulse radiolysis experiments in DNA,[149] where a potential of 1.22 ± 0.02 eV was found for guanine in multiple sequence contexts. Although the absolute potentials from electrocatalysis are approximate, they provide strong evidence for 5'-GG-3' being about 0.15 V lower in potential than G with a 5'- pyrimidine.[150]

The latter result, that the 5'-G of GG doublets are lower in oxidation potential versus G, has been extensively exploited in studies of the migration of charge in DNA, where GG sites are used as shallow hole traps. Calculation and oxidative yield experiments indicate that GGG acts as an even deeper well, although smaller differences in potential between these sequences are found experimentally than by calculations,[151] probably due to solvent interactions.[152] Both calculation and experimental work support preferential hole density on the 5'-G.[99,153-156] More generally, there is strong correlation between the calculated *ab initio* ionization potential of guanine in the different stacking environments and the relative oxidative damage found between different guanines under conditions that allow full equilibration of the injected charge.[157] Stacking affects the energies of all the bases, with the strongest perturbation due to the 5'-base.[150,158]

Vitally, all of these experiments probe the *equilibrium* potentials of the bases. Random sequences of DNA have rugged potential landscapes, corresponding to extensive

static disorder. There are many conformational modes in DNA and its hydration layer with time scales from picoseconds to seconds.[127] As discussed in more detail below, the energetics of the bases are coupled to these modes, introducing both static and dynamic disorder to the system.

Given the challenge in properly coupling an individual photooxidant to DNA, it is not surprising that few studies have attempted to determine rationally the driving force dependence of CT. It has been established from several studies that CT does not occur from an excited photooxidant hole donor to a higher energy hole acceptor. For example, the metallointercalator $[Rh(phi)_2(bpy')]^{3+}$, tethered to DNA, can oxidize A, G, or C from its excited state ($E^{3+}*/E^{2+}$ = 2.0 eV), but the metallointercalator $[Ru(phen)(dppz)(bpy')]^{3+}$ (E^{3+}/E^{2+} = 1.6 eV) oxidizes G, but not C.[76] Similarly, $[Ru(phen)(dppz)(bpy')]^{3+}$ and ethidium bromide (E^{*+}/E^{0} = 1.2V)[121] are not competent to repair thymine dimers, but photoexcited $[Rh(phi)_2(bpy')]^{3+}$ performs this repair, as does napthaldiimide (NDI) (E^{*}/E^{1-} > 1.9 V).[131,159] These studies include measurements with the hole donor tethered far from the acceptor, with intervening low-potential double guanine sites, indicating that even after charge is injected into DNA, there is some memory of the energy of its initial state (**Figure 1.6**).

In support of this interpretation, CT can still occur far below the potential of the DNA. In one example,[160] an oxidized nitroxide ($NO^{+}/NO^{\bullet}$ ~ 1 V) was incorporated into a duplex by covalent attachment to thymine. The [4Fe-4S] protein MutY (E^{3+}/E^{2+} = 0.1 V) was added, and the generation of the reduced nitroxide spin radical was observed by EPR (yield ~ 50%). This chemistry was demonstrated to be DNA-mediated by two controls. A

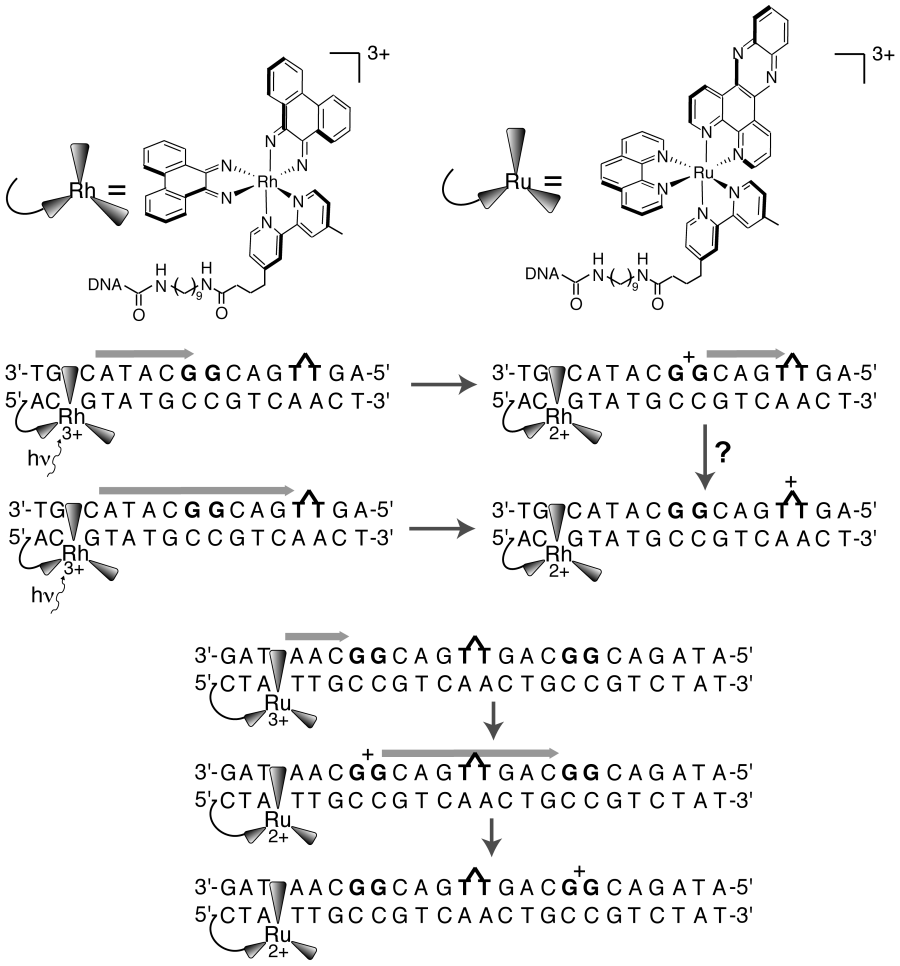

Figure 1.6. Oxidation and repair of thymine dimer (~1.8 eV) by tethered photoexcited $[Rh(phi)_2(bpy')]^{3+}$ (2.0 V) is unaffected by the intervening double guanine site (1.2 eV). Oxidation of double guanine sites by $[Ru(phen)(bpy')(dppz)]^{3+}$ (1.5 eV) is unaffected by the presence of thymine dimer, which this oxidant lacks sufficient driving force to repair. The latter result implies that guanine radical is not competent to repair thymine dimers, in accordance with the known potentials. Hence either the guanine radical oxidized by $[Rh(phi)_2(bpy')]^{3+}$ does not relax prior to migration to the thymine dimer, or the guanine radical is not an intermediate in DNA-mediated oxidation of thymine dimer by $[Rh(phi)_2(bpy')]^{3+}$.

noncleavable substrate analogue for MutY incorporated into DNA far from the label increased the reduction yield, and partially saturating the electronic conjugation between the label and the DNA substantially decreased the reduction yield.

A similar conundrum is involved in DNA-mediated CT in self-assembled monolayers on gold (**Figure 1.7**).[161] In these systems, a DNA monolayer is covalently self-assembled on an electrode, and CT through the DNA is measured with an electrochemical probe. At an applied potential greater than 0.4 V, the DNA adopts an upright conformation. Although elastic motions can bring the DNA in contact with the surface,[162] these conditions require high salt and fairly positive potentials. DNA mediation has been established for our system by the methods discussed above, i.e., mismatch and binding event discrimination, probe conjugation, linker-length dependence, and by differential redox potential between direct contact and DNA-mediated reduction.[31,163-165] The window for these experiments on Au is limited by the potential of Au-S reduction, about -0.5 V. DNA-mediated CT has been observed for a dozen different probes spanning a full volt below this value.[91,163-166] Importantly, the reductive limit is 600 mV below the reduction potential of cytosine.

Photooxidant-bridged DNA hairpins were employed to measure systematically the dependence of CT rate on driving force.[167] In these experiments, five photooxidants, stilbene-4,4'-dicarboxamide (Sa, $E^{*/-}$ = 1.68 V), naphthalene-2,6-dicarboxamide ($E^{*/-}$ = 1.74 V), diphenylacetylene-4,4'-dicarboxamide (PA, $E^{*/-}$ = 2.02 V), NDI ($E^{*/-}$ = 2.93 V), and phenanthrene-2,7-dicarboxamide ($E^{*/-}$ = 1.43 V), were employed as hole donors. Guanosine, inosine, deazaguanosine, and 8-oxoguanosine were used as the hole

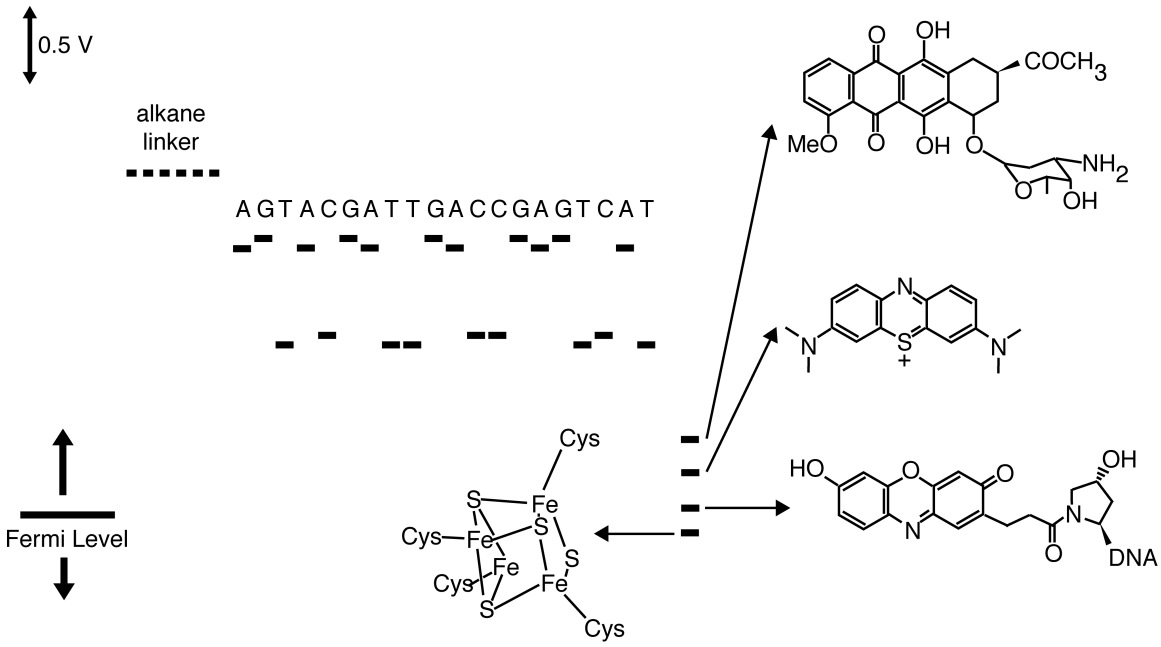

Figure 1.7. Scale diagram describing the relevant potentials for DNA-mediated CT through DNA self-assembled monolayers on gold. The potentials of the individual nucleotides are not accessible within the window of electrochemistry of DNA monolayers on Au. Nevertheless, facile DNA-mediated electrochemistry is observed for redox probes over DNA bridges. For all probes and sequences of well-matched duplexes, the tunneling through the alkane linker is rate limiting (~30 s^{-1}). Shown, in order from top, are daunomycin, methylene blue, Redmond Red, and a [4Fe-4S] cluster similar to those in the redox-active repair proteins EndoIII and MutY.

acceptors, either immediately adjacent to the bridging dye, or separated by a bridge of two A-T base pairs. The measured charge separation and recombination rates fit well to the Marcus-Levich-Jortner equation, with reorganization energies of 1.2 eV and 1.3 eV respectively (**Figure 1.8**). The agreement is improved if a molecular based model for the solvent is used and the Q-model is employed for the energy surfaces; in this case higher reorganization energies are found.[168] Further experiments varied the bridge length for the St and PA duplexes, and found that the distance dependence increased for greater donor-bridge energy separation.[169]

1.2.8. PROTON-COUPLED ELECTRON TRANSFER

If a participant in electron transfer is also an acid or base, the reduced and oxidized species will often have different pK_A values as well. In this case, it is likely that CT will be coupled to proton transfer.[170] Proton-coupled electron transfer (PCET) may be more the rule than the exception in biological systems. Most redox-active groups in biology are also subject to protonation or deprotonation, with the pK_A dependent on the redox state. Since complete proton transfer is unnecessary for substantial effects on the coupled electron transfer rate, the question is not whether the electron transfer is proton-coupled, but whether the coupling is significant so that proton transfer becomes rate-limiting. In the case of Class I *E. coli* ribonucleotide reductase, PCET has been found to occur over multiple steps.[171-173]

Each nucleotide in the double strand participates in stable hydrogen bonding with its complement in a base pair. Hence, it is not surprising that CT between nucleotides

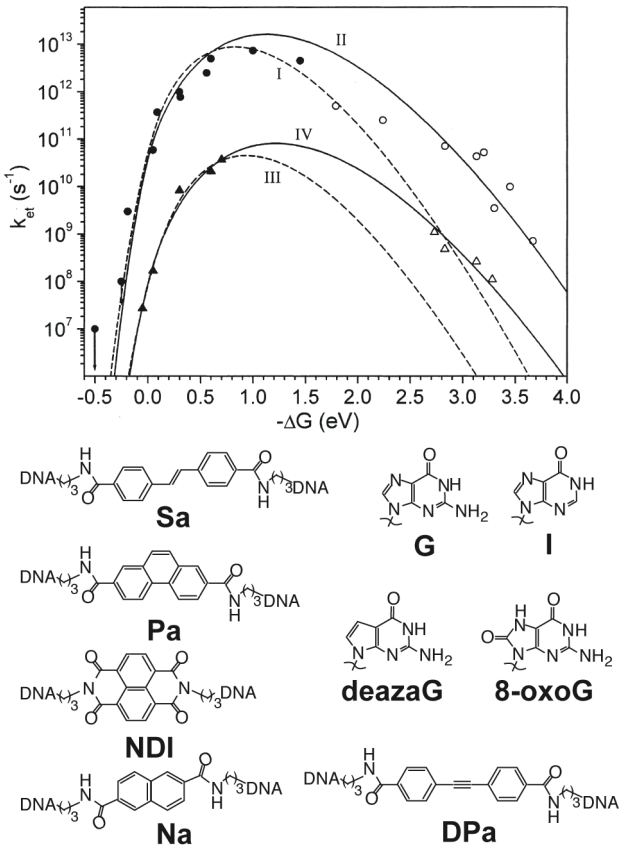

Figure 1.8. The driving force dependence for CT in photooxidant-bridged DNA hairpins is determined from time-resolved transient absorption studies of a series of five stilbene-derived photooxidants and four hole acceptor bases, following both charge separation (filled) and charge recombination (empty). Case I,II (circles): donor and acceptor are in contact. Case III,IV (triangles): donor and acceptor are separated by two TA base pairs. Case I,III are fit only to charge separation rates (dotted), while Case II,IV are fit to both charge separation and charge recombination rates (solid). Similar reorganization energies, about 1 eV for the nuclear reorganization energy and ~0.2 V for the solvent reorganization energy, are found for both Case II and Case IV. Adapted from Reference 167.

should be proton-coupled, although likely in a way that cannot be probed by the usual assay of pH dependence, given that the base-pair protons are excluded from solvent. It has been shown that oxidation of the aqueous, isolated nucleosides by Ap^* is not proton-coupled,[174] but that does not exclude the possibility of PCET in the context of protons in the base pair. Theoretical work predicts that double proton transfer between guanine and cytosine lowers the guanine potential.[175] Indeed, the cytosine radical has been directly observed by transient absorption spectroscopy, after oxidation of DNA by $SeO_3^{\bullet-}$ and $SO_4^{\bullet-}$ ions generated by pulse radiolysis.[176] This might not be general, though, as the mechanism of G-C oxidation in pulse radiolysis is strongly dependent on the chemical interaction with the oxidizing radical.[149,177] Similar evidence for PCET reduction of thymidine base-paired to adenine has also been found.[178]

Furthermore, the pK_A of the guanine cation radical has been measured to be 4, near that of cytosine (4.5),[179] and the neutral guanine radical is observed by nanosecond transient absorption and EPR after oxidation by intercalated Δ-$[Ru(phen)_2(dppz)]^{3+}$,[180,181] supporting deprotonation of the guanine cation radical, presumably to the paired cytosine, on a faster time scale. For DNA ionized by γ-irradiation at 77 K, ESR measurements find that the equilibrium strongly favors the neutral guanine radical over the cation radical; this held for guanine stacked between cytidine and for each guanine of the GGG triplet.[155] Although this evidence strongly supports proton transfer, it does not establish coherent PCET, as proton transfer consequent to oxidation has been shown to be favorable.[182]

Isotope experiments, which would establish whether proton transfer is rate-limiting, have not been straightforward. Certainly, for oxidation by $SO_4^{\bullet-}$ ions, the charge injection yield is decreased in D_2O.[177] In one experiment, deuterium replacement of acid protons led to a three-fold decrease in the relative yield of damage of distal GGG to proximal G sites.[87] In another, CT between Ap(-H)$^\bullet$ and G was found to exhibit a small differential between D_2O and H_2O, consistent with PCET.[183] A similar small differential was observed in some sequences, but not in others, for CT between photoexcited NI and Ptz.[184] However, in the fluorescence experiments, the substitution of D_2O for H_2O also affects excited state lifetimes.

At first, it might seem that the facile oxidation of ^{CP}C in competition with ^{CP}G supports a PCET model.[73] However, ^{CP}C oxidation is *increased* by base-pairing with inosine, a high potential guanine analogue, indicating that PCET is not the mechanism of ^{CP}C oxidation. Instead, this mechanism is enticingly similar to the proposed mechanism for excited state relaxation in GC base pairs,[185,186] which involves proton-coupled exciplex formation and has also received experimental support,[187,188] although it appears that guanine-guanine stacking might prevent this relaxation.[189] Based on this accumulated evidence, it seems likely that PCET is involved in at least some charge injections to guanine, and that neutral guanine radical is the persistent form of injected radical.

1.2.9. Characteristics of DNA CT

It is apparent that DNA mediates CT over long distances, and that the rate and yield are sensitive to both the donor and acceptor identities and to the integrity of the

intervening π-stack. Structural distortion of the DNA, or poor coupling of the donor or acceptor to the DNA, sharply attenuate long-range CT. Furthermore, rapid CT is conformationally gated, and the equilibrium conformation is not necessarily the CT-active conformation.

1.3. DNA-mediated CT Mechanisms

Tautologically, all mechanisms of charge transport incorporate an electron moving from a donor orbital to an acceptor orbital. The variation consists in the identification of orbitals that mediate this transition, and the pathways that are coupled to it. In a large biomolecule, such as DNA, complexity arises from the sheer number of atoms involved. In this section, we will evaluate postulated mechanisms of long-range CT in DNA in the context of the properties discussed above.

1.3.1. Transport through Water, Ions, Phosphates

An obvious source of conductivity in DNA is the highly charged phosphate backbone. Indeed, one of the earliest models of CT through DNA involved transport through the phosphates.[190] A recent measurement of delocalization of a hole produced on a single phosphate lends some credence to this model,[191] although it is unclear whether this delocalization can be transduced into conduction, and comparable measurements have not observed this delocalization.[192] In the phosphate conduction model, phosphates on the edge of the DNA are directly ionized, and the hole rapidly hops through isoenergetic phosphates. For this to occur, coupling between the phosphates must be

substantial. Even more importantly, oxidative damage must preferentially occur at phosphates versus the base stack. Some calculations found that this was the case,[193] but later work demonstrated that this was due to neglecting the presence of water and counterions that can shield the phosphate group's negative charge.[194] Theoretical and experimental work suggests that photoionization is initiated at bases and not at phosphates[195] and that the energies of the ions, phosphates and sugar states are far from the Fermi energy.[196]

Alternatively, the motions of water and ions can lead to apparent conduction. DNA adsorbs several layers of high dielectric water,[42] a primary condensation layer of cations, and a secondary layer of condensed anions. Even under relatively dry conditions, water and cations are still adsorbed. This layer plays a major role in the conformational dynamics of DNA and mediates molecular recognition events with other biomolecules. In particular, it seems certain that early conduction measurements were measuring ionic conduction along the DNA, rather than properties of the DNA molecule itself.[43]

Ultimately, however, it is difficult to rationalize these models with the marked sensitivity of long-range DNA-mediated CT to the integrity of stacking, as described in **Section 1.2**. In contrast, changing the pH, ionic strength, or the identity of the salt has at best a minor effect on CT, as long as well-coupled donors and acceptors are employed. Even the removal of a phosphate along the bridge does not cause a measurable difference in CT yield.[77,78] Adding extra intervening phosphates, via the construction of triplex DNA, actually lowers the competence for CT.[197] Hence, it is apparent that DNA CT must proceed through the base pairs, in the interior of the duplex.

1.3.2. SUPEREXCHANGE

Any medium is a superior pathway for charge transport in comparison to vacuum. Superexchange is coherent orbital-mediated tunneling, where, for electron (hole) transport, the high-energy LUMOs (HOMOs) on the pathway are virtually occupied, allowing a probability and corresponding rate of transmission from the donor to the acceptor. Following the Born-Oppenheimer approximation, the rate of superexchange can be separated into the nuclear factor, υ_n, and an electronic factor, υ_e:

$$k_{CT} = \nu_n \nu_e$$

where

$$\nu_n = exp\left(\frac{(\Delta G + \lambda)^2}{4\pi\lambda RT}\right)$$

and

$$\nu_e = \frac{2\pi}{\hbar\sqrt{4\pi\lambda RT}}\left|H_{DA}^0\right|^2 exp(-\beta d)$$

and ΔG is the driving force, H^0_{DA} is the donor-acceptor coupling extrapolated to zero bridge length, β is a decay parameter characteristic of the bridge, and d is the bridge length. The nuclear factor is a function solely of the identities and the environment of the donor and acceptor. The electronic factor represents the electronic coupling between the donor and acceptor, mediated by the bridge states. In the adiabatic limit, electronic coupling is sufficiently strong such that the nuclear motion will determine the rate of charge transfer. In the non-adiabatic limit, the electronic coupling is sufficiently weak such that the electronic transition probability is less than unity at the transition state.[9]

Hence, long-range (greater than 1 nm) CT systems are generally treated as non-adiabatic, though it has increasingly been recognized that changing the structure of even long bridges can have a non-trivial affect on both ΔG and λ.[7,168,185,198] Ignoring this effect, the only dependence of the rate on donor-acceptor distance is the exponential decay of the donor-acceptor coupling with d, the length of the bridge, characterized by the parameter β. It is important to note that β is generally not what is directly measured in experimental systems. For systems that measure the yield of irreversible chemical products, competing processes such as BET or equilibration will inevitably convolute with the inherent rate of charge separation. Even for very fast charge traps, or spectroscopic based measurements that can directly measure k_{CT}, the exponential drop-off will not necessarily correspond to β if the nuclear factor is itself distance dependent.[199] This restriction can be mitigated for long-range CT, where the iterative changes in the bridge length are unlikely to affect ΔG and λ, but is significant for short-range CT.[7]

Furthermore, it is important to note that calculation of the CT rate requires precise knowledge of the intervening electronic structure, which in turn is dependent on molecular structure. If the mechanism or pathway changes with an increase in bridge length, then the distance dependence will not be well represented by the electronic factor β. Also, conformational dynamics can lead to a time-dependent rate. If the equilibrium structure is the best-coupled structure, dynamics will decrease the apparent CT rate.

Another important consideration is that β is not independent of the bridge and donor energies. For increasing difference between the donor and bridge energies, β increases according to:

$$\beta = \frac{2}{a}\ln\left[\frac{\Delta\varepsilon}{2V} + \sqrt{1+\frac{\Delta\varepsilon^2}{4V^2}}\right]$$

where a is the intersite separation, V is the intersite coupling and $\Delta\varepsilon$ is the donor-bridge energy separation. As this separation decreases to below V, direct injection will successfully compete with tunneling. Hence, if tunneling is occurring, β is limited to about 0.3 $Å^{-1}$ (numerical calculations that properly treat the bridge as finite find about 0.2 $Å^{-1}$).[200] This supports the assignment of extremely shallow distance dependences to incoherent processes; at least it excludes superexchange mediated by orbitals on the individual bases of DNA. This model was supported by experiments in photooxidant capped adenine tract hairpins.[169] The oxidations of guanine by photoexcited Sa and of ^{Z}G by photoexcited phenanthrene-2,7-dicarboxamide are of similar driving force, but the latter pair are 0.25 eV lower in potential than the former pair. For each pair, the rate constants were measured for varying lengths of an intervening adenine tract, and the distance dependence was greater for the PA-^{Z}G pair.

Superexchange has been most thoroughly characterized as a mechanism for CT within and between redox-active proteins; charge-transfer reactions among proteins are essential to all organisms. To a rough approximation, proteins can be treated as a homogeneous medium with a single characteristic β of 0.9 $Å^{-1}$.[201] The scatter for individual proteins, however, spans several orders of magnitude, indicating that the electronic structure and pathways vary strongly with the identity of the protein, and the location of the donor and acceptor.[202] For some pathways in proteins, conformational dynamics have been shown to play an important role in dictating which pathways are

available.[203] It is clear that proteins optimize charge transport not only by controlling donor-acceptor distance and driving force, but by allowing a specific pathway, or combination of pathways, to be available for superexchange. An essential lesson from superexchange in proteins is that the most facile pathways determine the overall rate and yield. Although DNA might appear to be a simple one-dimensional system, owing to the extensive π-stacking, experiments suggest a more complicated system.

1.3.2.1. COUPLING CONSTANTS IN DNA

No model of superexchange can be properly constructed without first considering appropriate values for the coupling constants along the bridge.[204] Given the structural complexity, non-trivial assumptions are necessary to allow tractable calculations, each of which have certain disadvantages. Furthermore, the stacking interaction of bases is a particularly challenging one to computationally describe.[205] It is important to consider these couplings when developing a theoretical model. For example, a two-stranded model[206] for coherent DNA-mediated CT was recently published to fit the results of work[207] by Giese and coworkers. The model was only able to fit the data by taking intrastrand AA coupling to be 0.52 eV, nearly an order of magnitude greater than the time-averaged value found in typical calculations.[208,209] The average couplings appear to be about 80 meV for intrastrand GG, with somewhat lower intrastrand coupling between AA, and smaller values for interstrand purine-purine couplings.

Increasingly, it has been clear that couplings are highly dependent upon the geometry of the stacked bases. An early demonstration of this concept was the calculation

of coupling constants between base pairs for coordinates drawn for a large family of crystallized duplexes.[210] Even though this measurement was only for coordinates from a set of crystals, each of which presumably corresponds to an equilibrium conformation, variations in couplings were on the order of half of the values. In addition to this static disorder, DNA is subject to extensive dynamic disorder on a full spectrum of time-scales. A later study considered fluctuations from equilibrium conformations, using MD simulations to access the transient structures (**Figure 1.9**).[211] This study found even larger variations in coupling, and found that H_{DA} for GAAAAG varied by more than an order of magnitude over the course of the 40 ps simulation. Interestingly, they also found that transverse base motions, which affect stacking, are more significant than longitudinal motions; this is consistent with recent work that found that shear, twist, and stretching within base-pairs also affects coupling constants.[212] They also found that peaks in coupling over the bridge were more significant for GAAAAG than GTTTTG and nearly absent in GATATG, in accordance with measured CT yields. Since then, similarly large fluctuation-dependent variations have been found using a variety of computational approaches,[49,208,213,214] with fluctuations being most significant on the picosecond time-scale.[213] These studies have demonstrated that conformation also has a profound effect on the transient nucleobase energies, as does solvent polarization.[215] Interestingly, calculations indicated that base energies tend to be correlated in the duplex,[182] although the relative ordering of base energies is preserved.[208] These results offer a natural explanation for the conformational gating that has been observed in long-range systems.

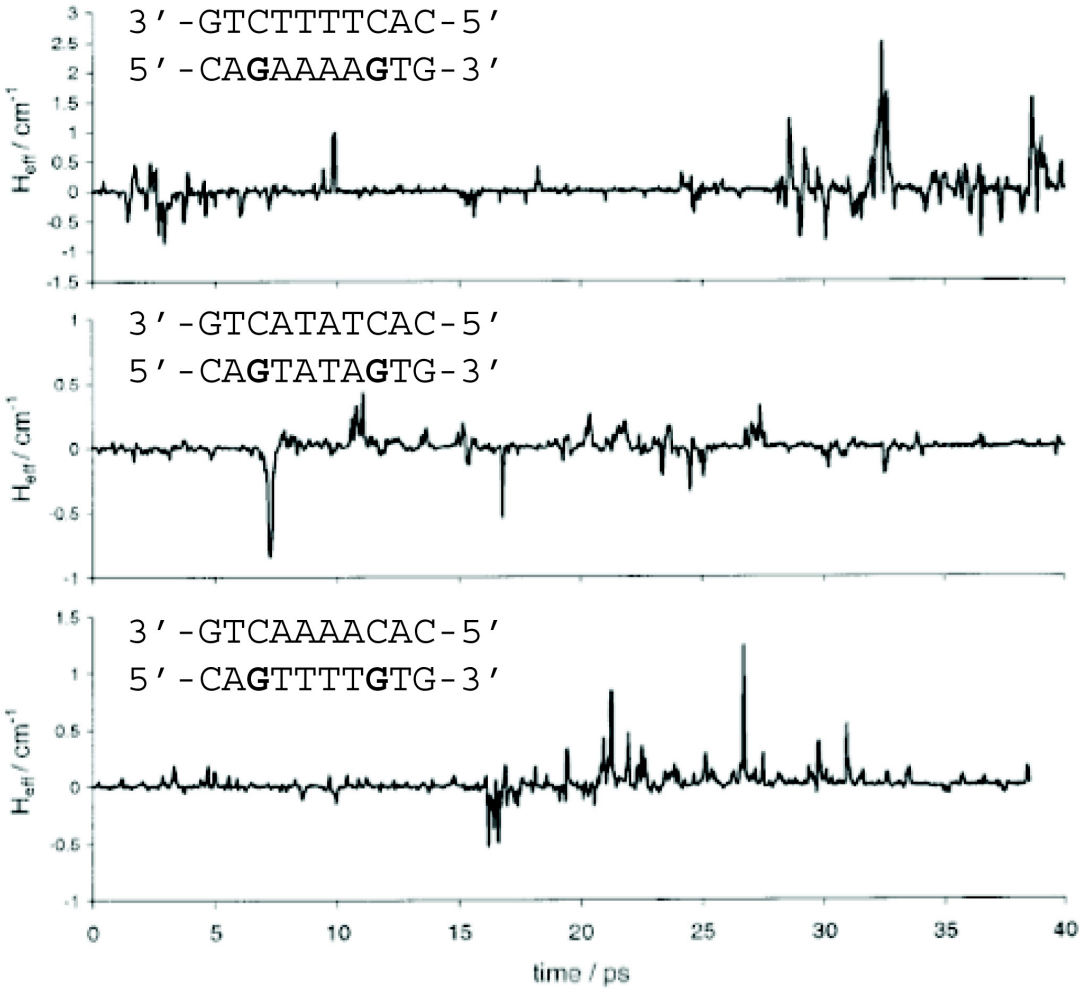

Figure 1.9. The time-dependent couplings between guanines separated by three different four-base sequence contexts, based on conformations generated through molecular dynamics. It is clear that the average value of coupling can be several orders of magnitude lower than the maximum coupling. For the poorly stacked, flexible ATAT sequence, strong coupling between the guanines is not achieved over the time-scale of the simulation. Adapted from Reference 211.

1.3.2.2 REORGANIZATION ENERGY

Given the excellent correlation of theory and experiment for the driving-force dependence of CT in stilbene-capped hairpins,[167] the reorganization energy for those systems is certainly close to 1 eV. For systems where the donor and acceptor are internal to the π-stack, as with intercalators, it is less clear, as these sites are far less solvent exposed than the end-capped agents, such as Sa, Ptz, AQ, and napthalimide (NI).

Even for transfers between sites in DNA, the reorganization energy can vary substantially. Sequence context, which affects couplings and site energies, is expected to affect reorganization energy as well. Delocalization among multiple bases, which decreases the effective amount of charge that must be transferred, lowers the reorganization energy.[216] One study found, by sampling many molecular dynamics configurations of oligopurine•oligopyrimidine DNA, reorganization energy for nearest neighbor hops to be about 1.1 eV for both adenine to adenine and for guanine to guanine.[49] Another study estimated 0.5 eV for adenine to adenine based on the spectral density of intercalated ethidium bromide.[217]

It has been found that for short-range CT in DNA, changes in bridge length can induce substantial changes in the reorganization energies.[7,118] This finding is consistent with Marcus' classical description of the solvent reorganization energy:

$$\lambda_s = \frac{\Delta q^2}{2}\left(\frac{1}{a_D} + \frac{1}{a_A} - \frac{2}{R_{DA}}\right)\left(\frac{1}{\varepsilon^{op}} - \frac{1}{\varepsilon^{st}}\right)$$

where Δq is the change in charge, a_D and a_A are the donor and acceptor radii respectively, and ε^{op} and ε^{st} are the optical and static dielectric constants, λ explicitly depends on the

donor-acceptor separation.[9] An indirect length dependence of λ will also be incorporated through the effect of molecular structure on the dielectric.

1.3.2.3. SUPEREXCHANGE IN DNA

Long-range charge transport over more than 50 Å seems incompatible with superexchange, given its inherently strong distance dependence. Even a β of 0.1 $Å^{-1}$ implies a loss of over eight orders of magnitude in rate over 200 Å. However, most long-range measurements either neglect yield[122,159] or measure products formed on long time scales.[3] In the former case, long-range transport can reflect a small yield, while in the latter case, products might be formed only on the time scale of milliseconds to seconds. Fluorescence quenching of photoexcited 2-aminopurine by guanine 35 Å away[54] has shown that long-range CT can occur on a time scale that is defined by the nanosecond lifetime of the 2-aminopurine excited state. Furthermore, the distance-independent decomposition of ^{CP}A by photoexcited $[Rh(phi)_2(bpy')]^{3+}$ over 40 Å[17] (**Figure 1.10**) demonstrates that CT occurs at high yield at least as fast as BET between oxidized adenine and $[Rh(phi)_2(bpy')]^{2+}$; the energetically similar reduction of $[Rh(phi)_2(phen')]^{3+}$ by $[Ru(phen')_2dppz]^{2+}$ over 41 Å is faster than 3 nanoseconds.[1] Hence, it is clear that DNA CT can occur over long distances on relatively short time scales, and any model must account for this. For these reasons, superexchange models are not satisfactory for DNA-mediated CT over long distances.

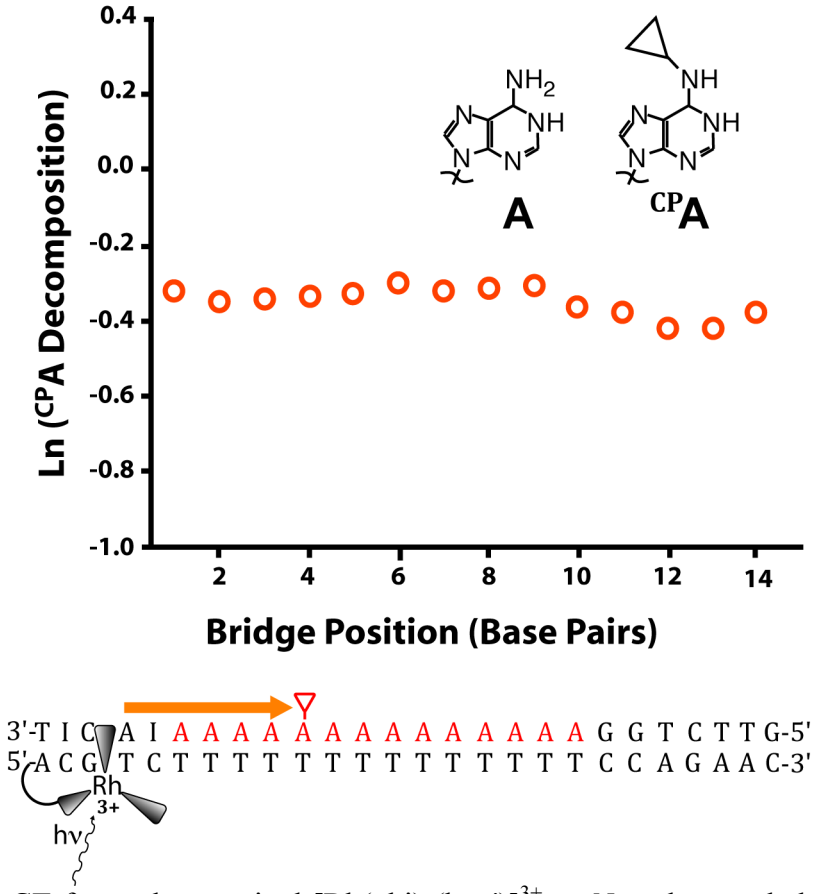

Figure 1.10. CT from photoexcited $[Rh(phi)_2(bpy')]^{3+}$ to *N*-cyclopropyladenosine (^{CP}A) across an adenine tract is distance-independent over 14 adenines. The rate of CT across the adenine tract, then, must be much faster than BET from the first adenine to the reduced rhodium. The driving force for recombination is only about 1.7 V, implying that BET should not be in the inverted region, consistent with evidence that BET from adenine to this rhodium complex is facile.[68] The lack of distance-dependence, in a system with a rapid competing process in BET and a charge trap that samples pre-equilibrium CT dynamics, implies extensive delocalization across the bridge. Adapted from Reference 17.

1.3.3. LOCALIZED HOPPING

The apparent contrast between theory and experiment led to extraordinary efforts to challenge the validity of the measured CT rates and yields. Hopping models offer an alternative that does not require exceptional coupling between bridge sites. Hopping, a type of diffusive, incoherent transport, is the concatenation of multiple superexchange steps, or "hops", in which charge occupies the bridge between each hop. Hopping has been proven as a mechanism in both natural[171] and synthetic[218] protein models. The distance dependence of hopping is geometric, and hence shallower than the distance dependence of superexchange.[202,219] The reason for the shallower distance dependence is intuitive; long, slow, superexchange steps are avoided.

1.3.3.1. NEAREST-NEIGHBOR MODELS

Although formal ballistic models do not distinguish superexchange from hopping, it is most straightforward to treat hopping as a multi-step process. In this case, an injected charge resides on the lowest potential base, guanine. This charge can diffusively migrate along the DNA, mediated by short single-step superexchange with neighboring guanines.[219] The rate of a hop will depend on the distance and sequence context. The fastest hop will be to neighboring guanine; hops through other nucleotides (e.g. GAG, GCG, or GTG) will be slower. For the case of GCG, hopping is also allowed to the guanine on the complementary strand ($G^+CG/CGC \rightarrow GCG/CG^+C \rightarrow GCG^+/CGC$).

The most impressive evidence in support of this model is a series of photooxidation experiments by the Majima group, and a series of STM conduction

experiments performed by the Tao group.[45] Using an elegant experimental setup,[220] they form unambiguously covalent contacts to single DNA molecules under aqueous conditions. They found a geometric dependence of the conductance on length for $(GC)_n$ sequences, but insertion of an $(AT)_m$ sequence into the $(GC)_n$ sequence led to an exponential decrease of the conductance with the length of the $(AT)_m$ sequence, as predicted by the hopping model. However, they did not investigate sequences that allowed purine-purine stacking, and were unable to find evidence for thermal activation,[221] although this was possibly due to the limited window of temperatures and potentials that allowed device stability. Calculations on averaged structures confirm that the alternating purine-pyrimidine sequence attenuates delocalization for this system and reproduce the data well.[222] Furthermore, more recent experiments using the same system[223] and a similar approach using a mechanical break junction[224] found a much smaller effect on conduction from increasing AT content. This was ascribed to the latter experiments being performed with DNA that was more likely to form the B-conformation versus the $(GC)_n$ sequences. For DNA covalently bridging a carbon nanotube gap, there appears to be no sequence dependence when the GC content of random sequence DNA is varied.[225]

Majima and colleagues have used transient absorption to study the oxidation of Ptz by photoexcited NI, linked by varying sequences of DNA.[4] The sequences near the hole acceptors and donors were kept constant, and a central region varied with $(GA)_n$ or $(GT)_n$; complementary studies separated the donor and acceptor by only adenines.[226,227] Each system fits well to a geometric dependence of rate on bridge length. They found the

rate of hopping to be $2x10^{10}$ s^{-1} for adenine to adenine hopping, $7.6x10^{7}$ s^{-1} for G^{+}-A-G → G-A-G^{+} hopping, and about $2x10^{5}$ s^{-1} for G^{+}-T-G → G-T-G^{+} hopping. Although this is strong evidence for multistep hopping in these systems, they have noted that it does not necessarily require that the intermediate states be completely localized on individual nucleotides.[227] More generally, the researchers were able to distinguish between hole injection and hole arrival, showing that the two are not coincident over long distances. Similar results have been observed for CT between DNA-capping stilbenes, with the transition between single and multistep CT at about two intervening AT base pairs.[125,126]

1.3.3.2. THERMALLY INDUCED HOPPING

Although hopping between guanine sites can explain many features of the propagation of holes in mixed sequences, it is not sufficient to explain facile charge transport through adenine tracts.[228] Occupation of adenines during CT has been demonstrated both by a direct chemical probe[73] and by the observation of facile and weakly distance-dependent transport of holes across long adenine bridges,[17,31,207,229-231] even when BET competes with equilibration.[31] This can be explained by a reasonable modification of the hopping model, whereby a hole on guanine can be thermally excited to occupy an adenine tract.[228,232,233] Although this will be disfavored in the case of mixed-sequence DNA in preference to guanine hopping, it can be much more favorable than the slow hop through a long AT sequence. For isoenergetic adenines, this model does not sufficiently explain the distance independence,[234] but if the adenines on the edge of the tract are higher in potential than the interior adenines, then the apparent yield of CT will

be distance-independent.[235] This explanation, although reasonable for $(A)_n$ bridges on the strand complementary to the guanine sites, does not support the shallow distance dependence observed when the $(A)_n$ bridge is in the same strand,[229,236] for which the edge adenines should be of lower energy versus internal adenines. It would be interesting to determine what effect incorporating the stacking-dependent adenine energetics would have on the theoretical predictions of the thermally induced hopping model.[228]

The most compelling evidence for thermal activation comes from a biochemical trapping assay of $G^+/A_n/GGG$, where the yield of GGG versus G damage was quantified after hole injection from a sugar radical near the single G site.[207] A steep distance dependence for $n \leq 3$ was followed by a flat distance dependence for $n \geq 3$. This is consistent with two mechanisms at play, where the steep distance dependence corresponds to CT through superexchange across the AT bridge, and the flat regime is where superexchange is sufficiently slow for thermally induced hopping across the adenine tract to become the dominant mechanism. It is important to note, however, that this dependence looks identical to that found for the rigid Et^+ base-pair surrogate.[27] In the latter case, the dependence was caused not by a fundamental shift in mechanism, but rather by the rate-limiting injection from the hole donor. Stilbene-capped hairpin systems[125] and AQ-capped duplexes[236] show a similar, though much more gradual, positive second-order change in the slope with distance. As shall be discussed in greater detail below, delocalized mechanisms can also explain facile transport through adenine tracts. Ultimately, a change in slope on its own is not sufficient to justify a crossover in mechanism.[237]

1.3.3.3. VARIABLE-RANGE MODELS

All the mechanisms listed above can be considered together, as components of a variable-range hopping model. Here, a hole is allowed to migrate by superexchange to any other site, rather than being limited to nearest neighbors.[238] The most probable sites will be the closest low-potential sites, i.e. guanines. Hence, the hole will hop from guanine to guanine through the DNA, preferring intrastrand transfer, but able to exploit interstrand transfer or thermally induced hopping onto adenine tracts where the sequence does not allow more favorable pathways. Even unfavorable pathways are possible, although slow. Theoretical treatments using this model have been successful in modeling some biochemical experiments,[239] although it was demonstrated that introducing static disorder substantially degrades the success of variable-range hopping models that rely on localized states (**Figure 1.11**).[217] In turn, dynamic disorder, analogous to the conformational gating discussed above, can assist hopping in a rugged landscape.[113]

One challenge that is common to all localized hopping models is the explanation of the mismatch discrimination that has been observed in nearly every system studied. One proposal was that mismatches allow water access to preferentially quench CT at guanine through proton abstraction or other chemical reaction.[232] This model was supported by the observation that GT mismatches affected distal yield more than AA mismatches, and that methylation of the most acidic residue of a guanine opposite an abasic site restores CT.[87] This model has not stood up to more extensive measurements, however, as AC mismatches attenuate CT more than GT mismatches. It has also been shown that GT mismatches lower the yield of CT by lowering the rate,[4] and GT

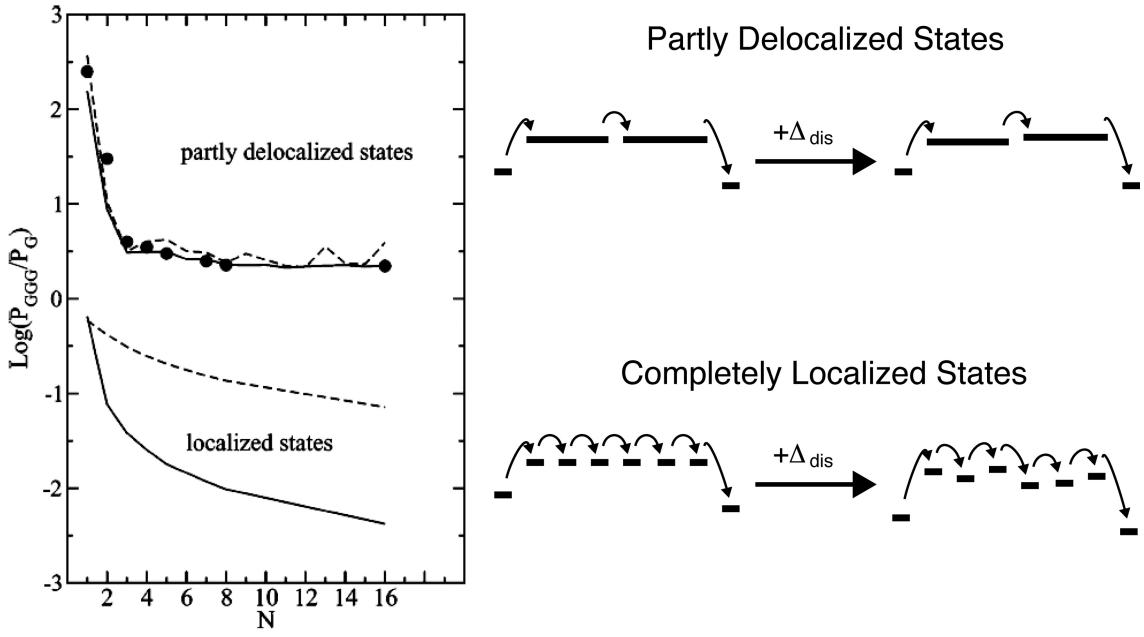

Figure 1.11. The variable-range hopping model predicts a shallow distance dependence for the rate of CT between G and GGG across an adenine tract of the opposing strand. Delocalized states, even in the absence of disorder (dashed lines), yield larger and shallower CT rates due to the smaller reorganization energy, and a shorter effective bridge length. In the presence of static disorder (solid lines), localized hopping is substantially attenuated due to the rugged energy landscape. Delocalized hopping, however, is relatively unaffected by static disorder, as the coupling is strong enough to allow tunneling through local barriers. Adapted from Reference 217, which fit data of Reference 207 using the interbase couplings of Reference 212, which are similar to the most recent calculated values.[208]

mismatches attenuate CT even under applied potentials insufficient for guanine oxidation.[30] Alternatively, mismatched base pairs might have lower couplings to the neighboring bases than matched pairs.[62] Particularly, they are less stacked, and sample more unstacked configurations. A similar argument can then be made to explain how DNA-binding proteins that bend the π-stack also attenuate CT.

A more profound problem with localized hopping models is the apparent "memory" that a charge has of the energy of the state from which it was injected. The intermediate in a localized hopping model is the cation or neutral radical on guanine or adenine. Oxidation of cytidine or thymidine by these species is taken to be highly unfavorable. Hence, the energy of injected charge should not affect the nature of the intermediate over long distances. This is not consistent with the evidence from thymine dimer[159] or ^{CP}C[75,76] oxidation, where oxidants competent for guanine oxidation, but not pyrimidine oxidation, were unable to decompose these species over long distance. Oxidants that are competent for thymine dimer repair or ^{CP}C decomposition, however, remain competent to decompose these oxidation reporters even with intervening low-energy guanines. For an extended $(A)_{20}$ bridge separating Ptz and photoexcited NI, central double guanine does attenuate CT yield by about half, indicating that over a very long piece of DNA relaxation of the cation does occur.[227]

Localized hopping is also inconsistent with electrochemical measurements, where the Fermi level is maintained up to a volt below the potentials of the bases.[58,88,164,240,241] Consider as an example where the electrode is at the potential of an [4Fe-4S]-containing protein (0.1 V), and injection is into cytidine (~ -1 V),[144,174] the most readily reduced

base, for an unfavorable driving force of at least 1.0 V. Although the coupling between cytidine and the metal is mediated by a long saturated linker, and hence will be small, let the coupling correspond to a generous value for two stacked bases, $H_{DA} \sim 0.2$ eV, and take the reorganization energy as being 0.5 V. According to a simple nonadiabatic Marcus-derived expression,[116,242] the injection rate is no greater than 0.002 s^{-1}; for realistic values for the molecule-metal coupling this injection rate would necessarily be far lower. This is slower than the linker-limited rate found through DNA of about 30 s^{-1}.[18,240] Effectively, this discrepancy reflects the inherent unfavorability of thermal activation far from the bridge potential.

1.3.4. Delocalized Mechanisms

The models discussed so far each assume localization of a hole on a single base. Although the couplings between bases might be expected to allow delocalization, disorder in the bath should rapidly localize charges onto a single site as long as reorganization energy is greater than interbase coupling. However, there is some experimental evidence for delocalization of charges, such as the effect of stacking interactions on the pK_A of the adenine cation radical,[243] or the competition of ^{CP}C with ^{CP}G for oxidation.[76] It has also been demonstrated that static disorder attenuates rapid hopping by creating low potential bottlenecks.[238] This can be alleviated by allowing delocalization of the charge; in this case, static disorder is partially averaged.[217,244] In conjuction with the known role of conformational gating, the obvious candidate for the delocalized state is the polaron.[245,246]

1.3.4.1. Polaron Hopping and Gating Mechanisms

Whenever charge is injected into a molecule, the environment will polarize in response, effectively partially delocalizing the charge and lowering the energy of the system.[247] Since the energy of the polaron is different than that of the purely localized charge, the presence of a polaron will affect the CT behavior of the system, in a way largely dependent on the polaron size. Much as PCET is inevitable for any charge-transfer participant with acidic protons, polaron formation is inevitable whenever CT proceeds with bridge occupation. The essential questions are whether the polarization occurs on a time-scale that can impact the CT process, which relaxation modes will be coupled to the polaron formation, and how much the polaron is stabilized relative to the completely localized state.

At first order, polarization of the environment in response to charge injection does not violate the tight-binding assumption. In this case, although DNA conformation, ion distribution, and water orientation all restructure as a result of charge migration, the effect on CT efficiency and rate will be *via* a change in the site energies on the bases, and gated by the time-scale of environmental polarization. It is important to note that small polaron formation slows charge migration, as the site energy is lowered, and hence the activation energy of each hop is increased; this leads to dynamic disorder, distinct from the static disorder discussed above. The exception is if the polaron can move by drift, where the orbitals of the donor and acceptor states overlap, so that CT occurs in the adiabatic limit. This results in transport that is faster than hopping, especially as it can be

activationless.[247] However, drift is most rapid between isoenergetic sites, so it is not a likely mechanism in the presence of static disorder, unless gated by conformational fluctuation of site energies.

Any description of polarons must take into account the structural rearrangement that provides the polarization. Lattice motion has been well treated in terms of deformations along the hydrogen bonds between the base pairs.[248-250] This treatment is particularly instructive regarding the effect of increased coupling between the lattice motion and the charge; high coupling implies a higher activation energy for individual hops and a higher probability for trapping. Hence, thermal activation is taken as evidence for small polaron trapping. There have been contradictory results on the temperature dependence of CT in conductivity measurements,[23,221] though photooxidation studies have unambiguously shown an increase in long-range CT rate[184] and yield[54,68] with temperature. Whether this temperature dependence is due to conformational gating, small polaron activation, or activation of localized hopping is not immediately obvious. Ultimately, the distinction between these cases is not sharp. Conformational dynamics influence bridge energy, and hence the activation energy for polaron drift. Calculations suggest that ion fluctuations, in particular, could sufficiently modulate the potential of a bridging sequence of DNA to permit polaron equilibration between two sites.[50] Given the ambiguity in experiments where counterion identity and concentration have been varied,[51-54] water re-orientation is more likely than ion motion to gate polaron formation.

Sufficient polarization of the environment will lead to formation of a large polaron. In this case, the polarization distortion extends far beyond the lattice site, i.e. the

individual base (**Figure 1.12**). Polarization over a large range must involve the medium, water. Calculation has supported that these polarons form by water reorientation delocalized over 2 to 5 base pairs, depending on the sequence.[251-252] Large polaron formation can have both positive and negative consequences for CT: self-trapping can decrease the rate of individual hopping steps, as is the case for small polarons, but delocalization decreases the distance between individual steps. Furthermore, for periodic sequences, drift can substantially increase the rate of individual hops, by lowering the activation energy for incoherent transport.

Critically, polaron drift can explain important features of DNA-mediated CT as discussed in the previous sections. As discussed above, the observed dependences of CT rates and yield on distance across adenine tracts is too shallow to be readily reconciled with thermal activation and localized hopping.[17,125,207,236] Rapid polaron drift across adenine tracts, in concert with inhibition of BET from adenine to guanine due to polaron self-trapping, has been predicted to provide a shallow distance dependence.[253] Furthermore, since the calculated polaron size is ~ 4 adenines, the steep distance dependence that has been found for tracts shorter than this length naturally corresponds to these sequences not supporting polaron formation.

This mechanism is not limited to adenine tracts, as polaron formation is predicted over mixed polypurine sites, with significant population of high-energy pyrimidines.[252,254] This is consistent with the oxidative damage observed at the fast trap ^{CP}C despite the presence of guanine[75] and the preferential damage at thymine in constructs containing only thymine or adenine.[69] As described above, the resulting

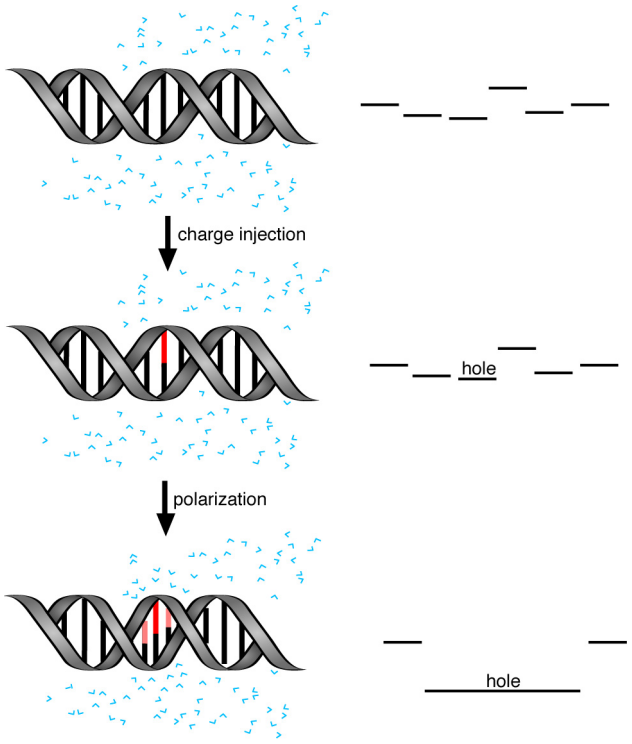

Figure 1.12. Formation of a large polaron. Upon charge injection, a hole is initially localized on a single base (red). Reorientation of the environment, including neighboring bases and the hydration layer, lowers the energy of the hole. Delocalization occurs to the extent that the coupling between the bases balances the unfavorable decrease in the reorganization energy.

delocalization serves as a mechanism for dynamic motions, that allow polaron formation, to alleviate the barrier to CT generated by the static disorder of site energies in DNA, and is consistent with the observed long-range migration of CT through mixed DNA sequences.[3,103] In this model, the effective hopping rates observed by the Majima group could correspond to hops between delocalized polaron sites.[4,226,227]

Physical identification of the polarization medium allows calculation of the polaron properties, particularly the speed limit on polaron migration imposed by the rate of repolarization. For drift along an adenine tract, water reorientation limits polaron mobility to about $3x10^{-3}$ $cm^2/(V\ s)$.[255] This mobility can be related to the conductivity of a single DNA between two carbon nanotubes,[34] where a mixed, aperiodic sequence should decrease the mobility of a polaron. Here, a resistance of about 3 MΩ was observed in a fifteen base-pair duplex. Although the number of charge carriers was unknown, it certainly cannot be less than unity or greater than fifteen, the number of base pairs. Within that range, the mobility is constrained to between 3×10^{-2} $cm^2/(V\ sec)$ and 5×10^{-1} $cm^2/(V\ sec)$. It will be interesting if theoretical evaluation is able to rationalize these values, as they appear inconsistent with polaron drift.

1.3.4.2. DOMAIN DELOCALIZATION

Evidence for delocalization in DNA has come from recent insights into long-lived excited states and exciplexes. It is well known that the individual nucleotides of DNA rapidly relax upon excitation, with a low fluorescence quantum yield.[256] This property is

essential for the molecule of life, as long-lived excited states would render the genetic material prone to photodamage. For mixed sequence DNA as well, relaxation is rapid (subpicosecond to picosecond), but in a manner highly dependent on the specific sequence context.[257] Recently, however, femtosecond studies of purine repeats in both oligonucleotides and duplexes have found much longer lifetimes for ground state recovery,[189] possibly due to exciton or exciplex states. Critically, for B-form DNA, it is base stacking rather than base-pairing interactions that are most critical in achieving long-lived states.[258] The extent of delocalization is still under debate. Although some states might extend over 4 to 8 base pairs,[259,260] others are delocalized over only two base pairs,[261] particularly in single strands. There is some computational support for this delocalization, as well. DFT calculations find that eximers can delocalize over several adenines,[262] and it has been found that fluctuations in the on-site energies of neighboring bases is highly correlated.[214] Recent calculations that incorporate static and dynamic disorder and solvent effects have shown that such transient delocalization can occur over several base pairs.[263]

Despite experimental and computational support for delocalization, as described above, there are profound theoretical arguments against delocalization models in DNA. A variety of computational studies have found that solvent and ion motions will strongly localize injected charge to a single or only a few nucleotides.[152,264,265] Importantly, these studies have mostly been limited to considerations of equilibrated or averaged structures. It will be important to determine whether solvent-induced localization is maintained in the presence of dynamic disorder.

A recent computational study[266] on the dynamics of electric fields produced by DNA, water, and ions was able to reproduce time-resolved Stokes shift data that directly measures those dynamics.[127] This study found no evidence of subpopulations where the DNA had particular electric fields beyond the Gaussian distribution. However, the Gaussian tails could in principle be the very states that mediate CT. All the data suggest that delocalization must be highly transient, and over very long distances, a substantial amount of incoherent hopping will also occur.

Perhaps the most distinctive feature of DNA-mediated CT that has been observed in recent years is the periodic length dependence of CT yield across adenine tracts for some systems (**Figure 1.13**). This dependence was clear, with the same period of 3 to 4 base pairs, for coherent transport from Ap^* to guanine[54] and for total CT from $[Rh(phi)_2(bpy')]^{*3+}$ to ^{CP}G, as will be discussed in Chapter 2.[68] This periodicity was shown to be with respect to adenine tract length, rather than with respect to donor-acceptor distance; by measuring the decomposition of ^{CP}A moved serially along an adenine tract of constant length, no periodicity is observed.[17] For CT from photoexcited AQ to guanine, the periodicity is less apparent, but this is likely due to the quenching of the radical anion of AQ by oxygen, which allows charge equilibration. Interestingly, Ap^* oxidation of ^{CP}G across adenine tracts is smoothly monotonic, but separating the Ap^* from the adenine tract with three inosines restores the periodicity. Clearly, the rapid BET associated with Ap^* allows duplexes that are well suited to forward transport also to better mediate BET, suppressing the periodicity. It should be noted that the inosine tract is a high potential barrier to oxidation by Ap.[120] It lowers both forward CT and BET, but

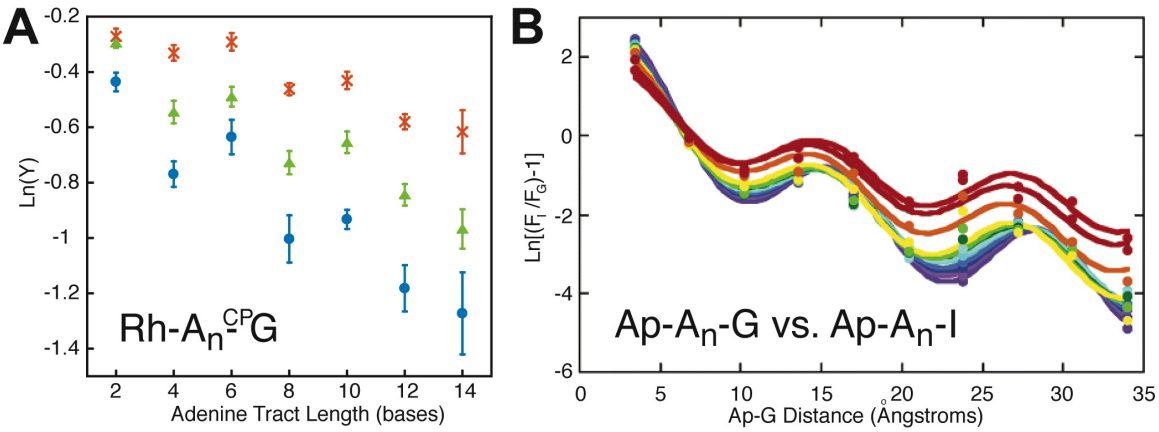

Figure 1.13. Equivalent periodicities with the same period and temperature dependence are observed for (B) the single-step oxidation of guanine by Ap^{*} and (A) the total oxidation of ^{CP}G by photoexcited $[Rh(phi)_2(bpy')]^{3+}$. Temperature increases from purple to red. Errors are given in (A) as 90% SEM.[54,68] Adapted from References 54 and 68.

since the former competes with the nanosecond Ap^* fluorescence lifetime, and the latter competes with picosecond ring opening, BET should be comparatively more attenuated. With BET suppressed, periodicity is again apparent.

A periodic A-tract dependence indicates that some adenine tract lengths mediate CT superior to others. Based on our experiments, this length is about three or four base pairs. In light of the extensive evidence for delocalization cited above, we characterize this CT-active tract as a delocalized domain. The role of conformational gating, then, is to generate this CT-active state. An adenine tract length that allows an integer number of these states allows facile CT; transport across other tracts requires dephasing processes, such as drift or hopping. Because these domains are, by their nature, transient, these effects will only be seen in experiments where the donor and acceptor are well-coupled to the bridge, and where injection and arrival can be observed on a fast time scale, decoupled from other pathways, such as BET. Critically, domain delocalization readily explains the facile competition between ^{CP}C and ^{CP}G,[74] and the ability of DNA to mediate CT far below the base potentials.[161,164]

1.4. SUMMARY

It is clear that DNA, when adequately coupled between the donor and acceptor, can competently mediate CT over long distances. This property is dependent on, and hence diagnostic of, the integrity of base stacking. Furthermore, long-range DNA-mediated CT is thermally activated in a manner dependent on the dynamical stacking of the bridge, indicating that conformational gating is convoluted with the CT rate.

Theoretically, CT over long molecular distances cannot be assigned to superexchange. Incoherent transport must play a role, although evidence does support coherent transport over at least 30 Å in some systems. Assigning the intermediates as guanine cation radicals in the context of a variable-range hopping model is sufficient to explain some gross features of DNA-mediated CT, but this model cannot explain long-range coherence. Transient delocalization plays an important role, at least with some sequences. Identifying the extent to which delocalization occurs, including *via* polaron formation, will be particularly important for understanding DNA CT mediated at potentials below those of the individual nucleotides.

Any model for DNA CT must consider the effects of static and dynamic disorder. For most models, static disorder attenuates long-range CT. Since DNA has many sources of static disorder in the site energies, inter-site couplings, and reorganization energies, it is unlikely that calculations performed on uniform ideal structures with a single repeating base pair will be relevant to understanding experimental results. On the other hand, dynamic disorder has the potential to alleviate the challenge posed by static disorder, by allowing transient structures to form with less rugged energetic landscapes. As long as the equilibrium conformation is not the most CT-active conformation, this condition will hold for most pathways, whether incoherent or coherent. Computational studies have begun to appear that consider what CT-active states look like;[267] it will be a challenge to experimentalists to evaluate these exciting predictions.

CT between a donor and acceptor will always proceed through the fastest pathways available. In a dynamic, structurally complex molecule like DNA, multiple

time scales describe the energetic and coupling landscapes, and hence there will be a time-dependent ensemble of pathways. This ensemble is even larger when delocalized states are allowed, whether they are transiently formed prior to, concurrently with, or after charge injection. For conditions that deplete available pathways, whether through rigidifying the duplex, disrupting donor and acceptor coupling to the bridge, or by introducing structural distortion, slower CT and conduction will inevitably result.

In this context, correlating the distance dependence to the β value of the electronic factor of the CT rate equation requires a high level of experimental support. It is unlikely that any of the measured distance dependences correspond to the distance dependence of the purely electronic component of CT through DNA. Nevertheless, the effective distance dependence over long distances compares favorably with common molecular wires such as oligophenylenevinylene and oligophenyleneethynylene, indicating a promising role for DNA in molecular electronics.

1.5. UNANSWERED QUESTIONS

It should be clear from this chapter that DNA-mediated CT does not pose a challenge to the fundamental theories of electron and hole transport. Ultimately, charge-transfer events only occur with the rates predicted by Marcus' theory. For a molecule as large and complicated as DNA, however, the parameters for the Marcus equation are not trivial to determine. Each conformation of a given DNA offers many pathways, and the extent of dynamical disorder can lead to the failure of the Condon approximation. Furthermore, in the context of hopping and drift, the nature of the states that mediate

charge transport vary with sequence and sequence-dependent dynamics. What these states are: localized radical cations, localized neutral radicals, large polarons, delocalized domains, or a combination, will be different based on the properties of the specific donor, DNA bridge, and acceptor. Understanding what conditions lead to what mechanism of transport is important, as the physical nature of charge injection and migration in DNA undoubtedly influences CT between DNA and redox-active DNA-binding proteins,[5,17,93,94] and the cellular defense against oxidizing radicals.[105,268-271]

Particular experiments that require more attention by theorists are the electrochemical experiments in DNA films. In these experiments, the Fermi level is held to potentials far from those of the bridge states, and yet many of the same properties are observed here as are observed in solution and device experiments that are at profoundly different energies. Insight into this process will undoubtedly also help elucidate DNA-mediated CT in general.

Ultimately, single-molecule conductivity experiments have the most potential for determining details of DNA-mediated CT, due to the strong control of driving force and online measurement of current. The main challenges for these experiments is maintaining the DNA in its native structure, and establishing that the observed current is, in fact, due to the DNA. These can be easily determined by the proper choice of controls.

If the past fifteen years of DNA-mediated CT are any indication, the synergy between the applications of DNA in devices and biology, and theoretical and experimental efforts to elucidate the mechanism, will continue to advance both areas of

study. Certainly, bringing these different perspectives together offers both a challenge and an opportunity.

1.6. REFERENCES

(1) Murphy, C.J.; Arkin, M.R.; Jenkins, Y.; Ghatlia, N.D.; Bossmann, S.H.; Turro, N.J.; Barton, J.K. *Science* **1993**, *262*, 1025.

(2) Murphy, C.J.; Arkin, M.R.; Ghatlia, N.D.; Bossman, S.H.; Turro, N.J.; Barton, J.K. *Proc. Natl. Acad. Sci. U.S.A.* **1994**, *91*, 5315.

(3) Nuñez, M.E.; Hall, D.B.; Barton, J.K. *Chem. Biol.* **1999**, *6*, 85.

(4) Takada, T.; Kawai, K.; Fujitsuka, M.; Majima, T. *Proc. Natl. Acad. Sci. U.S.A.* **2004**, *101*, 14002.

(5) Lee, P.E.; Demple, B.; Barton, J.K. *Proc. Natl. Acad. Sci. U.S.A.* **2009**, *106*, 13164.

(6) Osakada, Y.; Kawai, K.; Fujitsuka, M.; Majima, T. *Proc. Natl. Acad. Sci. U.S.A.* **2006**, *103*, 18072.

(7) Davis, W.B.; Hess, S.; Naydenova, I.; Haselsberger, R.; Ogrodnik, A.; Newton, M.D.; Michel-Beyerle, M.-E. *J. Am. Chem. Soc.* **2002**, *124*, 2422.

(8) von Feilitszch, T.; Tuma, J.; Neubauer, H.; Verdier, L.; Haselsberger, R.; Feick, R.; Gurzadyan, G.; Voityuk, A.A.; Griesinger, C.; Michel-Beyerle, M.E. *J. Phys. Chem. B* **2008**, *112*, 973.

(9) Marcus, R.A.; Sutin, N. *Biochim. Biophys. Acta* **1985**, *811*, 265.

(10) Turro, N.J.; Barton, J.K. *J. Biol. Inorg. Chem.* **1998**, *3*, 201.

(11) Endres, R.G.; Cox, D.L.; Singh, R.R.P. *Rev. Mod. Phys.* **2004**, *76*, 195.

(12) Chen, F.; Hihath, J.; Huang, Z.; Li, X.; Tao, N.J. *Annu. Rev. Phys. Chem.* **2007**, *58*, 535.

(13) Müller, K.-H. *Phys. Rev. B* **2006**, *73*, 045403.

(14) Kelley, S. O.; Barton, J. K. *Science* **1999**, *283*, 375.

(15) Delaney, S.; Pascaly, M.; Bhattacharya, P.K.; Han, K.; Barton, J.K. *Inorg. Chem.* **2002**, *41*, 1966.

(16) Tada, T.; Kondo, M.; Yoshizawa, K. *ChemPhysChem* **2003**, *4*, 1256.

(17) Augustyn, K.E.; Genereux, J.C.; Barton, J.K. *Angew. Chem. Int. Ed.* **2007**, *46*, 5731.

(18) Gorodetsky, A.A.; Green, O.; Yavin, E.; Barton, J.K. *Bioconjugate Chem.* **2007**, *18*, 1434.

(19) Fink, H.W.; Schoenberger, C. *Nature* **1999**, *398*, 407.

(20) de Pablo, P.J.; Moreno-Herrero, F.; Colchero, J.; Gómez Herrero, J.; Herrero, P.; Baró, A.M.; Ordejón, P.; Soler, J.M.; Artacho, E. *Phys. Rev. Lett.* **2000**, *85*, 4992.

(21) Kasumov, A.Yu.; Kociak, M.; Guéron, S.; Reulet, B.; Volkov, V.T.; Klinov, D.V.; Bouchiat, H. *Science* **2001** *291* 280.

(22) Storm, A.J.; van Noort, J.; de Vries, S.; Dekker, C. *Appl. Phys. Lett.* **2001**, *79*, 3881.

(23) Yoo, K.-H.; Ha, D.H.; Lee, J.-O.; Park, J.W.; Kim, J.; Kim, J.J.; Lee, H.-Y.; Kawai, T.; Choi, H.Y. *Phys. Rev. Lett.* **2001**, *87*, 198102.

(24) Odom, D.T.; Dill, E.A.; Barton, J.K. *Chem. Biol.* **2000**, *7*, 475.

(25) Schuster, G. B., Ed. *Long-Range Charge Transfer in DNA, I and II;* Springer: New York, **2004**; Vols. 236, 237.

(26) Wagenknecht, H. A., Ed. *Charge Transfer in DNA*; Wiley-VCH: Weinheim, **2005**.

(27) Valis, L.; Wang, Q.; Raytchev, M.; Buchvarov, I.; Wagenknecht, H.-A.; Fiebig, T. *Proc. Natl. Acad. Sci. U.S.A.* **2006** *103*, 10192.

(28) Meade, T.J.; Kayyem, J.F. *Angew. Chem. Int. Ed.* **1995**, *34*, 352.

(29) Lyndon Pittman, T.; Miao, W. *J. Phys. Chem. C* **2008** *112*, 16999.

(30) Boon, E.M.; Jackson, N.M.; Wrightman, M.D.; Kelley, S.O.; Hill, M.G.; Barton, J.K. *J. Phys. Chem. B* **2003**, *107*, 11805.

(31) Drummond, T.G.; Hill, M.G.; Barton, J.K. *J. Am. Chem. Soc.* **2004,** *126*, 15010.

(32) Watson, J.D.; Crick, F.H.C. *Nature* **1953**, *171***,** 737.

(33) Watson, J.D.; Crick, F.H.C. *Nature* **1953**, *171*, 964.

(34) Guo, X.; Gorodetsky, A.A.; Hone, J.; Barton, J.K.; Nuckolls, C. *Nat. Nanotech.* **2008**, *3*, 163.

(35) O'Neill, M.A.; Becker, H.C.; Wan, C.; Barton, J.K.; Zewail, A.H. *Angew. Chem. Int. Ed.* **2003**, *42*, 5896.

(36) Melvin, T.; Botchway, S.; Parker, A.W.; O'Neill, P. *J. Chem. Soc., Chem. Commun.* **1995**, *6*, 653.

(37) Cohen, H.; Nogues, C.; Naaman, R.; Porath, D. *Proc. Natl. Acad. Sci. U.S.A.* **2005***, 102,* 11589.

(38) Cohen, H.; Nogues, C.; Ullien, D.; Daube, S.; Naaman, R. ; Porath, D. *Far. Disc.* **2006**, *131*, 367.

(39) Ceres, D.M.; Barton, J.K. *J. Am. Chem. Soc.* **2003**, *125*, 14964.

(40) Boon, E. M.; Ceres, D. M.; Drummond, T. G.; Hill, M. G.; Barton J. K. *Nat. Biotech.* **2000**, *18*, 1096.

(41) Calladine, C.R.; Drew, H.R.; Luisi, B.F.; Travers, A.A., *Understanding DNA: The Molecule and How it Works*, Elsevier Academic Press: San Diego, **2004**, 304.

(42) Pal, S.K.; Zewail, A.H. *Chem. Rev.* **2004**, *104*, 2099.

(43) Yamahata, C.; Collard, D.; Takekawa, T.; Kumemura, M.; Hashiguchi, G.; Fujita, H. *Biophys. J.* **2008**, *94*, 63.

(44) Han Ha, D.; Nham, H.; Yoo, K.-H.; So, H.-m.; Lee, H.-Y.; Kawai, T. *Chem. Phys. Lett.* **2002**, *355*, 405.

(45) Xu, B.; Zhang, P.; Li, X.; Tao, N. *Nano Lett.* **2004**, *4*, 1105.

(46) Nogues, C.; Cohen, S.R.; Daube, S.; Apter, N.; Naaman, R. *J. Phys. Chem. B* **2006**, *110*, 8910.

(47) Xiao, X.; Xu, B.; Tao, N.J. *Nano Lett.* **2004**, *4*, 267.

(48) Boon, E.M.; Barton, J.K. *Bioconjugate Chem.* **2003**, *14*, 1140.

(49) Steinbrecher, T.; Koslowski, T.; Case, D.A. *J. Phys. Chem. B* **2008**, *112*, 16935.

(50) Barnett, R. N.; Cleveland, C. L.; Joy, A.; Landman, U.; Schuster, G. B. *Science* **2001**, *294*, 567.

(51) Williams, T.T.; Odom, D.T.; Barton. J.K. *J. Am. Chem. Soc.* **2000**, *122*, 9048.

(52) Williams, T.T.; Barton, J.K. *J. Am. Chem. Soc.* **2002**, *124*, 1841.

(53) Douki, T.; Angelov, D.; Cadet, J. *J. Am. Chem. Soc.* **2001**, *123*, 11360.

(54) O'Neill, M.A.; Barton, J.K. *J. Am. Chem. Soc.* **2004**, *126*, 11471.

(55) Blaustein, G.S.; Demas, B.; Lewis, F.D.; Burin, A.L. *J. Am. Chem. Soc.* **2009**, *131*, 400.

(56) Abdou, I.M.; Sartor, V.; Cao, H.; Schuster, G.B. *J. Am. Chem. Soc.* **2001**, *123*, 6696.

(57) O'Neill, M.A.; Barton, J.K. *J. Am. Chem. Soc.* **2002**, *124*, 13053.

(58) Boon, E. M.; Salas, J. E.; Barton, J. K. *Nat. Biotech.* **2002**, *20*, 282.

(59) Okamoto, A.; Kamei, T.; Saito, I. *J. Am. Chem. Soc.* **2006**, *128*, 658.

(60) Kelley, S.O.; Barton, J.K. *Chem. Biol.* **1998**, *5*, 413.

(61) Bhattacharya, P. K.; Barton, J. K., *J. Am. Chem. Soc.* **2001**, *123*, 8649.

(62) Osakada, Y.; Kawai, K.; Fujitsuka, M.; Majima, T. *Nuc. Acids Res.* **2008**, *36*, 5562.

(63) Bhattacharya, P.K.; Cha, J.; Barton, J.K. *Nuc. Acids Res.* **2002**, *30*, 4740.

(64) Buzzeo, M.C.; Barton, J.K. *Bioconjugate Chem.* **2008**, *19*, 2110.

(65) Boal, A.K.; Barton, J.K. *Bioconjugate Chem.* **2005**, *16*, 312.

(66) Williams, T.T.; Dohno, C.; Stemp, E.D.A.; Barton, J.K. *J. Am. Chem. Soc.* **2004**, *126*, 8148.

(67) Furrer, E.; Giese, B. *Helv. Chim. Acta* **2003**, *86*, 3623.

(68) Genereux, J.C.; Augustyn, K.E.; Davis, M.L.; Shao, F.; Barton, J.K. *J. Am. Chem. Soc.* **2008**, *130*, 15150.

(69) Joy, A.; Ghosh, A.K.; Schuster, G.B. *J. Am. Chem. Soc.* **2006**, *128*, 5346.

(70) Delaney, S.; Yoo, J.; Stemp, E.D.A.; Barton, J.K. *Proc. Natl. Acad. Sci. U.S.A.* **2004**, *101*, 10511.

(71) Nakatani, K.; Dohno, C.; Saito, I. *J. Am. Chem. Soc.* **2001**, *123*, 9681.

(72) O'Neill, M. A.; Dohno, C.; Barton, J. K. *J. Am. Chem. Soc.* **2004**, *126*, 1316.

(73) Dohno, C.; Ogawa, A.; Nakatani, K.; Saito, I. *J. Am. Chem. Soc.* **2003**, *125*, 10154.

(74) Elias, B.; Genereux, J.C.; Barton, J.K. *Angew. Chem. Int. Ed.* **2008**, *47*, 9067.

(75) Shao, F.; O'Neill, M. A.; Barton, J. K. *Proc. Natl. Acad. Sci. U.S.A.* **2004**, *101*, 17914.

(76) Shao, F.; Augustyn, K. E.; Barton, J. K. *J. Am. Chem. Soc.* **2005**, *127*, 17445.

(77) Liu, T.; Barton, J.K. *J. Am. Chem. Soc.* **2005**, *127*, 10160.

(78) Osakada, Y.; Kawai, K.; Fujitsuka, M.; Majima, T. *Chem. Communications* **2008**, *23*, 2656.

(79) Nakatani, K.; Dohno, C.; Saito, I. *J. Am. Chem. Soc.* **2000**, *122*, 5893.

(80) Kodera, H.; Osakada, Y.; Kawai, K.; Majima, T. *Nat. Chem.* **2009**, *1*, 156.

(81) Okamoto, A.; Nakatani, K.; Saito, I. *J. Am. Chem. Soc.* **2003,** *125*, 5066.

(82) Hunter, W.N.; Brown, T.; Kennard, O. *Nuc. Acids. Res.* **1987**, *15*, 6589.

(83) Hunter, W.N.; Brown, T.; Kneale, G.; Anand, N.N.; Rabinovich, D.; Kennard, O. *J. Biol. Chem.*, **1987**, *262*, 9962.

(84) Kumamoto, S.; Watanabe, M.; Kawakami, N.; Nakamura, M.; Yamanato, K. *Bioconjugate Chem.* **2008**, *19*, 65.

(85) Takada, T.; Fujitsuka, M.; Majima, T. *Proc. Natl. Acad. Sci. U.S.A.* **2007**, *104*, 11179.

(86) Elias, B.; Shao, F.; Barton, J. K. *J. Am. Chem. Soc.* **2008**, *130*, 1152.

(87) Giese, B.; Wessely, S. *Chem. Communications* **2001**, *20*, 2108.

(88) Boal, A. K.; Yavin, E.; Lukianova, O. A.; O'Shea, V. L.; David, S. S.; Barton, J. K. *Biochemistry.* **2005**, *44*, 8397.

(89) Gasper, S.M.; Schuster, G.B. *J. Am. Chem. Soc.* **1997**, *119*, 12762.

(90) Hickerson, R.P.; Prat, F.; Muller, J.G.; Foote, C.S.; Burrows, C.J. *J. Am. Chem. Soc.* **1999**, *121*, 9423.

(91) Drummond, T.G.; Hill, M.G.; Barton, J.K. *Nat. Biotech.* **2003**, *21*, 1192.

(92) Inouye, M.; Ikeda, R.; Takase, M.; Tsuri, T.; Chiba, J. *Proc. Natl. Acad. Sci. U.S.A.* **2005**, *102*, 11606.

(93) Boal, A.K.; Yavin, E.; Barton, J.K. *J. Inorg. Biochem.* **2007**, *101*, 1913.

(94) Gorodetsky, A.A.; Dietrich, L.E.P.; Lee, P.E.; Demple, B.; Newman, D.K.; Barton, J.K. *Proc. Natl. Acad. Sci. U.S.A.* **2008**, *105*, 3684.

(95) Watanabe, S.; Kita, A.; Kobayashi, K.; Miki, K. *Proc. Natl. Acad. Sci. U.S.A.* **2008**, *105*, 4121.

(96) Gorodetsky, A.A.; Ebrahim, A.; Barton, J.K. *J. Am. Chem. Soc.* **2008**, *130*, 2924.

(97) Rajski, S. R.; Barton, J. K., *Biochemistry* **2001**, *40*, 5556.

(98) Nakatani, K.; Dohno, C.; Ogawa, A.; Saito, I. *Chem. Biol.* **2002**, *9*, 361.

(99) Kurbanyan, K.; Nguyen, K.L.; To, P.; Rivas, E.V.; Lueras, A.M.K.; Kosinski, C.; Steryo, M.; González, A.; Mah, D.A.; Stemp, E.D.A. *Biochemistry* **2003**, *42*, 10269.

(100) Perrier S.; Hau, J.; Gasparutto, D.; Cadet, J.; Favier, A.; Ravanat, J.L. *J. Am. Chem. Soc.* **2006**, *128*, 5703.

(101) Cadet, J.; Douki, T.; Ravanat, J.-L. *Acc. Chem. Res.* **2008**, *41*, 1075.

(102) Bjorklund, C.C.; Davis, W.B. *Biochemistry* **2007**, *46*, 10745.

(103) Nuñez, M.E.; Noyes, K.T.; Barton, J.K. *Chem. Biol.* **2002**, *9*, 403.

(104) Nuñez, M.E.; Holmquist, G.P.; Barton, J.K. *Biochemistry* **2001**, *40*, 12465.

(105) Merino, E.J.; Barton, J.K. *Biochemistry* **2008**, *47*, 1511.

(106) Nguyen, K.L.; Steryo, M.; Kurbanyan, K.; Nowitzki, K.M.; Butterfield, S.M.; Ward, S.R.; Stemp, E.D.A. *J. Am. Chem. Soc.* **2000**, *122*, 3585.

(107) Johansen, M.E.; Muller, J.G.; Xu, X.Y.; Burrows, C.J. *Biochemistry* **2005**, *44*, 5660.

(108) Peng, X.; Pigli, Y.Z.; Rice, P.A.; Greenberg, M.M. *J. Am. Chem. Soc.* **2008**, *130*, 12890.

(109) Liu, C.-S. Schuster, G.B. *J. Am. Chem. Soc.* **2003**, *125*, 6098.

(110) Lewis, F.D.; Daublain, P.; Cohen, B.; Vura-Weiss, J.; Shafirovich, V.; Wasielewski, M.R. *J. Am. Chem. Soc.* **2007**, *129*, 15130.

(111) O'Neill, M.A.; Barton, J.K. *Proc. Natl. Acad. Sci U.S.A.* **2002**, *99*, 16543.

(112) Shao, F.; Barton, J.K. *J. Am. Chem. Soc.* **2007**, *129,* 14733.

(113) Grozema, F.C.; Tonzani, S.; Berlin, Y.A.; Schatz, G.C.; Siebbeles, L.D.A.; Ratner, M.A. *J. Am. Chem. Soc.* **2008**, *130*, 5157.

(114) Davis, W.B.; Ratner, M.A.; Wasielewski, M.R. *J. Am. Chem. Soc.* **2001**, *123*, 7877.

(115) Smalley, J.F.; Sachs, S.B.; Chidsey, C.E.D.; Dudek, S.P.; Sikes, H.D.; Creager, S.E.; Yu, C.J.; Feldberg, S.W.; Newton, M.D. *J. Am. Chem. Soc.* **2004**, *126*, 14620.

(116) Newton, M.D.; Smalley, J.F. *Phys. Chem. Chem. Phys.* **2007**, 9, 555.

(117) O'Neill, M. A.; Barton, J. K. *J. Am. Chem. Soc.* **2004**, *126*, 13234.

(118) Siriwong, K.; Voityuk, A.A.; Newton, M.D.; Rösch, N. *J. Phys. Chem. B* **2003**, *107*, 2595.

(119) Kocherzhenko, A.A., Patwardhan, S.; Grozema, F.C.; Anderson, H.L.; Siebbeles, L.D.A. *J. Am. Chem. Soc.* **2009**, *131*, 5522.

(120) Wan, C.Z.; Fiebig, T.; Kelley, S.O.; Treadway, C.R.; Barton, J.K.; Zewail, A.H. *Proc. Natl. Acad. Sci. U.S.A.* **1999**, *96*, 6014.

(121) Kelley, S.O.; Holmlin, R.E.; Stemp, E.D.A.; Barton, J. K. *J. Am. Chem. Soc.* **1997**, *199*, 9861.

(122) Lewis, F.D.; Wu, T.; Xhang, Y.; Letsinger, R.L.; Greenfield, M.R.; Wasielewski, M.R. *Science* **1997**, *277*, 673.

(123) Lewis, F.D.; Wu, T.; Liu, X.; Letsinger, R.L.; Greenfield, S.R.; Miller, S.E.; Wasielewski, M.R. *J. Am. Chem. Soc.* **2000**, *122*, 2889.

(124) Lewis, F.D.; Zhu, H.; Daublain, P.; Fiebig, T.; Raytchev, M.; Wang, Q.; Shafirovich, V. *J. Am. Chem. Soc.* **2006**, *128*, 791.

(125) Lewis, F.D.; Zhu, H.; Daublain, P.; Cohen, B.; Wasielewski, M.R. *Angew. Chem. Int. Ed.* **2006**, *45*, 7982.

(126) Lewis, F.D.; Zhu, H.; Daublain, P.; Sigmund, K.; Fiebig, T.; Raytchev, M.; Wang, Q.; Shafirovich, V. *Photochem. Photobiol. Sciences* **2008**, *7*, 534.

(127) Andreatta, D.; Pérez Lustres, J.L.; Kovalenko, S.A.; Ernsting, N.P.; Murphy, C.J.; Coleman, R.S.; Berg, M.A. *J. Am. Chem. Soc.* **2005**, *127*, 7270.

(128) Dohno, C.; Stemp, E. D. A.; Barton, J. K. *J. Am. Chem. Soc.* **2003**, *125*, 9586.

(129) Armitage, B.; Yu, C.; Devadoss, C.; Schuster, G.B. *J. Am. Chem. Soc.* **1994**, *116*, 9847.

(130) Sanii, L.; Schuster, G.B. *J. Am. Chem. Soc.* **2000**, *122*, 11545.

(131) Vicic, D.A.; Odom, D.T.; Núñez, M.E.; Gianolio, D.A.; McLaughlin, L.W.; Barton, J.K. *J. Am. Chem. Soc.* **2000**, *122*, 8603.

(132) Dotse, A.K.; Boone, E.K.; Schuster, G.B. *J. Am. Chem. Soc.* **2000**, *122*, 6825.

(133) Kawai, K.; Osakada, Y.; Takada, T.; Fujitsuka, M.; Majima, T. *J. Am. Chem. Soc.* **2004**, *126*, 12843.

(134) Kawai, K.; Osakada, Y.; Fujitsuka, M.; Majima, T. *Chem. Eur. J.* **2008**, *14*, 3721.

(135) Kawai, K.; Takada, T.; Nagai, T.; Cai, X.; Sugimoto, A.; Fujitsuka, M. ; Majima, T. *J. Am. Chem. Soc.* **2003**, *125*, 16198.

(136) Kawai, K.; Osakada, Y.; Fujitsuka, M.; Majima, T. *J. Phys. Chem. B* **2008**, *112*, 2144.

(137) Arkin, M.R.; Stemp, E.D.A.; Holmlin, R.E.; Barton, J.K.; Hörmann, A.; Olson, E.J.C.; Barbara, P.F. *Science* **1996**, *273*, 475.

(138) Wan, C.Z.; Fiebig, T.; Schiemann, O.; Barton, J.K., Zewail, A.H. *Proc. Natl. Acad. Sci. U.S.A.* **2000**, *97*, 14052.

(139) Lewis, F.D.; Liu, J.; Zuo, X.; Hayes, R.T.; Wasielewski, M.R. *J. Am. Chem. Soc.* **2003**, *125*, 4850.

(140) Senthilkumar, K.; Grozema, F.C.; Guerra, C.F.; Bilkelhaupt, F.M.; Lewis, F.D.; Berlin, Y.A.; Ratner, M.A.; Siebbeles, L.D.A. *J. Am. Chem. Soc.* **2005**, *127*, 14894.

(141) Santhosh, U.; Schuster, G.B. *J. Am. Chem. Soc.* **2002**, *124*, 10986.

(142) O'Neill, M.A.; Barton, J.K. In *Topics in Current Chemistry*; Schuster, G.B., Ed.; Springer: Berlin, 2004; Vol. 237, p. 67.

(143) Boussicault, F.; Robert, M. *Chem. Rev.* **2008**, *108*, 2622.

(144) Seidel, C.A.M.; Shulz, A.; Sauer, M.H.M. *J. Phys. Chem.* **1996**, *100*, 5541.

(145) Caruso, T.; Carotenuto, M.; Vasca, E.; Peluso, A. *J. Am. Chem. Soc*. **2005**, *127*, 15040.

(146) Sheu, C.; Foote, C.S. *J. Am. Chem. Soc.* **1995**, *117*, 6439.

(147) Thorp, H.H. In *Topics in Current Chemistry*; Schuster, G.B., Ed.; Springer: Berlin, 2004; Vol. 237, p. 159.

(148) Johnston, D.H.; Glasgow, K.C.; Thorp, H.H. *J. Am. Chem. Soc.* **1995**, *117*, 8933.

(149) Shinde, S.S.; Maroz, A.; Hay, M.P.; Anderson, R.F. *J. Am. Chem. Soc.* **2009**, *131,* 5203.

(150) Sistare, M.F.; Codden, S.J.; Heimlich, G.; Thorp, H.H. *J. Am. Chem. Soc.* **2000**, *122*, 4742.

(151) Lewis F.D.; Liu, X.; Hayes, R.T.; Wasielewski, M.R. *J. Am. Chem. Soc.* **2000**, *122*, 12037.

(152) Kurnikov, I.V.; Tong, G.S.M.; Madrid, M.; Beratan, D.N. *J. Phys. Chem. B* **2002**, *106*, 7.

(153) Saito, I.; Takayama, M.; Sugiyama, H.; Nakatani, K. *J. Am. Chem. Soc.* **1995**, *117*, 6406.

(154) Sugiyama, H.; Saito, I. *J. Am. Chem. Soc.* **1996**, *118*, 7063.

(155) Adhikary, A.; Khanduri, D.; Sevilla, M.D. *J. Am. Chem. Soc.* **2009**, *131*, 8614.

(156) Hall, D.B.; Holmlin, R.E.; Barton, J.K. *Nature* **1996**, *382*, 731.

(157) Saito, I.; Nakamura, T.; Nakatani, K.; Yoshioka, Y.; Yamaguchi, K.; Sugiyama, H. *J. Am. Chem. Soc.* **1998**, *120*, 12686.

(158) Voityuk, A.A. ; Jortner, J. ; Bixon, M. ; Rösch, N. *Chem. Phys. Lett.* **2000**, *324*, 430.

(159) Dandliker, P.J. ; Nuñez, M.E. ; Barton, J.K. *Biochemistry* **1998**, *37*, 6491.

(160) Yavin, E.; Stemp, E.D.A.; O'Shea, V.L.; David, S.S.; Barton, J.K. *Proc. Natl. Acad. Sci. U.S.A.* **2006**, *3610.*

(161) Treadway, C.R.; Hill, M.G.; Barton, J.K. *Chem. Phys.* **2002**, *281*, 409.

(162) Anne, A.; Demaille, C. *J. Am. Chem. Soc.* **2008**, *130*, 9822.

(163) Wong, E.L.S.; Gooding, J.J. *Anal. Chem.* **2006** *78*, 2138.

(164) Gorodetsky, A.A.; Buzzeo, M.C.; Barton, J.K. *Bioconjugate Chem.* **2008**, *19*, 2285.

(165) Ikeda, R.; Akaishi, A.; Chiba, J.; Inouye, M. *ChemBioChem* **2007**, *8*, 2219.

(166) Hartwich, G.; Caruana, D.J.; de Lumley-Woodyear, T.; Wu, Y.; Campbell, C.N.; Heller, A. *J. Am. Chem. Soc.* **1999**, *121*, 10803.

(167) Lewis, F.D.; Kalgutkar, R.S.; Wu, Y.; Liu, X.; Liu, J.; Hayes, R.T.; Miller, S.E.; Wasielewski, M.R. *J. Am. Chem. Soc.* **2000**, *122*, 12346.

(168) LeBard, D.N.; Lilichenko, M.; Matyushov, D.V.; Berlin, Y.A.; Ratner, M.A. *J. Phys. Chem. B* **2003**, *107*, 14509.

(169) Lewis, F.D.; Liu, J.; Weigel, W.; Rettig, W.; Kurnikov, I.V.; Beratan, D.N. *Proc. Natl. Acad. Sci. U.S.A.* **2002**, *99*, 12536.

(170) Huynh, M.H.V.; Meyer, T.J. *Chem. Rev.* **2007**, *107*, 5004.

(171) Stubbe, J.; Nocera, D.G.; Yee, C.S.; Chang, M.C.Y. *Chem. Rev.* **2003**, *103*, 2167.

(172) Reece, S.Y.; Hodgkiss, J.M.; Stubbe, J.; Nocera, D.G. *Phil. Trans. R. Soc. B.* **2006**, *361*, 1351.

(173) Seyedsayamdost, M.R.; Yee, C.S.; Reece, S.Y.; Nocera, D.N.; Stubbe, J. *J. Am. Chem. Soc.* **2006**, *128*, 1562.

(174) Fiebig, T.; Wan, C.; Zewail, A.H. *ChemPhysChem* **2002**, *3*, 781.

(175) Gervasio, F.L.; Boero, M.; Parrinello, M. *Angew. Chem. Int. Ed.* **2006**, *45*, 5606.

(176) Anderson, R.F.; Shinde, S.S.; Maroz, A. *J. Am. Chem. Soc.* **2006**, *128*, 15966.

(177) Kobayashi, K.; Yamagami, R.; Tagawa, S. *J. Phys. Chem. B* **2008**, *112*, 10752.

(178) Yamagami, R.; Kobayashi, K.; Tagawa, S. *J. Am. Chem. Soc.* **2008**, *130*, 14772.

(179) Huber, R.; Fiebig, T.; Wagenknecht, H.-A. *Chem. Comm.* **2003**, *15*, 1878.

(180) Stemp, E.D.A.; Arkin, M.; Barton, J.K. *J. Am. Chem. Soc.* **1997**, *119*, 2921.

(181) Schiemann, O.; Turro, N.J.; Barton, J.K. *J. Phys. Chem. B* **2000**, *104*, 7214.

(182) Kumar, A.; Sevilla, M.D. *J. Phys. Chem. B* **2009**, *113*, 11359.

(183) Shafirovich, V.; Dourandin, A.; Geacintov, N.E. *J. Phys. Chem. B* **2001**, *105*, 8431.

(184) Takada, T.; Kawai, K.; Fujitsuka, M.; Majima, T. *Chem. Eur. J.* **2005,** *11*, 3835.

(185) Sobolewski, A.L.; Domcke, W. *Phys. Chem. Chem. Phys.* **2004**, *6*, 2763.

(186) Sobolewski, A.L.; Domcke, W.; Hattig, C. *Proc. Natl. Acad. Sci. U.S.A.* **2005**, *102*, 17903.

(187) Abu-Riziq, A.; Grace, L., Nir, E.; Kabelac, M. ; Hobza, P. ; de Vries, M.S. *Proc. Natl. Acad. Sci. U.S.A.* **2005**, *102*, 20.

(188) Schwalb, N.K.; Temps F. *J. Am. Chem. Soc.* **2007**, *129,* 9272.

(189) Crespo-Hernández, C.E.; de La Harpe, K.; Kohler, B. *J. Am. Chem. Soc.* **2008**, *130*, 10844.

(190) Brillouin, L. in *Horizons in Biochemistry* **1962** ed. M. Kasha and B. Pullman Academic Press: New York City, **1962**, 295.

(191) Sekiguchi, I.-S.; Sekiguchi, T. *Phys. Rev. Lett.* **2007**, *99*, 228102.

(192) Baba, Y.; Sekiguchi, T.; Shimoyama, I.; Hirao, N.; Nath, K.G. *Phys. Rev. B* **2006**, *74*, 205433.

(193) Zakjevskii, V.V.; King, S.J.; Dolgounitcheva, O.; Zakrzewski, V.G.; Ortiz, J.V. *J. Am. Chem. Soc.* **2006**, *128*, 13350.

(194) Close, D.M.; Øhman, K.T. *J. Phys. Chem. A* **2008**, *112*, 11207.

(195) Gabelica, V.; Rosu, F.; Tabarin, T.; Kinet, C.; Rodolphe, A.; Broyer, M.; De Pauw, E.; Dugourd, P. *J. Am. Chem. Soc.* **2007**, *129,* 4706.

(196) Hübsch, A.; Enders, R.G.; Cox, D.L.; Singh, R.R.P. *Phys. Rev. Lett.* **2005**, *94*, 178102.

(197) Haruna, K.-I.; Iida, H.; Tanabe, K.; Nishimoto, S.-I. *Org. Biomolec. Chem.* **2008**, *6*, 1613.

(198) Vladimirov, E.; Ivanova, A.; Rösch, N. *J. Phys. Chem. B* **2009**, *113*, 4425.

(199) Yonemoto, E.H.; Saupe, G.B.; Schmehl, R.H.; Hubig, S.M.; Riley, R.L.; Iverson, B.L.; Mallouk, T.E. *J. Am. Chem. Soc.* **1994**, *116*, 4786.

(200) Berlin, Y.A.; Grozema, F.C.; Siebbeles, L.D.A.; Ratner, M.A. *J. Phys. Chem. C* **2008**, *112*, 10988.

(201) Page, C.C.; Moser, C.C.; Chen, X.; Dutton, P.L. *Nature* **1999**, *402*, 47.

(202) Gray, H.B.; Winkler, J.R. *Q. Rev. Biophys.* **2003**, *36*, 341.

(203) Balabin, I.A.; Beratan, D.N.; Skourtis, S.S. *Phys. Rev. Lett.* **2008**, *101*, 158102.

(204) Rösch, N.; Voityuk, A.A. In *Topics in Current Chemistry*; Schuster, G.B., Ed.; Springer: Berlin, 2004; Vol. 237, p. 37.

(205) Sponer, J.; Riley, K.E.; Hobza, P. *Phys. Chem. Chem. Phys.* **2008**, *10*, 2595.

(206) Wang, X.F.; Chakraborty, T. *Phys. Rev. Lett.* **2006**, *97*, 106602.

(207) Giese, B.; Amaudrut; Köhler, A.-K.; Sporman, M.; Wessely, S. *Nature* **2001**, *412*, 318.

(208) Voityuk, A.A. *J. Chem. Phys.* **2008**, *128*, 115101.

(209) Migliore, A.; Corni, S.; Varsano, D.; Klein, M.L.; Di Felice, R. *J. Phys. Chem. B* **2009**, *113*, 9402.

(210) Troisi, A.; Orlandi, G. *Chem. Phys. Lett.* **2001**, *344*, 509.

(211) Troisi, A.; Orlandi, G. *J. Phys. Chem. B* **2002**, *106*, 2093.

(212) Mallajosyula, S.S.; Gupta, A.; Pati, S.K. *J. Phys. Chem. A* **2009**, *113*, 3955.

(213) Reha, D.; Barford, W.; Harris, S. *Phys. Chem. Chem. Phys.* **2008**, *10*, 5437.

(214) Kubař, T.; Elstner, M.; *J. Phys. Chem. B* **2008**, *112*, 8788.

(215) Bongiorno, A. *J. Phys. Chem. B* **2008**, *112*, 13945.

(216) Kubař, T.; Elstner, M.; *J. Phys. Chem. B* **2009**, *113*, 5653.

(217) Renger, T., Marcus, R. A. *J. Phys. Chem. A* **2003**, *107*, 8404.

(218) Shih, C.; Museth, A.K.; Abrahamsson, M.; Blanco-Rodriguez, A.M.; Di Bilio, A.J.; Sudhamsu, J.; Crane, B.R.; Ronayne, K.L.; Towrie, M.; Vicek, A.; Richards, J.H.; Winkler, J.R.; Gray, H.B. *Science* **2008**, *320*, 1760.

(219) Jorner, J.; Bixon, M.; Langenbacher, T.; Michel-Beyerle, M.E. *Proc. Natl. Acad. Sci U.S.A.* **1998**, *95*, 12759.

(220) Xu, B.; Tao, N. *Science* **2003**, *301*, 1221.

(221) Hihath, J.; Chen, F.; Zhang, P.; Tao, N. *J. Phys. Condens. Matter* **2007**, *19*, 215202.

(222) Mallajosyula, S.S.; Lin, J.C.; Cox, D.L.; Pati, S.K.; Singh, R.R.P. *Phys. Rev. Lett.* **2008**, *101*, 176805.

(223) Hihath, J.; Xu, B.; Zhang, P.; Tao, N. *Proc. Natl. Acad. Sci. U.S.A.* **2005**, *102*, 16979.

(224) Dulic, D., Tuukkanen, S., Chung, C.-L.; Isambert, A.; Lavie, P.; Filoramo, A. *Nanotech.* **2009**, *20*, 115502.

(225) Barton, J.K.; Nuckols, C. *Unpublished results.*

(226) Takada, T.; Kawai, K.; Cai, X.; Sugimoto, A.; Fujitsuka, M.; Majima, T. *J. Am. Chem. Soc.* **2004**, *126*, 1125.

(227) Takada, T.; Kawai, K.; Fujitsuka, M.; Majima, T.; *J. Am. Chem. Soc.* **2006**, *128*, 11012.

(228) Jortner, J.; Bixon, M.; Voityuk, A.A.; Rösch, N. *J. Phys. Chem. A* **2002**, *106*, 7599.

(229) Sartor, V.; Boone, E.; Schuster, G.B. *J. Phys. Chem. B* **2001**, *105*, 11057.

(230) Yoo, J.; Delaney, S.; Stemp, E.D.A.; Barton, J.K. *J. Am. Chem. Soc.* **2003**, *125*, 6640.

(231) Kendrick, T.; Giese, B. *Chem. Comm.* **2002**, *18*, 2016.

(232) Giese, B.; Wessely, S. *Angew. Chem. Int. Ed.* **2000**, *39*, 3490.

(233) Bixon, M.; Jortner, J. *J. Am. Chem. Soc.* **2001**, *123*, 12556.

(234) Bixon, M.; Jortner, J. *Chem. Phys.* **2002**, *271*, 393.

(235) Bixon, M.; Jortner, J. *Chem. Phys.* **2006**, *326*, 252.

(236) Liu, C.-S.; Hernandez, R.; Schuster, G.B. *J. Am. Chem. Soc.* **2004**, *126*, 2877.

(237) Goldsmith, R.H.; DeLeon, O.; Wilson, T.M.; Finkelstein-Shapiro, D.; Ratner, M.A.; Wasielewski, M.R. *J. Phys. Chem. A* **2008**, *112*, 4410.

(238) Yu, Z.G.; Song, X. *Phys. Rev. Lett.* **2001**, *86*, 6018.

(239) Berlin, Y.A.; Burin, A.L.; Ratner, M.A. *J. Am. Chem. Soc.* **2001**, *123*, 260.

(240) Kelley, S. O.; Jackson, N. M.; Hill, M. G.; Barton, J. K. *Angew. Chem., Int. Ed*. **1999**, *38*, 941.

(241) Hartwich, G.; Caruana, D.J.; de Lumley-Woodyear, T.; Wu, Y.; Campbell, C.N.; Heller, A. *J. Am. Chem. Soc.* **1999**, *121*, 10803.

(242) Traub, M.C.; Brunschwig, B.S.; Lewis, N.S. *J. Phys. Chem. B* **2007**, *111*, 6676.

(243) Adhikary, A.; Kumar, A.; Khanduri, D.; Sevilla, M.D. *J. Am. Chem. Soc.* **2008**, *130*, 10282.

(244) Jakobsson, M.; Stafström, S. *J. Chem. Phys.* **2008**, *129*, 125102.

(245) Schuster, G.B. *Acc. Chem. Res.* **2000**, *33*, 253.

(246) Conwell, E. M.; Rakhmanova, S. V. *Proc. Natl. Acad. Sci. U.S.A.* **2000**, *97*, 4556.

(247) Kuznetsov, A.M. *Charge Transfer in Physics, Chemistry and Biology: Physical Mechanisms of Elementary Processes and an Introduction to the Theory* Gordon and Breach Science Publishers: Amsterdam, **1995**, 2.

(248) Maniadis, P.; Kalosakas, G; Rasmussen, K.Ø.; Bishop, A.R. *Phys. Rev. B.* **2003**, *68*, 174304.

(249) Komineas, S.; Kalosakas, G.; Bishop, A.R. *Phys. Rev. E* **2002**, *65*, 061905.

(250) Chang, C.-M.; Castro Neto, A.H.; Bishop, A.R. *Chem. Phys.* **2004**, *303*, 189.

(251) Conwell, E.M. *Proc. Natl. Acad. Sci. U.S.A.* **2005**, *102*, 8795.

(252) Conwell, E. M.; Bloch, S. M. *J. Phys Chem. B* **2006**, *110*, 5801.

(253) Conwell, E.M.; Park, J.-H.; Choi, H.-Y. *J. Phys. Chem. B* **2005**, *109*, 9760.

(254) Conwell, E.M.; Bloch, S.M.; McLaughlin, P.M.; Basko, D.M. *J. Am. Chem. Soc.* **2007**, *129*, 9175.

(255) Conwell, E.M.; Basko, D.M. *J. Phys. Chem. B* **2006**, *110*, 23603.

(256) Middleton, C.T.; de La Harpe, K.; Su, C. ; Law, Y.K.; Crespo-Hernández, C.E.; Kohler, B. *Ann. Rev. Phys. Chem.* **2009**, *60*, 217.

(257) Schwalb, N.K.; Temps, F. *Science* **2008**, *322*, 243.

(258) Crespo-Hernández, C.E.; Cohen, B.; Kohler, B. *Nature* **2005**, *436*, 1141.

(259) Buchvarov, I.; Wang, Q.; Raytchev, M.; Trifonov, I.; Fiebig, T. *Proc. Natl. Acad. Sci. U.S.A.* **2007**, *104*, 4794.

(260) Kadhane, U.; Holm, A.I.S.; Hoffmann, S.V.; Nielsen, S. *Phys. Rev. E* **2008**, *77*, 021901.

(261) Takaya, T,; Su, C.; de La Harpe, K.; Crespo-Hernández, C.E.; Kohler, B. *Proc. Natl. Acad. Sci. U.S.A.* **2008**, *105*, 10285.

(262) Lange, A.W.; Herbert, J.M. *J. Am. Chem. Soc.* **2009**, *131*, 3913.

(263) Hatcher, E.; Balaeff, A.; Keinan, S.; Venkatramani, R.; Beratan, D.N. *J. Am. Chem. Soc.* **2008**, *130*, 11752.

(264) Uskov, D.B.; Burin, A.L. *Phys. Rev. B* **2008**, *78*, 073106.

(265) Voityuk, A.A. *J. Chem. Phys.* **2005**, *122*, 204904.

(266) Sen, S.; Andreatta, D.; Ponomarev, S.Y.; Beveridge, D.L.; Berg, M.A. *J. Am. Chem. Soc.* **2009**, *131*, 1724,

(267) Voityuk, A.A. *J. Chem. Phys.* **2008**, *128*, 045104.

(268) Friedman, K.A.; Heller, A. *J. Phys. Chem. B* **2001**, *105*, 11859.

(269) Heller, A. *Farad. Disc.* **2000**, *116*, 1.

(270) Merino, E.J.; Barton, J.K. *Biochemistry* **2007**, *46*, 2805.

(271) Merino, E.J.; Barton, J.K. *Biochemistry* **2009**, *48*, 660.

(272) Steenken, S.; Jovanovic, S.V. *J. Am. Chem. Soc.* **1997**, *119*, 617.

(273) Crespo-Hernández, C.E.; Close, D.M.; Gorb, L.; Leszczynski, J. *J. Phys. Chem. B* **2007**, *111*, 5386.

Chapter 2:

Interpreting Periodicity in DNA-mediated Charge Transport across Adenine Tracts[†§]

[†] adapted from Augustyn, K. E.; Genereux, J. C.; Barton, J. K. *Angew. Chem. Int. Ed.* **2007**, *46*, 5731 and Genereux, J.C.; Augustyn, K.E.; Davis, M.L.; Shao, F.; Barton, J.K. *J. Am. Chem. Soc.* **2008**, *130*, 15150.

[§] Dr. Kate Augustyn and Ms. Molly Davis performed the Rh experiments, while Dr. Fangwei Shao performed the AQ experiments.

2.1. INTRODUCTION

The DNA π-stack has the inherent ability to act as an efficient medium for charge transport (CT).[1] Long-range DNA-mediated CT is exquisitely sensitive both to the coupling of donors and acceptors into the π-stack,[2] and to the presence of lesions, mismatches, protein-induced distortions, and other defects in the integrity of base stacking.[3] This sensitivity has been exploited in the development of novel classes of DNA-based sensing technologies[4] and might be utilized *in vivo* by transcriptional activation and DNA repair pathways.[5] To fully realize the potential of this technology, it is necessary to further understand the mechanistic underpinnings of DNA-mediated CT.

Recently, a periodic dependence on adenine tract length was observed for the fluorescence quenching of photoexcited 2-aminopurine (Ap^*) by DNA-mediated CT to guanine across the adenine tract.[6] By standardizing to a system containing the redox-inactive base inosine, the contribution to quenching solely due to CT between Ap^* and guanine was isolated. The amplitudes associated with this periodicity are substantial and greater than the observed associated errors. Non-monotonicity of CT rate vs. distance has since been observed between gold and ferrocene across methyl-substituted oligophenyleneethynylene, but that result was attributed to substantial torsional variations between polymers of different lengths, an explanation that is not adaptable to these adenine tracts[7]. Instead, we interpreted our surprising result in the context of four or five base pairs being conducive to forming a CT-active domain, leading to higher CT over an adenine tract that is an integer multiple of this number. This interpretation is consistent with the conformationally-gated character of DNA-mediated CT over long distances,[8] with evidence for delocalization of the injected hole,[9] and with evidence for a similar

delocalization length in the formation of excimers along adenine tracts.[10] A similar argument has been made to explain this result in the context of a polaron hopping model,[11] and non-monotonicity was also observed in calculations that permitted delocalization.[12]

Importantly, Ap^* fluorescence quenching is insensitive to processes that occur after the CT event, including radical trapping, incoherent hopping or back electron transfer (BET). For hole acceptors in DNA, product yields for different photooxidants scale inversely to the propensity for BET,[13] and attenuating BET, both between the hole donor and the oxidized bridge and between the hole donor and oxidized acceptor, extends the lifetime of the charge separated state.[14] While other spectroscopic investigations of CT across adenine tracts have not revealed a similar periodicity, these other studies have been performed on systems for which BET is known to be substantial[15,16] or where slow trapping allows charge equilibration after the initial CT step.[17,18] We have recently shown that for both hole and electron transport, CT efficiency is dictated in the same manner by the dynamics and structure of the intervening DNA bases.[19] If the periodicity is the result of CT-active states that serve as more efficient pathways for forward CT, then they will also mediate more efficient BET. Hence, we propose that conformations that promote forward CT also promote BET, and this BET will serve to suppress the apparent periodicity.

To test this hypothesis and determine whether this periodicity is a general property of long-range DNA-mediated CT, in this chapter we consider disparate donor-acceptor systems with varying extents of BET (**Figure 2.1**). Previously, by measuring the quantum yield of damage at double guanine sites, we ranked a series of photooxidants by

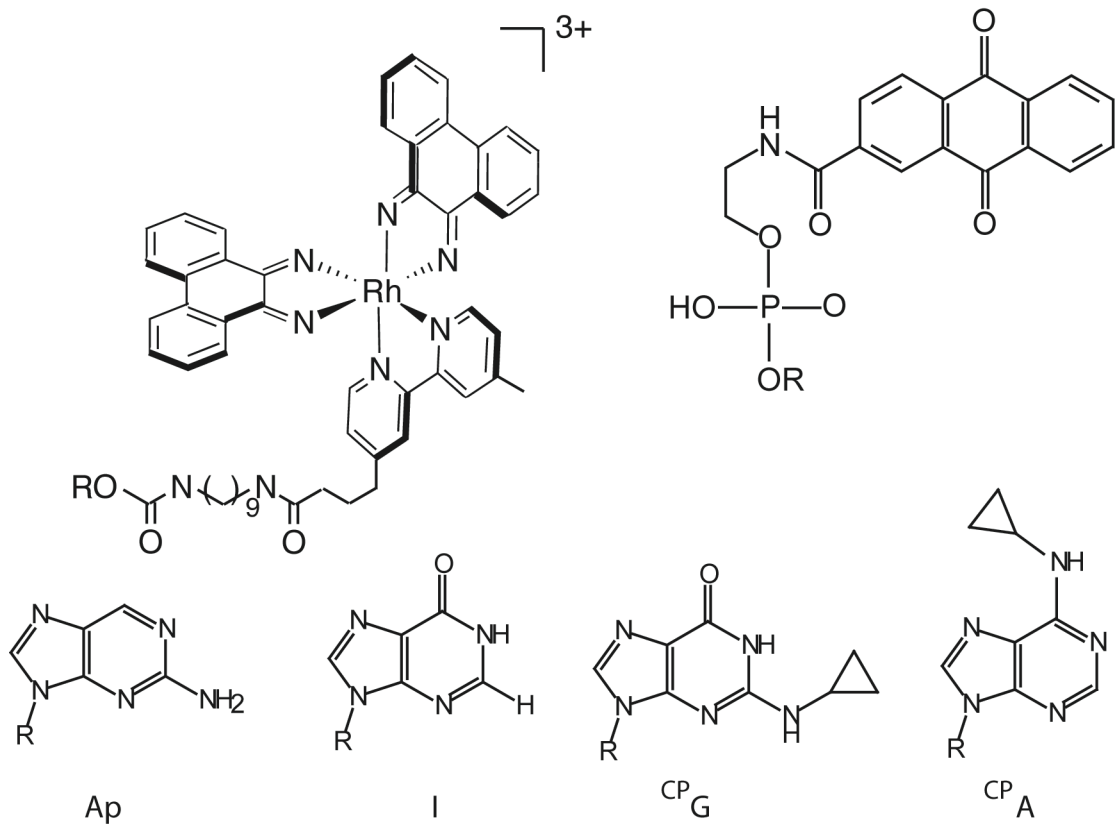

Figure 2.1. Photooxidants and modified bases used to probe CT events in DNA. At top are the structures of the rhodium and anthraquinone complexes utilized, and below are structures of aminopurine, inosine, ^{CP}G, and ^{CP}A. The rhodium complex is tethered to the 5' end of amino modified DNA by a nine carbon linker, and the anthraquinone caps the 5' end through the phosphate.

propensity for charge recombination between the guanine cation radical and the reduced hole donor.[13] Two photooxidants that are subject to only moderate BET are $Rh(phi)_2(bpy')^{3+}$ (Rh) and anthraquinone (AQ), while BET is highly efficient for Ap. Although these and other photooxidants typically induce oxidation of native guanine sites to 8-oxoguanine and further base-labile damage products,[18,20] facile BET between guanine cation radical and aminopurine anion radical renders Ap^* oxidation of guanine only observable with the ^{CP}G trap. Furthermore, to limit post-injection charge equilibration, we assay for arrival using N_2-cyclopropylguanine (^{CP}G) instead of guanine as a hole acceptor.[21] This fast[22] trap for cation and anion radicals allows detection of pre-equilibrium CT processes that are obscured by the slow trapping of guanine cation radical by water or superoxide.[26] By modulating the extent of BET for a series of ^{CP}G-containing duplexes, we demonstrate that the periodic length dependence is inherent to adenine tracts, but attenuated with increasing BET.

2.2. METHODS

2.2.1. OLIGONUCLEOTIDE SYNTHESIS

DNA oligonucleotides were synthesized trityl-on using standard phosphoramidite chemistry on an ABI DNA synthesizer with Glen Research reagents. 2-aminopurine was incorporated as the N_2-dimethylaminomethylidene-protected phosphoramidite (Glen Research). ^{CP}G-modified oligonucleotides were prepared by incorporating the precursor base, 2-fluoro-O_6-paraphenylethyl-2'-deoxyinosine (Glen Research), as a phosphoramidite at the desired position. The resin was then reacted with 1 M diaza(1,3)bicyclo[5.4.0]undecane (DBU, Aldrich) in acetonitrile to effectively remove

the O_6 protecting group. Similarly, ^{CP}A-modified oligonucleotides were prepared by incorporating the precursor base, *O*$_6$-phenylinosine (Glen Research), as a phosphoramidite at the desired position. For both ^{CP}G- and ^{CP}A- containing strands, the oligonucleotides were subsequently incubated overnight in 6 M aqueous cyclopropylamine (Aldrich) at 60 ^{o}C, resulting in substitution, base deprotection, and simultaneous cleavage from the resin. The cleaved strands were dried *in vacuo* and purified by reversed-phase HPLC, detritylated by 80% acetic acid for 15 min, and repurified by reversed-phase HPLC. Oligonucleotides were characterized by MALDI-TOF mass spectrometry.

Rhodium-modified oligonucleotides were synthesized as described previously.[27] Briefly, the detritylated resin-bound oligonucleotides were first modified with a nine carbon amine linker by reaction with carbonyldiimidazole and diaminononane in dioxane. The amine-modified strands were then reacted with $[Rh(phi)_2(bpy')]Cl_3$ (bpy' = 4-(4'-methyl-2,2'-bipyridyl) valerate) in 1:1:1 methanol:acetonitrile:isopropanol using *O*-(*N*-succinimidyl)-1,1,3,3-tetramethyl uranium tetrafluoroborate (TSTU) as the coupling reagent. Cleavage from the resin was accomplished by incubation in NH_4OH at 60 ^{o}C for 6 hours. Strands were HPLC-purified using a Varian C_4 reversed-phase column. The two diasteromeric conjugates, differing in configuration at the metal center, have different retention times. However, both isomers were collected together and used for subsequent experiments. MALDI-TOF mass spectrometry was used to characterize the metallated DNA conjugates.

Anthraquinone (AQ)-tethered oligonucleotides were synthesized as described previously by incorporating an anthraquinone phosphoramidite at the 5´-end of the

oligonucleotides.[28] The DNA was deprotected in NH_4OH at 60 ^oC overnight. The resulting oligonucleotides were purified once by reversed-phase HPLC and characterized by MALDI-TOF mass spectrometry.

All oligonucleotides were suspended in a buffer containing 50 mM NaCl, 20 mM or 5 mM sodium phosphate, pH 7 and quantified using UV-visible spectroscopy. Duplexes were prepared by heating equal concentrations of complementary strands to 90 ^oC for 5 min and slow cooling to ambient temperature. Melting temperatures (T_m) were obtained for all duplexes. All duplexes melted between 50 ^oC and 60 ^oC at a 1.5 μM concentration in phosphate buffer (PBS, 20 mM sodium phosphate, 50 mM NaCl, pH 7).

2.2.2. PHOTOOXIDATION EXPERIMENTS

Photooxidations of Rh-tethered oligonucleotides were carried out by irradiating 30 μL aliquots of 10 μM duplex in PBS for 30 sec at 365 nm on a 1000 W Hg/Xe lamp equipped with a 320 nm long pass filter and monochromator. AQ-containing duplexes in PBS (30 μL, 10 μM) were irradiated at 350 nm using the same apparatus for 5 min. Irradiation times were varied and the decomposition was linear over the times used (supplementary information). Samples were irradiated at various temperatures ranging from 20 to 80 ^oC. Ap-containing duplexes (30 μL, 10 μM) in PBS were irradiated as above at 325 nm without the long pass filter for 30 sec or 30 min.

To analyze for ^{CP}A or ^{CP}G decomposition following irradiation, samples were digested to the component nucleosides by phosphodiesterase I (USB) and alkaline phosphatase (Roche) at 37 ^oC, to completion. The resulting deoxynucleosides were analyzed by reversed-phase HPLC using a Chemcobond 5-ODS-H, 4.6 mm × 100 mm

column. The amount of ^{CP}G per duplex was determined by taking the ratio of the area of the HPLC peak for d^{CP}G to the area of the peak for dT. The amount of ^{CP}A per duplex was determined in the same manner, using dI as the internal reference. For 30 minute irradiations, a small amount of thymine decomposition was observed, as has been described previously.[29] Hence, redox-inactive deoxyinosine was used as the internal standard for these experiments as well. The decomposition yield is taken as the percent loss of ^{CP}G or ^{CP}A between an irradiated sample and the dark control. Dark control HPLC traces were confirmed to yield the correct relative amounts of dA, dC, dG, dI, dT, d^{CP}A and d^{CP}G based on duplex sequence. Irradiations were performed at least three times and the results averaged. Due to the long irradiation times used for the Ap–I_3A_n strands, actinometry was performed using a 6 mM ferrioxalate standard[30] to allow comparison between experiments performed on separate days. The given quantum yield is for the efficiency from the Ap* state to the ring-opened product. Fluorescence quenching for the Ap–I_3A_n was not expected to be observable based on the quantum yield of ^{CP}G damage, and hence was not explored.

For ^{CP}G decomposition, errors are presented at 90% standard error of the mean, using the Student's t-distribution at the appropriate degrees of freedom to determine confidence intervals. For ^{CP}A decomposition, three trials were performed and data are reported with 2 standard errors for a 95% confidence level.

Table 2.1. DNA assemblies for oxidative decomposition experiments

Rh–A_2	3′-TICTI-AA-G^{CP}GTCTAATAACTG-5′ 5′-Rh-ACIAC-TT-C CAGATTATTGAC-3′
Rh–A_4	3′-TICTI-AAAA-G^{CP}GTCTAATCTG-5′ 5′-Rh-ACIAC-TTTT-C CAGATTAGAC-3′
Rh–A_6	3′-TICTI-AAAAAA-G^{CP}GTCTTCTG-5′ 5′-Rh-ACIAC-TTTTTT-C CAGAAGAC-3′
Rh–A_8	3′-TICTI-AAAAAAAA-G^{CP}GTCTTG-5′ 5′-Rh-ACIAC-TTTTTTTT-C CAGAAC-3′
Rh–A_8′	3′-TICTI-AAAAAAAA-G^{CP}GTCTCTATCTTG-5′ 5′-Rh-ACIAC-TTTTTTTT-C CAGAGATAGAAC-3′
Rh–A_{10}	3′-TICTI-AAAAAAAAAA-G^{CP}GTCTATCTTG-5′ 5′-Rh-ACIAC-TTTTTTTTTT-C CAGATAGAAC-3′
Rh–A_{12}	3′-TICTI-AAAAAAAAAAAA-G^{CP}GTCTCTTG-5′ 5′-Rh-ACIAC-TTTTTTTTTTTT-C CAGAGAAC-3′
AQ–A_{14}	3′-TICTI-AAAAAAAAAAAAAA-G^{CP}GTCTTG-5′ 5′-AQ-ACIAC-TTTTTTTTTTTTTT-C CAGAAC-3′
AQ–A_2	3′-TICTI-AA-G^{CP}GTCTAATAACTG-5′ 5′-AQ-ACIAC-TT-C CAGATTATTGAC-3′
AQ–A_4	3′-TICTI-AAAA-G^{CP}GTCTAATCTG-5′ 5′-AQ-ACIAC-TTTT-C CAGATTAGAC-3′
AQ–A_6	3′-TICTI-AAAAAA-G^{CP}GTCTTCTG-5′ 5′-AQ-ACIAC-TTTTTT-C CAGAAGAC-3′
AQ–A_8	3′-TICTI-AAAAAAAA-G^{CP}GTCTTG-5′ 5′-AQ-ACIAC-TTTTTTTT-C CAGAAC-3′
AQ–A_8′	3′-TICTI-AAAAAAAA-G^{CP}GTCTCTATCTTG-5′ 5′-AQ-ACIAC-TTTTTTTT-C CAGAGATAGAAC-3′
AQ–A_{10}	3′-TICTI-AAAAAAAAAA-G^{CP}GTCTATCTTG-5′ 5′-AQ-ACIAC-TTTTTTTTTT-C CAGATAGAAC-3′

AQ-A_{12} 3′-TICTI-AAAAAAAAAAAA-G^{CP}GTCTCTTG-5′
5′-AQ-ACIAC-TTTTTTTTTTTT-C CAGAGAAC-3′

AQ-A_{14} 3′-TICTI-AAAAAAAAAAAAAA-G^{CP}GTCTTG-5′
5′-AQ-ACIAC-TTTTTTTTTTTTTT-C CAGAAC-3′

Rh-A_4-$^{CP}A_2$ 3′-TICTI-^{CP}AAAA-GGTCTAATCTG-5′
5′-Rh-ACIAC- TTTT-CCAGATTAGAC-3′

Rh-A_4-$^{CP}A_2$ 3′-TICTI-A^{CP}AAA-GGTCTAATCTG-5′
5′-Rh-ACIAC-T TTT-CCAGATTAGAC-3′

Rh-A_4-$^{CP}A_3$ 3′-TICTI-AA^{CP}AA-GGTCTAATCTG-5′
5′-Rh-ACIAC-TT TT-CCAGATTAGAC-3′

Rh-A_4-$^{CP}A_4$ 3′-TICTI-AAA^{CP}A-GGTCTAATCTG-5′
5′-Rh-ACIAC-TTT T-CCAGATTAGAC-3′

Rh-A_6-$^{CP}A_1$ 3′-TICTI-^{CP}AAAAAA-GGTCTAATCTG-5′
5′-Rh-ACIAC- TTTTTT-CCAGATTAGAC-3′

Rh-A_6-$^{CP}A_2$ 3′-TICTI-A^{CP}AAAAA-GGTCTAATCTG-5′
5′-Rh-ACIAC-T TTTTT-CCAGATTAGAC-3′

Rh-A_5-$^{CP}A_3$ 3′-TICTI-AA^{CP}AAAA-GGTCTAATCTG-5′
5′-Rh-ACIAC-TT TTTT-CCAGATTAGAC-3′

Rh-A_5-$^{CP}A_4$ 3′-TICTI-AAA^{CP}AAA-GGTCTAATCTG-5′
5′-Rh-ACIAC-TTT TTT-CCAGATTAGAC-3′

Rh-A_5-$^{CP}A_5$ 3′-TICTI-AAAA^{CP}AA-GGTCTAATCTG-5′
5′-Rh-ACIAC-TTTT TT-CCAGATTAGAC-3′

Rh-A_5-$^{CP}A_6$ 3′-TICTI-AAAAA^{CP}A-GGTCTAATCTG-5′
5′-Rh-ACIAC-TTTTT T-CCAGATTAGAC-3′

Rh-A_{14}-$^{CP}A_1$ 3′-TICTI-^{CP}AAAAAAAAAAAAAA-GGTCTAATCTG-5′
5′-Rh-ACIAC- TTTTTTTTTTTTTT-CCAGATTAGAC-3′

Rh-A_{14}-$^{CP}A_2$ 3′-TICTI-A^{CP}AAAAAAAAAAAAA-GGTCTAATCTG-5′
5′-Rh-ACIAC-T TTTTTTTTTTTTT-CCAGATTAGAC-3′

Rh-A_{14}-$^{CP}A_3$ 3′-TICTI-AA^{CP}AAAAAAAAAAAA-GGTCTAATCTG-5′
5′-Rh-ACIAC-TT TTTTTTTTTTTT-CCAGATTAGAC-3′

Rh-A_{14}-$^{CP}A_4$ 3′-TICTI-AAA^{CP}AAAAAAAAAAA-GGTCTAATCTG-5′
5′-Rh-ACIAC-TTT TTTTTTTTTTT-CCAGATTAGAC-3′

$Rh-A_{14}-^{CP}A_5$ 3′-TICTI-AAAA^{CP}AAAAAAAAAA-GGTCTAATCTG-5′
5′-Rh-ACIAC-TTTT TTTTTTTTTT-CCAGATTAGAC-3′

$Rh-A_{14}-^{CP}A_6$ 3′-TICTI-AAAAA^{CP}AAAAAAAAA-GGTCTAATCTG-5′
5′-Rh-ACIAC-TTTTT TTTTTTTTT-CCAGATTAGAC-3′

$Rh-A_{14}-^{CP}A_7$ 3′-TICTI-AAAAAA^{CP}AAAAAAAA-GGTCTAATCTG-5′
5′-Rh-ACIAC-TTTTTT TTTTTTTT-CCAGATTAGAC-3′

$Rh-A_{14}-^{CP}A_8$ 3′-TICTI-AAAAAAA^{CP}AAAAAAA-GGTCTAATCTG-5′
5′-Rh-ACIAC-TTTTTTT TTTTTTT-CCAGATTAGAC-3′

$Rh-A_{14}-^{CP}A_9$ 3′-TICTI-AAAAAAAA^{CP}AAAAAA-GGTCTAATCTG-5′
5′-Rh-ACIAC-TTTTTTTT TTTTTT-CCAGATTAGAC-3′

$Rh-A_{14}-^{CP}A_{10}$ 3′-TICTI-AAAAAAAAA^{CP}AAAAA-GGTCTAATCTG-5′
5′-Rh-ACIAC-TTTTTTTTT TTTTT-CCAGATTAGAC-3′

$Rh-A_{14}-^{CP}A_{11}$ 3′-TICTI-AAAAAAAAAA^{CP}AAAA-GGTCTAATCTG-5′
5′-Rh-ACIAC-TTTTTTTTTT TTTT-CCAGATTAGAC-3′

$Rh-A_{14}-^{CP}A_{12}$ 3′-TICTI-AAAAAAAAAAA^{CP}AAA-GGTCTAATCTG-5′
5′-Rh-ACIAC-TTTTTTTTTTT TTT-CCAGATTAGAC-3′

$Rh-A_{14}-^{CP}A_{13}$ 3′-TICTI-AAAAAAAAAAAA^{CP}AA-GGTCTAATCTG-5′
5′-Rh-ACIAC-TTTTTTTTTTTT TT-CCAGATTAGAC-3′

$Rh-A_{14}-^{CP}A_{14}$ 3′-TICTI-AAAAAAAAAAAAA^{CP}A-GGTCTAATCTG-5′
5′-Rh-ACIAC-TTTTTTTTTTTTT T-CCAGATTAGAC-3′

$Ap-A_2$ 5′-TIACTIAp-A-G^{CP}GTCTTAATCTACATCTTG-3′
3′-ACTIACT -T-C CAGAATTAGATGTAGAAC-5′

$Ap-A_4$ 5′-TIACTIAp-AAA-G^{CP}GTCTATCTACATCTTG-3′
3′-ACTIACT -TTT-C CAGATAGATGTAGAAC-5′

$Ap-A_6$ 5′-TIACTIAp-AAAAA-G^{CP}GTCTCTACATCTTG-3′
3′-ACTIACT -TTTTT-C CAGAGATGTAGAAC-5′

$Ap-A_8$ 5′-TIACTIAp-AAAAAAA-G^{CP}GTCTACATCTTG-3′
3′-ACTIACT -TTTTTTT-C CAGATGTAGAAC-5′

$Ap-A_{10}$ 5′-TIACTIAp-AAAAAAAAA-G^{CP}GTCTATCTTG-3′
3′-ACTIACT -TTTTTTTTT-C CAGATAGAAC-5′

$Ap-A_{12}$ 5′-TIACTIAp-AAAAAAAAAAA-G^{CP}GTCTCTTG-3′
3′-ACTIACT -TTTTTTTTTTT-C CAGAGAAC-5′

Ap-A_{14}	5′-TIACTIAp-AAAAAAAAAAAAA-G^{CP}GTCTTG-3′ 3′-ACIIACT -TTTTTTTTTTTTT-C CAGAAC-5′
Ap-I_3A_2	5′-TIACTIApIII-A-G^{CP}GTCTTAATCTACATCTTG-3′ 3′-ACTIACT CCC-T-C CAGAATTAGATGTAGAAC-5′
Ap-I_3A_4	5′-TIACTIApIII-AAA-G^{CP}GTCTATCTACATCTTG-3′ 3′-ACTIACT CCC-TTT-C CAGATAGATGTAGAAC-5′
Ap-I_3A_6	5′-TIACTIApIII-AAAAA-G^{CP}GTCTCTACATCTTG-3′ 3′-ACTIACT CCC-TTTTT-C CAGAGATGTAGAAC-5′
Ap-I_3A_8	5′-TIACTIApIII-AAAAAAA-G^{CP}GTCTACATCTTG-3′ 3′-ACTIACT CCC-TTTTTTT-C CAGATGTAGAAC-5′
Ap-I_3A_{10}	5′-TIACTIApIII-AAAAAAAAA-G^{CP}GTCTATCTTG-3′ 3′-ACTIACT CCC-TTTTTTTTT-C CAGATAGAAC-5′
Ap-I_3A_{12}	5′-TIACTIApIII-AAAAAAAAAAA-G^{CP}GTCTCTTG-3′ 3′-ACTIACT CCC-TTTTTTTTTTT-C CAGAGAAC-5′
Ap-I_3A_{14}	5′-TIACTIApIII-AAAAAAAAAAAAA-G^{CP}GTCTTG-3′ 3′-ACIIACT CCC-TTTTTTTTTTTTT-C CAGAAC-5′

2.3 RESULTS

2.3.1. EXPERIMENTAL DESIGN

Figure 2.1 illustrates typical DNA-photooxidant assemblies. The Rh-A_n, AQ-A_n and Ap-A_n series contain rhodium, anthraquinone, or aminopurine separated from ^{CP}G by a bridge containing increasing numbers of adenines, while Rh-A_n-^{CP}A sequences contain ^{CP}A serially inserted along the adenine tract. For all Rh-modified assemblies there is a four base-pair segment surrounding the rhodium binding site to provide optimum intercalation of the photooxidant. Likely a mixture of binding sites (one and two bases in) are available to the rhodium diastereomers.[27] On the side distal to the hole trap, there is a constant three-base sequence so that end effects are minimized. Guanine can serve as a thermodynamic well if placed near the rhodium intercalation site and, although the trapping rate is slow, BET to rhodium is comparably fast at short distance.[13] Therefore, inosine was employed as a substitute for guanine near the rhodium binding site to enhance ^{CP}G decomposition.[9,19] Note that the first four adenine tract sequences, Rh–A_2 through Rh–A_8 are composed of 20 base pairs, while that of Rh–A_8' through Rh–A_{14} are slightly longer, with 26 base pairs (**Table 2.1**). Rh–A_8 and Rh–A_8', both containing the 8 base-pair long adenine tract but differing in length, yield equivalent decomposition profiles with both time and temperature, and in subsequent results and figures, the data from Rh-A_8' are presented. A series of HPLC traces from the time-course of AQ-A_2 degradation shows the well-resolved peaks corresponding to the six different natural and unnatural nucleosides (**Figure 2.2**).

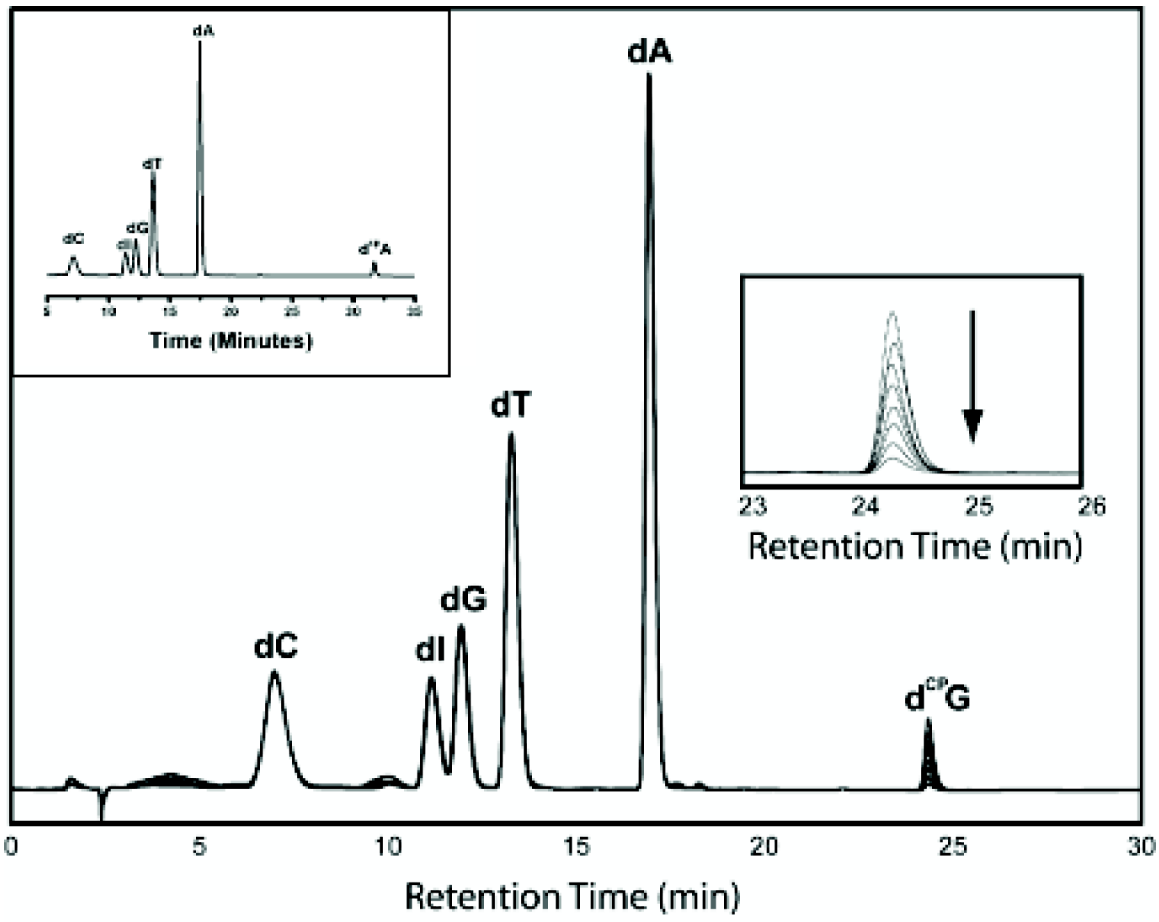

Figure 2.2. Overlaid HPLC traces at 260 nm for digested nucleosides from AQ–A_2 irradiated at 350 nm for 0, 1, 2, 3, 5, 7, 10, and 15 min. Traces are normalized to the height of the dT peak, and the righthand inset demonstrates that the peak corresponding to $d^{CP}G$ steadily degrades with respect to increased irradiation time. The lefthand inset is a chromatogram generated from digested nucleosides from a ^{CP}A-containing oligonucleotide. Conditions are as described in Methods.

2.3.2. DNA-MEDIATED OXIDATIVE DECOMPOSITION OF ^{CP}G BY RH AND AQ

Irradiation leads to the first-order decomposition of ^{CP}G by Rh and AQ, and of ^{CP}A by Rh (**Figure 2.3**). **Figure 2.4** shows the variation in the decomposition yield (Y) as a function of bridge length for the Rh-A_n and AQ-A_n series. Notably, the same non-monotonic, apparently periodic decay is observed for the Rh-A_n series as was seen for the Ap^* fluorescence quenching.[6] The apparent period of about five base pairs is similar as well, as is the temperature dependence for the Rh-A_n sequences. Below the T_m of the duplex, increasing temperature leads to increased ^{CP}G decomposition, but the amplitude of the periodicity is suppressed. Once the duplexes begin to melt, unstacking the base pairs, the decomposition efficiencies sharply drop to zero (**Figure 2.5**). This decrease in decomposition occurs between 50 and 60 ^{o}C.

Although the apparent periodicity is dampened, a similar profile is apparent with anthraquinone as the pendant photooxidant (**Figure 2.4**). As with the Rh-A_n series, photooxidation of the AQ-A_n assemblies show a shallow, non-monotonic periodic length dependence in yield. Decay parameters and apparent period are comparable.

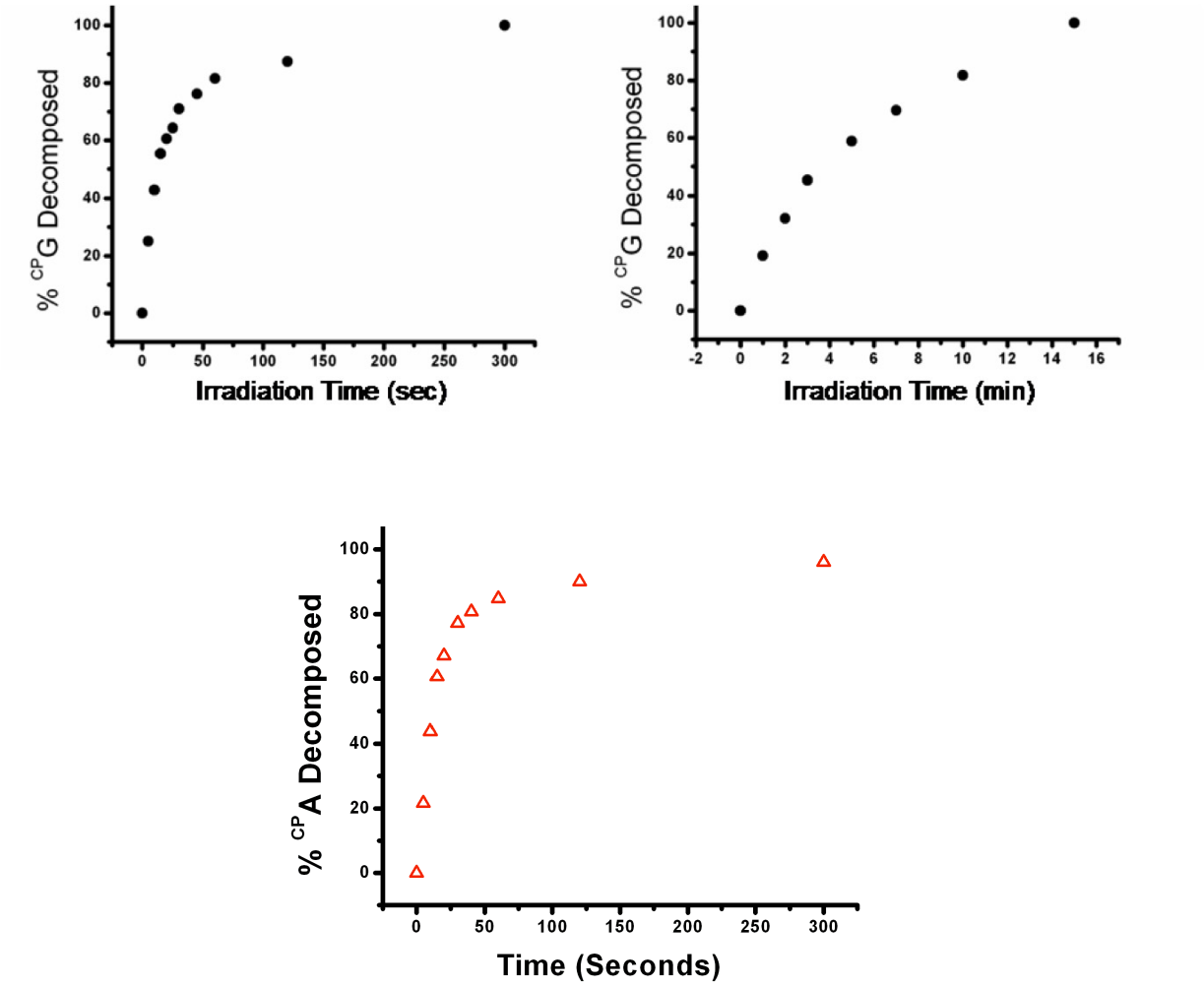

Figure 2.3. Time courses of ^{CP}G decomposition by irradiation of Rh–A_2 (top left), AQ–A_2 (top right), and Rh–A_{14}–$^{CP}A_1$. 10 μM duplexes were irradiated at 365 nm (Rh) or 350 nm (AQ). Conditions are as provided in Methods.

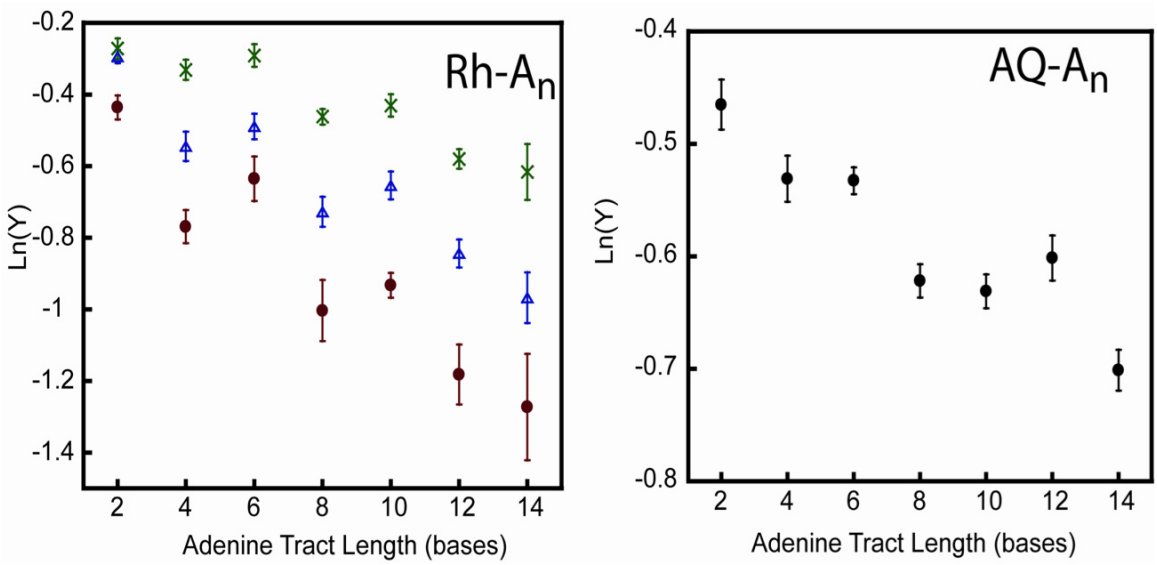

Figure 2.4. CT yields (Y) as a function of bridge length for the Rh–A_n series and AQ–A_n series. Results at three temperatures are shown for the Rh–A_n series: 20 ^{o}C (red circles), 30 ^{o}C (blue triangles), and 40 ^{o}C (green x's); AQ–A_n experiments are at ambient temperature. Duplexes (10 μM) were irradiated at 365 nm in 20 mM sodium phosphate, 50 mM NaCl, pH 7.0 as described in the text. The bridge length is defined as the number of adenines between the photooxidant and the trap. The experiments were repeated at least three times, the results averaged, and the error is expressed as 90% confidence intervals of the mean.

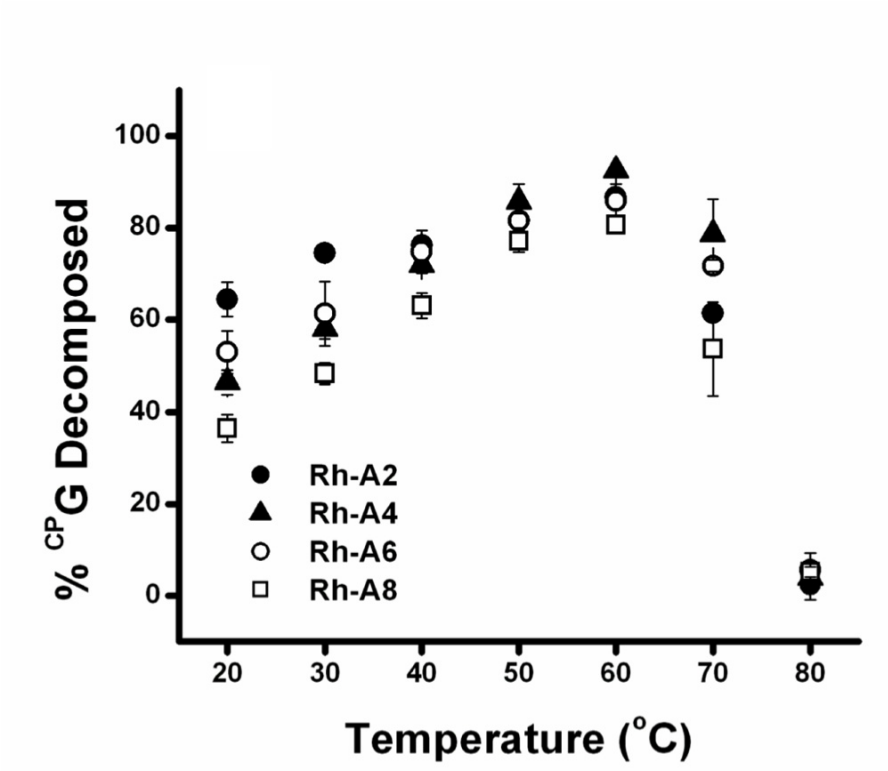

Figure 2.5. Temperature dependence for Rh–A_2 through Rh–A_8, conditions as in text. As each duplex becomes dehybridized, DNA-mediated CT is completely attenuated. Errors are single standard deviation.

2.3.3. DNA-MEDIATED OXIDATIVE DECOMPOSITION OF ^{CP}G BY AP.

To determine if periodicities could be observed in the presence of facile BET, we prepared the series of duplexes ApA_n. **Figure 2.6** directly compares the CT yield for ^{CP}G decomposition and Ap^* fluorescence quenching. Although oxidative damage to ^{CP}G is observed, ^{CP}G immediately neighboring Ap does not allow a sufficiently long-lived charge-separated state, and BET depletes the oxidized base faster than ring-opening.[13] This initial low yield for a single intervening adenine, and much higher yield for three intervening adenines, is characteristic of a system with rapid charge recombination.[14,15] Notably, although the length dependence is comparable to the fluorescence quenching result, the corresponding periodicity is completely suppressed.

To suppress BET, we tested separating the Ap from the adenine tract with a variety of higher energy sequences, including a single inosine and the sequence CTI; we found that with I_3A_n as the bridge, there is more ^{CP}G decomposition for Ap–I_3A_1 than for Ap–I_3A_3 indicating suppression of BET. For the Ap-I_3A_n sequences (**Figure 2.7**), there is substantially less damage, such that 30 min of irradiation is necessary to achieve significant decomposition of the ^{CP}G. BET is suppressed, as only slightly more decomposition is observed for the Ap-I_3A_3 sequence versus the Ap-I_3A_1 sequence. The non-monotonicity is now recovered, and is qualitatively similar to that observed for the Ap^* fluorescence quenching and Rh-A_n systems.

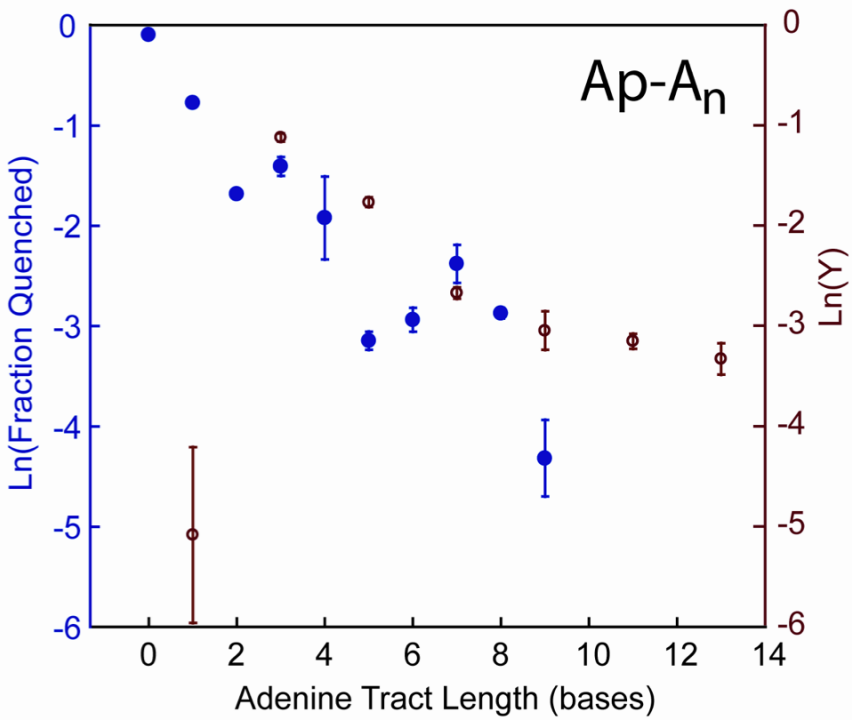

Figure 2.6. CT yields (Y) as a function of bridge length for the Ap–A_n series (red, open circles), as determined by ring-opening of ^{CP}G. Duplexes (10 μM) were irradiated at ambient temperature for 30 sec at 325 nm in 5 mM sodium phosphate, 50 mM NaCl, pH 7.0 as described in the text. The experiments were repeated at least three times, the results averaged, and the error is expressed as 90% confidence intervals of the mean. On the same plot, fluorescence quenching from reference (6) is shown for comparison (blue, closed circles).

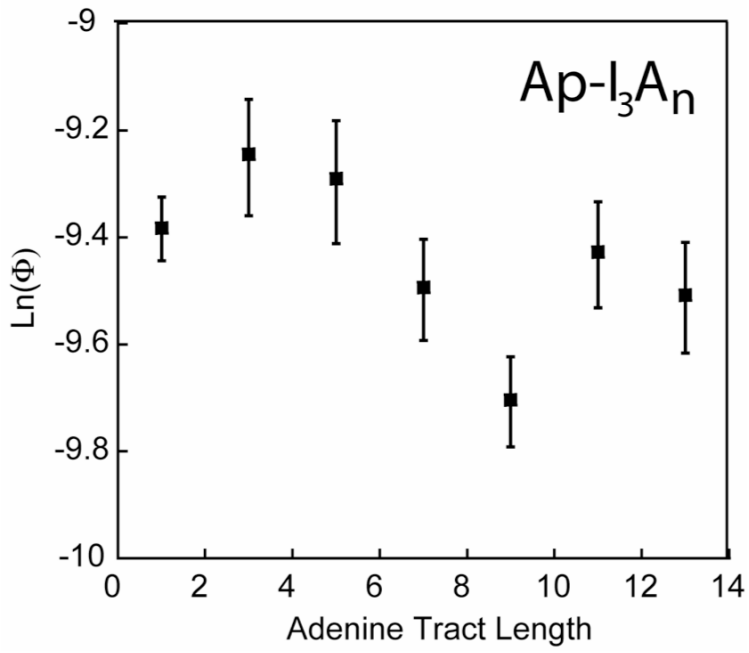

Figure 2.7. CT quantum yields (Φ) as a function of bridge length for the Ap–I_3A_n series, as determined by ring-opening of ^{CP}G. Duplexes (10 μM) were irradiated at ambient temperature for 30 min at 325 nm in 5 mM sodium phosphate, 50 mM NaCl, pH 7.0 as described in the text. The experiments were repeated at least eight times, the results averaged, and the error is expressed as 90% confidence intervals of the mean. Quantum yields were determined using actinometry on 6 mM ferrioxalate.

2.3.4. DNA-MEDIATED OXIDATIVE DECOMPOSITION OF ^{CP}A BY RH

To discriminate whether the periodicity for ^{CP}G decomposition in Rh–A_n constructs is dependent on the length of the adenine tract or on the donor-acceptor distance, we studied a series of assemblies where ^{CP}A is serially moved along the adenine tract. For these studies, we varied donor-acceptor distance while keeping the adenine tract length constant, for three sets of adenine tract lengths. Remarkably, over the 14 base pair A-tract, we find essentially no decay, with $\beta = 0.0013(3)$ Å^{-1} (**Figure 2.8**).

2.4. DISCUSSION

2.4.1. OBSERVATION OF PERIODICITIES IN LENGTH DEPENDENCE OF ^{CP}G DECOMPOSITION

The dependence of ^{CP}G oxidation by Rh or AQ on the length of the intervening adenine tract is periodic. It is striking that this result is so similar to that seen with the Ap* fluorescence quenching assay and that the periods are identical. The driving forces for photooxidation by Ap*, Rh*, and AQ* vary over a range of 700 mV.[2,31,32] The fluorescence quenching assay measures direct hole injection from Ap* into an orbital that includes the acceptor guanine, while the ^{CP}G assays directly measure the total CT yield to the hole acceptor, regardless of mechanism. Nevertheless, despite these fundamental differences between the experiments, a periodic length dependence is observed for all three cases and approximately the same apparent period is observed. Importantly, when the slow, unmodified guanine trap is used, no periodicity is observed, indicating the importance of assaying pre-equilibrium states in CT experiments. Although the ^{CP}G decomposition is a chemical event, the fast timescale of ring-opening defines a fast clock

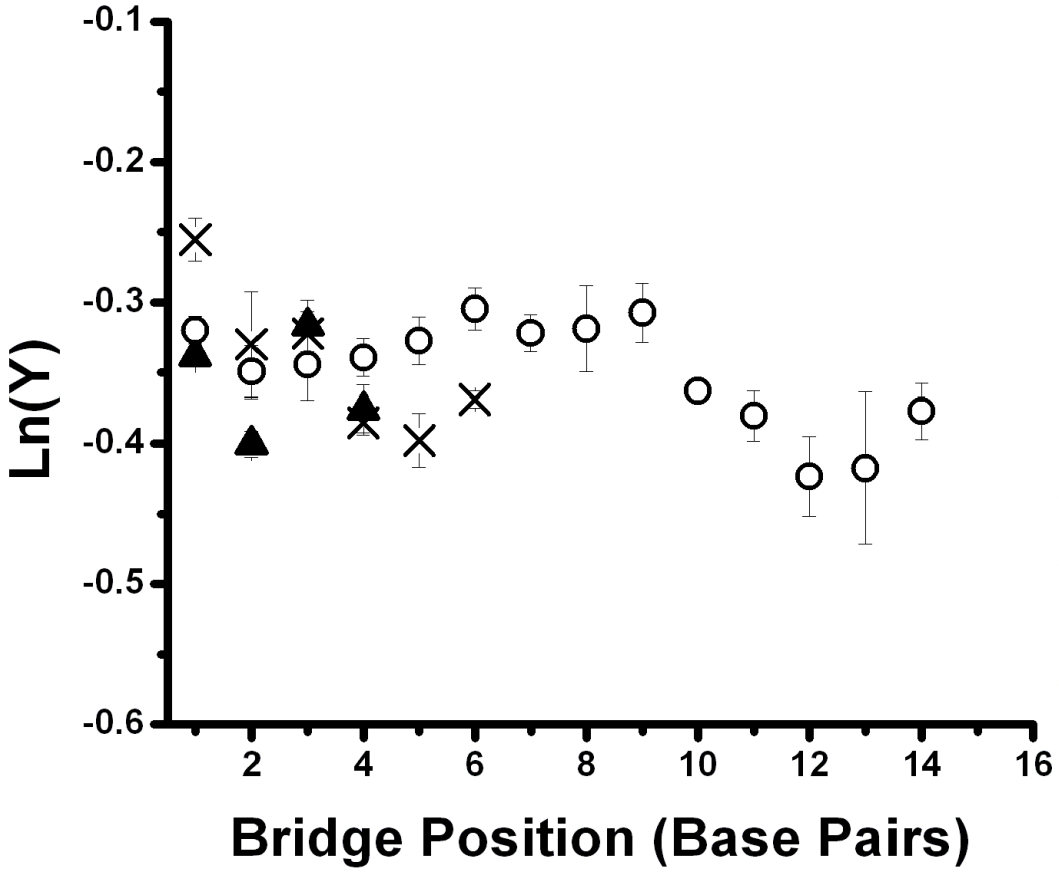

Figure 2.8. Decomposition (Y), as a function of bridge position for the Rh–A_4–$^{CP}A_m$ (closed triangles), Rh–A_6–$^{CP}A_m$ (X), and Rh–A_{14}–$^{CP}A_m$ (open circles) series following a 30 second irradiation at 365 nm. Decomposition was determined by integrating the HPLC ^{CP}A peak in an irradiated sample relative to a non-irradiated sample. Each HPLC trace was normalized to an internal inosine standard. The bars correspond to two standard errors for a 95% confidence level.

such that CT is still rate-limiting, in contrast to biochemical experiments measuring guanine decomposition.

For the Rh–A_n series, with increasing temperature, the overall yield of CT increases, the length dependence becomes shallower, and the periodicity is attenuated. For a direct CT event between a donor and acceptor in contact, in which the donor and acceptor orbitals are already aligned, higher temperatures are likely to decrease the probability that the orbitals will remain aligned, and decreased CT results. In contrast, when the donor and acceptor are separated by a dynamic bridge of base pairs, increasing the temperature allows a greater fraction of these duplexes to access a CT-active domain, resulting in enhanced CT. Increased temperature has a more prominent effect on CT through longer adenine bridges because there is a lower initial probability of each bridging base being aligned in a CT-active conformation. This effect is identical to that observed for Ap^* fluorescence quenching.[6] Furthermore, for both cases, the apparent periodicity is suppressed with increasing temperature, implying that the underlying cause of the periodicity is the same. Periodicity is not as evident for the AQ–A_n system as for the Rh–A_n sequences. This apparent decrease in amplitude could be because the AQ is separated from the adenine tract by five bases, introducing dephasing processes. Furthermore, anionic AQ can equilibrate between singlet and triplet states, the former of which is competent to reduce oxygen[34], generating a persistent hole in the DNA that can equilibrate over a long time scale and damage ^{CP}G independently of the bridging sequence, although previous work[13] has shown only a modest effect of oxygen on ^{CP}G ring-opening rates by AQ. Nevertheless, there is clear deviation from monotonicity that is

greater than experimental error, and a period equivalent in length to that observed for the Rh–A_n is evident.

In a sense, the Ap–A_n-^{CP}G sequences should represent an intermediate system between the Ap^* fluorescence quenching and ^{CP}G decomposition assays. The photooxidant is the same as in the fluorescence quenching study, and ^{CP}G decomposition is used as a proxy for charge separation, as with the Rh–A_n and AQ–A_n series. Remarkably, the decay is monotonic (**Figure 2.4**), with a decreasing slope similar to that observed in a system using stilbene as a photooxidant.[16] This could be due to a higher proportion of initial CT-active conformations for short lengths[8] or to changing distribution of yield with length between superexchange, localized hopping, and delocalized hopping mechanisms. Nevertheless, the only consistent difference between the Ap–A_n system and the other three is the presence of efficient BET. Clearly, we can control this non-monotonic effect by changing the extent of BET.

We next considered the effect of eliminating BET while still assaying for ring-opening. The timescale required for efficient charge injection is the nanosecond lifetime of Ap^*, while BET must compete with the faster ring-opening. Hence, we speculated that a bridge modification that sufficiently decreased the rate of CT in both directions could eliminate BET while still maintaining some efficiency for forward transfer.[14,35] Ap^* does not oxidize inosine, and the introduction of inosine into an adenine bridge substantially affects the CT yield. We introduced three inosines between the aminopurine and the adenine tract (**Figure 2.5**). As expected, the total CT efficiency dropped substantially, but the Ap–I_3A_1 sequence has equivalent damage yield to the Ap-I_3A_3 sequence, indicating that BET has been mostly excluded from the system. Importantly, the non-monotonicity

is now restored, supporting the hypothesis that BET was responsible for suppressing the periodicity.

These results are straightforward to reconcile with two recent studies on CT across adenine tracts. In one system, transient absorption spectroscopy was used to measure the production of NDI radical, with PTZ across an A tract participating as the hole acceptor.[15] No periodicity was observed, but it was found that BET substantially depletes the charge-separated state. Similarly, another series of experiments considered CT across an adenine tract between two capping stilbenes.[16] The length dependence found in this study is identical to that for Ap–A_n–^{CP}G, and no periodicity was observed. Furthermore, BET of the injected hole is rapid in this system as well. Notably, although a recent theoretical treatment of three-adenine tracts implied that the stiffness introduced by the bridging stilbene used in this study does not profoundly influence local coupling constants[36], this environment might well affect formation of delocalized domains.

2.4.2. Distance Dependence for RH–A_N–$^{CP}A_M$ Decomposition

The distance dependence for CT yield is dependent on the injection yield, the contribution of incoherent and coherent channels, and the relative rates of charge recombination, charge migration, and charge trapping. It is unlikely that measured effective logarithmic distance dependences of CT in DNA correspond to the inherent electronic coupling factor β, particularly for cases where hopping is the dominant mechanism.

Adenine tracts are particularly interesting as a medium for CT due to their resistance to inherent charge trapping,[15,29] structural homogeneity, and established

efficient CT.[6,15,16] Yields of CT from sugar radicals to triple guanine sites were found to decrease exponentially with increasing A-tract length up to three adenine base pairs, but yields through longer A-tracts followed a weaker distance dependence.[17] The kinetics of CT through A-tracts were examined later by transient absorption of stilbene-capped hairpins; rates with increasingly weak distance dependences were attributed to superexchange, localized hopping, and delocalized hopping with limiting $\beta \sim 0.1$ Å^{-1}.[16] Studies to examine injection yields of CT through A-tracts have also been performed with phenothiazine as the hole acceptor and naphthaldiimide as the hole donor, with $\beta = 0.08$ Å^{-1}.[15] With phenothiazine and 8-oxo guanine, a β value of 0.2 Å^{-1} is observed. Interestingly, when the A-tract is disrupted by insertion of a double guanine site, CT is attenuated. We have investigated charge injection through increasing length A-tracts by monitoring the quenching of photoexcited 2-aminopurine by guanine and also observe a shallow distance dependence ($\beta \sim 0.1$ Å^{-1}).[6]

CT over the 14 base pair A-tract is distance-independent (**Figure 2.8**), contrasting strongly with previous studies using acceptors that are external to the bridge. This is not merely a consequence of attenuated BET, as a steeper distance dependence of roughly 0.02 Å^{-1} is found for the Rh–A_n assemblies, where both the photooxidant and the injection environment are identical. The flatness implies that all holes reach the adenine tract terminus following injection. Thus, the timescale for transport over the entire 48 Å adenine tract must be faster than BET from the first bridge position. These data cannot be explained by a localized hopping mechanism through the 14 bases of the A-tract.

These results also demonstrate the importance of fast traps. Guanine damage experiments[13,17] also result in a shallow distance dependence across adenine tracts over

longer distance, but with a guanine trap there is charge equilibration prior to the millisecond trapping event.[37] Here, the cyclopropylamine ring opening occurs faster than charge equilibration. We previously found that the stacking of the donor and acceptor with the DNA bases has a dramatic effect on the distance dependence of CT through adenine tracts.[2] With ethenoadenine, a poorly stacked adenine analogue, as the photooxidant, a steeper β value of 1.0 $Å^{-1}$ is found, consistent with poorly coupled superexchange. This is a characteristic value found for purely σ bonded systems.[38] With the well-stacked adenine analogue 2-aminopurine as photooxidant, the distance dependence is that expected in well-stacked systems. In this context, the present results are not surprising.

Thus, a well-coupled trap incorporated into an A-tract bridge can be oxidized through DNA-mediated CT without significant attenuation over 5 nm. This is not due to suppression of BET, but rather to the competition between BET and oxidation of the trap being sensitive to the nature of the trap, even for large separation. These results are completely consistent with a fully delocalized transport model.

2.4.3. CONFORMATIONAL GATING THROUGH DELOCALIZED CT-ACTIVE DOMAINS

Previously, we interpreted the periodic length dependence in the context of a certain number of bases being ideal for forming a CT-active domain.[6] When an integer number of CT-active domains can readily form between the acceptor and donor, CT is accelerated, either coherently through two mutually CT-active domains or incoherently by hopping between such domains. For a non-integer number of domains, dephasing processes, such as domain drift, are required. These processes are slower and decrease the

probability of CT to the acceptor before charge recombination. A similar argument has been made in the context of polaron hopping.[11] The experiments described here do not distinguish between the two mechanistic arguments. Nevertheless, the fact that BET suppresses the periodicity supports the notion that increased CT across certain bridge lengths is the inherent source of the periodicity.

Since the conformationally gated domain hopping model ascribes the periodicity to the change in A-tract length, it is interesting to compare distance dependences to a system in which the A-tract length is fixed. This was accomplished by monitoring decomposition of cyclopropyladenine (^{CP}A) serially substituted at each position within a 14 base-pair adenine tract. In contrast to the ^{CP}G trapping situation, there is no periodic variation of the yield with ^{CP}A position for a given A-tract length. This result is consistent with our domain hopping model, as a given length A-tract will accommodate a similar domain structure regardless of the placement of the trap.

2.4.4. OTHER THEORETICAL PREDICTIONS OF PERIODIC DISTANCE DEPENDENCE

There have been theoretical predictions of a periodic length dependence of CT. In particular, when the energies of the donor, bridge, and acceptor are similar, on-resonance CT has been calculated to have a periodic length dependence.[39-41] In these theoretical studies of molecular wires, though an exponential distance dependence was found for off-resonance CT, smooth, bounded periodicities were predicted for on-resonance coupling; energetic inhomogeneities along the bridge could attenuate the periodicities.[40] Although these studies modeled the wire between metals, the same analyses could apply to a sufficiently gated charge-transfer system, such that the donor can be excited

independently of the bridge. It is possible that DNA fulfills that requirement based on the apparent conformational gating. A separate novel approach to determine the coupling across a molecular bridge formulated the lengthening of the bridge as iterative perturbations. Here, too, a non-monotonicity was predicted for on-resonant transfer, but was aperiodic and unstable with respect to the coupling parameters.[41]

Interestingly, Renger and Marcus have calculated a periodic length dependence for CT across an A-tract DNA bridge using a model that allowed delocalization of the electron hole over several bases.[12] These periodicities were eliminated by incorporation of a static disorder term.

The periodic length dependence found in this study does not appear to be related to on-resonance CT. The periods are the same for the different photooxidants, Ap, Rh, AQ, with different oxidation potentials; this similarity argues that the periodicity is not electronic in nature. More importantly, these theoretical periodicities are all with regard to donor-acceptor separation, not adenine tract length. Only the CT-active domain model predicts that serially inserting a ^{CP}A trap along an adenine tract of constant length will eliminate the periodicity; a quantum or symmetry effect would be, if anything, more pronounced in such a system.

It is remarkable that we are able to observe these periodicities in DNA CT using disparate assays so long as the experiments probe events on a fast timescale and isolate convoluting processes such as BET and trapping events. The observations here underscore the utility of applying cyclopropylamine-modified bases as fast traps for CT. More importantly, it is clear that engineering differing extents of BET allows control over the extent of length-dependent periodic behavior.

2.5. REFERENCES

(1) (a) Schuster, G. B., Ed. *Long-Range Charge Transfer in DNA, I and II;* Springer: New York, 2004; Vols. 236, 237. (b) Wagenknecht, H. A., Ed. *Charge Transfer in DNA*; Wiley-VCH: Weinheim, 2005. (c) Guo, X.; Gorodetsky, A. A.; Hone, J.; Barton, J. K.; Nuckolls, C. *Nat. Nanotech.* **2008** *3*, 163-167.

(2) (a) Kelley, S. O.; Barton, J. K. *Science* **1999**, *283*, 375-381. (b) Delaney, S.; Pascaly, M.; Bhattacharya, P. K.; Han, K.; Barton, J. K. *Inorg. Chem.* **2002**, *41*, 1966-1974.

(3) (a) Kelley, S. O.; Holmlin, E. R.; Stemp, E. D. A.; Barton, J. K. *J. Am. Chem. Soc.* **1997**, *199*, 9861-9870. (b) Bhattacharya, P. K.; Barton, J. K., *J. Am. Chem. Soc.* **2001**, *123*, 8649-8656. (c) Takada, T.; Fujitsuka, M.; Majima, T. *Proc. Natl. Acad. Sci. U.S.A.* **2007**, *104*, 11179-11183. (d) Boal, A. K.; Barton, J. K. *Bioconugate Chem.* **2005**, *16*, 312-321. (e) Rajski, S. R.; Barton, J. K., *Biochemistry* **2001**, *40*, 5556-5564.

(4) (a) Boon, E. M.; Ceres, D. M.; Drummond, T. G.; Hill, M. G.; Barton J. K. *Nat. Biotech.* **2000**, *18*, 1096-1100. (b) Boon, E. M.; Salas, J. E.; Barton, J. K. *Nat.. Biotech.* **2002**, *20*, 282-286. (c) Kelley, S. O.; Jackson, N. M.; Hill, M. G.; Barton, J. K. *Angew. Chem., Int. Ed*. **1999**, *38*, 941-945. (d) Inouye, M.; Ikeda, R.; Takase, M.; Tsuri, T.; Chiba, J. *Proc. Natl. Acad. Sci. U.S.A.* **2005**, 11606-11610.

(5) (a) Merino, E. J.; Boal, A. K.; Barton, J. K. *Curr. Op. Chem. Biol.* **2008**, *12*, 1-9. (b) Boal, A. K.; Yavin, E.; Lukianova, O. A.; O'Shea, V. L.; David, S. S.; Barton, J. K. *Biochemistry* **2005**, *44*, 8397-8407. (c) Augustyn, K. E., Merino, E. J.; Barton, J. K. *Proc. Natl. Acad. Sci. U.S.A.* **2007**, *104*, 18907-18912. (d) Gorodetsky, A. A.; Dietrich, L. E.

P.; Lee, P. E.; Demple, B.; Newman, D. K.; Barton, J. K. *Proc. Natl. Acad. Sci. U.S.A.* **2008**, *105*, 3684-3689. (e) Merino, E. J.; Barton, J. K. *Biochemistry* **2008**, *47*, 1511-1517.

(6) O'Neill, M. A.; Barton, J. K. *J. Am. Chem. Soc.* **2004**, *126*, 11471-11486.

(7) Smalley, J.F.; Sachs, S.B.; Chidsey, C.E.D.; Dudek, S.P.; Sikes, H.D.; Creager, S.E.; Yu, C.J.; Feldberg, S.W.; Newton, M.D. *J. Am. Chem. Soc.* **2004**, *126*, 14620-14630.

(8) (a) O'Neill, M. A.; Barton, J. K. *J. Am. Chem. Soc.* **2004**, *126*, 13234-13235. (b) Wan, C. Z.; Fiebig, T.; Kelley, S. O.; Treadway, C. R.; Barton, J. K.; Zewail, A. H. *Proc. Natl. Acad. Sci. U.S.A.* **1999**, 96, 6014-6019. (c) O'Neill, M. A.; Becker, H. C.; Wan, C.; Barton, J. K.; Zewail, A. H., *Angew. Chem. Int. Ed.* **2003**, *42*, 5896-5900.

(9) (a) Shao, F.; Augustyn, K. E.; Barton, J. K. *J. Am. Chem. Soc.* **2005**, *127*, 17445-17452. (b) Conwell, E. M.; Rakhmanova, S. V. *Proc. Natl. Acad. Sci. U.S.A.* **2000**, *97*, 4556-4560. (c) Kendrick, T.; Giese, B. *Chem. Commun.* **2002**, 2016-2017. (d) Barnett, R. N.; Cleveland, C. L.; Joy, A.; Landman, U.; Schuster, G. B. *Science* **2001**, *294*, 567-571.

(10) (a) Buchvarov, I.; Wang, Q.; Raytchev, M.; Trifonov, I.; Fiebig, T. *Proc. Natl. Acad. Sci. U.S.A.* **2007**, *104*, 4794-4797. (b) Crespo-Hernández, C.E.; Cohen, B.; Kohler, B. *Nature* **2005**, *436*, 1141-1144. (c) Kadhane, U.; Holm, A.I.S.; Hoffmann, S.V.; Nielsen, S. *Phys. Rev. E* **2008**, *77*, 021901.

(11) Conwell, E. M.; Bloch, S. M. *J. Phys Chem. B* **2006**, *110*, 5801-5806.

(12) Renger, T., Marcus, R. A. *J. Phys. Chem. A* **2003**, *107*, 8404-8419.

(13) (a) Williams, T. T.; Dohno, C.; Stemp, E. D. A.; Barton, J. K. *J. Am. Chem. Soc.* **2004**, *126*, 8148-8158. (b) O'Neill, M. A.; Dohno, C.; Barton, J. K. *J. Am. Chem. Soc.* **2004**, *126*, 1316-1317. (c) Dohno, C.; Stemp, E. D. A.; Barton, J. K. *J. Am. Chem. Soc.*

2003, *125*, 9586-9587. (d) Yoo, J.; Delaney, S.; Stemp, E.D.A.; Barton, J.K. *J. Am. Chem. Soc.* **2003**, *125*, 6640-6641.

(14) (a) Kawai, K.; Osakada, Y.; Fujitsuka, M.; Majima, T. *J. Phys. Chem. B* **2008**, *112*, 2144-2149. (b) Takada, T.; Lin, C.; Majima, T. *Angew. Chem. Int. Ed.* **2007** *46,* 6681-6683. (c) Kawai, K.; Osakada, Y.; Fujitsuka, M.; Majima, T. *Chem. Eur. J.* **2008**, *14*, 3721-3726. (d) Sanii, L.; Schuster, G.B. *J. Am. Chem. Soc.* **2000**, *122*, 11545-11546.

(15) (a) Takada, T.; Kawai, K.; Cai, X.; Sugimoto, A.; Fujitsuka, M.; Majima, T. *J. Am. Chem. Soc.* **2004**, *126*, 1125-1129. (b) Kawai, K.; Takada, T.; Nagai, T.; Cai, X.; Sugimoto, A.; Fujitsuka, M. ; Majima, T. *J. Am. Chem. Soc.* **2003**, *125*, 16198-16199. (c) Kawai, K.; Takada, T.; Tojo, S.; Majima, T. *J. Am. Chem. Soc.* **2003**, *125*, 6842-6843.

(16) (a) Lewis, F. D.; Zhu, H.; Daublain, P.; Fiebig, T.; Raytchev, M.; Wang, Q.; Shafirovich, V. *J. Am. Chem. Soc.* **2006**, *128*, 791-800. (b) Lewis, F. D.; Zhu, H.; Daublain, P.; Cohen, B.; Wasielewski, M. R. *Angew. Chem. Int. Ed.* **2006**, *45*, 7982-7985. (c) Lewis, F.D.; Zhu, H.; Daublain, P.; Sigmund, K.; Fiebig, T.; Raytchev, M.; Wang, Q.; Shafirovich, V. *Photochem. Photobiol. Sciences* **2008**, *7*, 534-539.

(17) Giese, B.; Amaudrut; Köhler, A.-K.; Sporman, M.; Wessely, S. *Nature* **2001**, *412*, 318-320.

(18) (a) Stemp, E.D.A.; Arkin, M.; Barton, J.K. *J. Am. Chem. Soc.* **1997**, *119*, 2921-2925. (b) Burrows, C.J.; Muller, J.G. *Chem. Rev.* **1998**, *93*, 1109-1151.

(19) Elias, B.; Shao, F.; Barton, J. K. *J. Am. Chem. Soc.* **2008**, *130*, 1152-1153.

(20) (a) Kino, K.; Sugiyama, H. *Chem. Biol.* **2001**, *8*, 369-378. (b) Cadet, J.; Douki, T.; Ravanat, J.-L. *Acc. Chem. Res.* **2008**, *41*, 1075-10783.

(21) (a) Nakatani, K.; Dohno, C.; Saito, I. *J. Am. Chem. Soc.* **2001**, *123*, 9681-9682. (b) Shao, F.; O'Neill, M. A.; Barton, J. K. *Proc. Natl. Acad. Sci. U.S.A.* **2004**, *101*, 17914-17919.

(22) The rate of ring-opening for ^{CP}G has not been directly measured, though indirect results from experiments in DNA suggest a subnanosecond rate. BET from guanine cation radical to non-covalent thionine anion radical has been measured as subpicosecond[23], consistent with thionine's lack of competence in producing base-labile guanine decomposition products despite clear evidence from transient absorption spectroscopy that photooxidation occurs[13]. However, ^{CP}G is facilely decomposed by covalent thionine, indicating that the ring-opening rate is at least nanosecond. Similar results are obtained with Ap*, for which forward transport to guanine is 200 ps over a three adenine tract[24], and no damage is observed to guanine due to facile BET, but ^{CP}G ring-opening is observed [13]. These results confirm that ^{CP}G ring-opening is much faster than charge trapping at unmodified guanine. There is no ideal model study. A neutral N-alkylcyclopropylaminyl radical[25] was observed to ring-open with a rate of at least 7.2×10^{11} s^{-1}. This rate is most likely accelerated by the phenyl substitution on the cyclopropyl group, but attenuated by virtue of being the neutral, rather than cation radical.

(23) Reid, G.D.; Whittaker, D.J.; Day, M.A.; Turton, D.A.; Kayser, V.; Kelly, J.M., Beddard, G.S. *J. Am. Chem. Soc.* **2002**, *124*, 5518-5527.

(24) Wan, C.Z.; Fiebig, T.; Schiemann, O.; Barton, J.K., Zewail, A.H. *Proc. Natl. Acad. Sci. U.S.A.* **2000**, *97*, 14052-14055.

(25) Musa, O. M.; Horner, J. H.; Shahin, M.; Newcomb, J. *J. Am. Chem. Soc.* **1996**, *118*, 3862-3868.

(26) Shafirovich, V.; Dourandin, A.; Huang, W.; Geacintov, N.E. *J. Biol. Chem.* **2001**, *276*, 24621.

(27) Holmlin, R.E.; Dandliker, P.J.; Barton, J.K. *Bioconjugate Chem.* **1999**, *10*, 1122-1130.

(28) Gasper, S.M.; Schuster, G.B. *J. Am. Chem. Soc.* **1997**, *119*, 12762-12771.

(29) (a) Joy, A.; Ghosh, A.K.; Schuster, G.B. *J. Am. Chem. Soc.* **2006**, *128*, 5346-5347. (b) Ghosh, A.; Joy, A.; Schuster, G.B.; Douki, T.; Cadet, J. *Org. Biomolec. Chem.* **2008**, *6*, 916-928.

(30) Hatchard, C. G.; Parker, C. A. *Proc. R. Soc. Lon. Ser. A* **1956**, *235*, 518-536.

(31) (a) Turro, C.; Hall, D.B.; Chen, W.; Zuilhof, H.; Barton, J.K.; Turro, N.J. *J. Phys Chem. A* **1998**, *102*, 5708-5715. (b) Dotse, A.K.; Boone, E.K.; Schuster, G.B. *J. Am. Chem. Soc.* **2000**, *122*, 6825-6833. (c) Ly, D.; Sanii, L.; Schuster, G.B. *J. Am. Chem. Soc.* **1999**, *121*, 9400-9410.

(32) The currently accepted oxidation potential for guanosine is ~1.29 V[33], although it is notable that this value is based on irreversible electrochemistry of the isolated nucleoside in acetonitrile.

(33) Steenken, S.; Jovanovic, S.V. *J. Am. Chem. Soc.* **1997**, *119*, 617-618.

(34) Armitage, B.; Yu, C.; Devadoss, C.; Schuster, G.B. *J. Am. Chem. Soc.* **1994**, *116*, 9847-9859.

(35) O'Neill, M. A.; Barton, J. K. *Proc. Natl. Acad. Sci U.S.A.* **2002**, *99*, 16543-16550.

(36) Siriwong K.; Voityuk, A. A. *J. Phys. Chem. B* **2008**, *112*, 8181-8187.

(37) Delaney, S.; Yoo, J.; Stemp, E.D.A.; Barton, J.K. *Proc. Natl. Acad. Sci. U.S.A.* **2004** *101*, 10511.

(38) Gray, H.B.; Winkler, J.R. *Annu. Rev. Biochemistry* **1996**, *65*, 573-561.

(39) Reimers, J.R.; Hush, N.S. *Chem. Phys.* **1990**, *146*, 89-103.

(40) (a) Mujica, V.; Kemp, M.; Ratner, M.A. *J. Chem. Phys.* **1994**, *101*, 6856-6864.

(b) Kemp, M.; Mujica, V.; Ratner, M.A. *J. Chem. Phys.* **1994**, *101*, 5172-5178.

(41) Hsu, C.P.; Marcus, R.A. *J. Chem. Phys.* **1997**, *106*, 584-598.

Chapter 3:

Comparison of Incoherent and Coherent Yields of DNA-mediated Charge Transport[§]

[§] This work was performed in collaboration with Ms. Stephanie Wuerth.

3.1. INTRODUCTION

Molecular charge transport (CT) has been subject to extensive theoretical and experimental studies,[1-4] since nanoscale device elements provide both novel sensing platforms and the potential to extend Moore's Law beyond the current limits of solid-state lithography. The properties of individual assemblies can be difficult to predict, however, because the mechanism of CT can change as a result of small variations in donor and bridge energies, bridge length, or environmental factors. A transition from exponential to geometric distance dependence is frequently interpreted as being due to a change in the dominant mechanism from coherent superexchange over short bridges to incoherent hopping over long bridges. In fact, it is assumed that fast, coherent CT over long distances is impossible, as a bridge low enough in potential to mediate long-range superexchange will be rapidly occupied by charge itself, and that incoherent CT will then dominate.[5] Given these conditions, it is not surprising that a variety of bridging systems have been found to transition between superexchange and hopping for increasing bridge length and decreasing separation of bridge and donor energy levels.[6-7]

DNA has been extensively studied as a molecular bridge, due to the synthetic accessibility of diverse, well-defined structures,[8,9] the biotechnological applications of DNA sensors,[10,11] and the relevance of DNA-mediated charge migration to biological function.[12] DNA CT is mediated by the π-stack of the base pairs, and for well-coupled donors and acceptors, can lead to charge migration over 200 Å.[13] Importantly, fluorescence quenching by CT through DNA has been observed for donor-acceptor separations of up to eight base pairs, indicating that single-step CT can occur over long distances as well.[14] For the quenching of the fluorescent adenine analogue 2-aminopurine

(Ap) by guanine across an adenine tract, the distance dependence is shallow and periodic. The periodicity has been assigned as a consequence of transient delocalization over 3 to 4 base pairs being ideal for forming a CT-active state[14]; this delocalization length has also been found from other experimental and theoretical studies.[15-17] Furthermore, these CT-active states are non-equilibrium states, and their formation is conformationally gated.[14,18,19]

Another approach for studying DNA CT is to measure the decomposition yields of the bases themselves, with guanine being the most reactive to oxidative damage.[20-22] Because guanine radical decomposition is slow in the absence of additional reactive species, such as superoxide,[23] this measure is convoluted with the trapping rate.[21] We have recently studied CT yield using fast *N*-cyclopropyl radical traps,[24] as substituents on guanine,[19,25] adenine,[26] and cytosine[17] through the exocyclic amines. N_2-cyclopropylguanine, incorporated into DNA, is facilely decomposed by photoexcited thionine, despite the femtosecond recombination that has been measured between guanine radical cation and thionine radical anion, indicating the power of these subnanosecond traps for measuring pre-equilibrium hole occupation.[19,22,25]

By using fast radical traps at the hole acceptor, we can determine the yield of total CT. Herein, we measure the quantum yields of total CT in comparable assemblies containing Ap and ^{CP}G separated by adenine tracts. Single-step CT yield is derived from previous measurements of steady-state fluorescence quenching.[14] By comparing the yields of total and single-step CT, we can see the relative contributions of coherent and incoherent channels.

3.2. METHODS

3.2.1. OLIGONUCLEOTIDE SYNTHESIS.

DNA oligonucleotides were synthesized trityl-on using standard phosphoramidite chemistry on an ABI DNA synthesizer with Glen Research reagents. 2-aminopurine (Ap) was incorporated as the N_2-dimethylaminomethylidene protected phosphoramidite (Glen Research). ^{CP}G-modified oligonucleotides were prepared by incorporating the precursor base, 2-fluoro-O_6-paraphenylethyl-2'-deoxyinosine (Glen Research), as a phosphoramidite at the desired position. The resin was then reacted with 1 M diaza(1,3)bicyclo[5.4.0]undecane (DBU, Aldrich) in acetonitrile to effectively remove the O_6 protecting group. Similarly, ^{CP}A-modified oligonucleotides were prepared by incorporating the precursor base, O_6-phenylinosine (Glen Research) as a phosphoramidite at the desired position. For both ^{CP}G- and ^{CP}A- containing strands, the oligonucleotides were subsequently incubated overnight in 6 M aqueous cyclopropylamine (Aldrich) at 60 ^{o}C resulting in substitution, base deprotection, and simultaneous cleavage from the resin. The cleaved strands were dried *in vacuo* and purified by reversed-phase HPLC, detritylated by 80% acetic acid for 15 min, and repurified by reversed-phase HPLC. Oligonucleotides were characterized by MALDI-TOF mass spectrometry. Sequences are provided in **Table 3.1**.

All oligonucleotides were suspended in a buffer containing 50 mM NaCl, 5 mM sodium phosphate, pH 7 and quantified using UV-visible spectroscopy. Duplexes were prepared by heating equal concentrations of complementary strands to 90 ^{o}C for 5 min and slow cooling to ambient temperature.

Table 3.1. DNA assemblies for oxidative decomposition experiments

Ap-A_0-^{CP}G	5'-GATTATAGACATATT**IAp-^{CP}GI**TATTAAGTACATTAC-3' 3'-CTAATATCTGTATAA**CT - CC**ATAATTCATGTAATG-5'
Ap-A_1-^{CP}G	5'-GATTATAGACATATT**IAp-A-^{CP}GI**TATTAAGTACATTAC-3' 3'-CTAATATCTGTATAA**CT -T- CC**ATAATTCATGTAATG-5'
Ap-A_2-^{CP}G	5'-GATTATAGACATATT**IAp-AA-^{CP}GI**TATTAAGTACATTAC-3' 3'-CTAATATCTGTATAA**CT -TT- CC**ATAATTCATGTAATG-5'
Ap-A_3-^{CP}G	5'-GATTATAGACATATT**IAp-AAA-^{CP}GI**TATTAAGTACATTAC-3' 3'-CTAATATCTGTATAA**CT -TTT - CC**ATAATTCATGTAATG-5'
Ap-A_4-^{CP}G	5'-GATTATAGACATATT**IAp-AAAA-^{CP}GI**TATTAAGTACATTAC-3' 3'-CTAATATCTGTATAA**CT -TTTT- CC**ATAATTCATGTAATG-5'
Ap-A_5-^{CP}G	5'-GATTATAGACATATT**IAp-AAAAA-^{CP}GI**TATTAAGTACATTAC-3' 3'-CTAATATCTGTATAA**CT -TTTTT - CC**ATAATTCATGTAATG-5'
Ap-A_6-^{CP}G	5'-GATTATAGACATATT**IAp-AAAAAA-^{CP}GI**TATTAAGTACATTAC-3' 3'-CTAATATCTGTATAA**CT -TTTTTT - CC**ATAATTCATGTAATG-5'
Ap-A_7-^{CP}G	5'-GATTATAGACATATT**IAp-AAAAAAA-^{CP}GI**TATTAAGTACATTAC-3' 3'-CTAATATCTGTATAA**CT -TTTTTTT - CC**ATAATTCATGTAATG-5'
Ap-A_8-^{CP}G	5'-GATTATAGACATATT**IAp-AAAAAAAA-^{CP}GI**TATTAAGTACATTAC-3' 3'-CTAATATCTGTATAA**CT - TTTTTTTT - CC**ATAATTCATGTAATG-5'
Ap-A_9-^{CP}G	5'-GATTATAGACATATT**IAp-AAAAAAAAA-^{CP}GI**TATTAAGTACATTAC-3' 3'-CTAATATCTGTATAA**CT -TTTTTTTTT - CC**ATAATTCATGTAATG-5'
Ap-A_{11}-^{CP}G	5'-GATTATAGACATATT**IAp-AAAAAAAAAAA-^{CP}GI**TATTAAGTACATTAC-3' 3'-CTAATATCTGTATAA**CT -TTTTTTTTTTT - CC**ATAATTCATGTAATG-5'
Ap-A_{12}-^{CP}G	5'-GATTATAGACATATT**IAp-AAAAAAAAAAAA-^{CP}GI**TATTAAGTACATTAC-3' 3'-CTAATATCTGTATAA**CT -TTTTTTTTTTTT - CC**ATAATTCATGTAATG-5'
Ap-A_7-^{CP}A^4	5'-GATTATAGACATATT**IAp-AAA^{CP}AAAA-I**TATTAAGTACATTAC-3' 3'-CTAATATCTGTATAA**CT -TTT TTTT -C**ATAATTCATGTAATG-5'
Ap-A_7-^{CP}A^7	5'-GATTATAGACATATT**IAp-AAAAAA^{CP}A-I**TATTAAGTACATTAC-3' 3'-CTAATATCTGTATAA**CT -TTTTTT T-C**ATAATTCATGTAATG-5'
LC-A_7-^{CP}A^7	5'-GATTATAGACATATT**I A-AAAAAA^{CP}A-I**TATTAAGTACATTAC-3' 3'-CTAATATCTGTATAA**CT-TTTTTT T-C**ATAATTCATGTAATG-5'
Ap-A_5-^{CP}A^3	5'-GATTATAGACATATT**IAp-AA^{CP}AAA-II**TATTAAGTACATTAC-3' 3'-CTAATATCTGTATAA**CT -TT TTT-CC**ATAATTCATGTAATG-5'

Ap-A_5-$^{CP}A^3$-G	5'-GATTATAGACATATT**IAp-AA^{CP}AAA-GI**TATTAAGTACATTAC-3' 3'-CTAATATCTGTATAA**CT -TT TTT-CC**ATAATTCATGTAATG-5'
Ap-A_5-$^{CP}A^3$-^{CP}G	5'-GATTATAGACATATT**IAp-AA^{CP}AAA-^{CP}GI**TATTAAGTACATTAC-3' 3'-CTAATATCTGTATAA**CT -TT TTT - CC**ATAATTCATGTAATG-5'
Ap-A_5-$^{CP}A^2$	5'-GATTATAGACATATT**IAp-A^{CP}AAAA- II**TATTAAGTACATTAC-3' 3'-CTAATATCTGTATAA**CT -T TTTT-CC**ATAATTCATGTAATG-5'
Ap-A_5-$^{CP}A^4$	5'-GATTATAGACATATT**IAp-AAA^{CP}AA-II**TATTAAGTACATTAC-3' 3'-CTAATATCTGTATAA**CT -TTT TT-CC**ATAATTCATGTAATG-5'
Ap-A_5-$^{CP}A^5$	5'-GATTATAGACATATT**IAp-AAAA^{CP}A - I I**TATTAAGTACATTAC-3' 3'-CTAATATCTGTATAA**CT -TTTT T-CC**ATAATTCATGTAATG-5'
Ap-A_6-$^{CP}A^3$	5'-GATTATAGACATATT**IAp-AA^{CP}AAAA-I I**TATTAAGTACATTAC-3' 3'-CTAATATCTGTATAA**CT -TT TTTT-CC**ATAATTCATGTAATG-5'
Ap-A_6-$^{CP}A^3$-G	5'-GATTATAGACATATT**IAp-AA^{CP}AAAA-GI**TATTAAGTACATTAC-3' 3'-CTAATATCTGTATAA**CT -TT TTTT-CC**ATAATTCATGTAATG-5'
Ap-A_6-$^{CP}A^3$-^{CP}G	5'-GATTATAGACATATT**IAp-AA^{CP}AAAA-^{CP}GI**TATTAAGTACATTAC-3' 3'-CTAATATCTGTATAA**CT -TT TTTT- C C**ATAATTCATGTAATG-5'

3.2.2. PHOTOOXIDATION EXPERIMENTS

Samples were irradiated at ambient temperature. Duplexes (30 mL, 10 mM) in PBS were irradiated on a 1000 W Hg/Xe lamp equipped with a monochromator at 325 nm for 30 sec unless otherwise indicated. To analyze for ^{CP}A or ^{CP}G decomposition following irradiation, samples were digested to the component nucleosides by phosphodiesterase I (USB) and alkaline phosphatase (Roche) to completion. The resulting deoxynucleosides were analyzed by reversed-phase HPLC using a Chemcobond 5-ODS-H, 4.6 mm × 100 mm column. The amount of ^{CP}G or ^{CP}A per duplex was determined by taking the ratio of the area of the HPLC peak for d^{CP}G or d^{CP}A to the area of the peak for dT, the internal reference. The decomposition yield is taken as the percent loss of ^{CP}G or ^{CP}A between an irradiated sample and the dark control; at least nine samples and three dark controls are performed for each sequence. Dark control HPLC traces were quantified for the relative amounts of dA, dC, dG, dI, dT, d^{CP}A and d^{CP}G based on duplex sequence, to confirm strand stoichiometry. Actinometry was performed using a 6 mM ferrioxalate standard.[27] The given quantum yield is for the efficiency from the Ap* state to the ring-opened product. Errors are presented at 90% standard error of the mean, using the Student's t-distribution at the appropriate degrees of freedom to determine confidence intervals.

3.3. RESULTS AND DISCUSSION

3.3.1. EXPERIMENTAL DESIGN

To determine the quantum yield of guanine oxidation by photoexcited 2-aminopurine (Ap), we constructed a series of duplex assemblies with Ap separated

from ^{CP}G by adenine tracts of varying length, and measured the decomposition of the radical trap upon irradiation. Inosines are used as barriers for CT from Ap* to bases outside of the tract; the high-potential inosine serves as a tunneling barrier, preventing depopulation of the aminopurine excited state by nucleotides outside of the bridge.[28] Because ^{CP}G is a fast radical trap, its decomposition yield represents the total yield of all pathways that lead to oxidation of guanine, as long as back electron transfer is slower than ring-opening. Importantly, in this work we have determined quantum yields for Ap-$(A)_n$-^{CP}G duplexes that are identical to sequences for which single-step CT yields have been determined,[14] allowing us to compare the relative yields of single-step and multi-step CT (**Figure 3.1**). For direct comparison of guanine and adenine oxidation, we also constructed assemblies containing the ^{CP}A radical trap at various positions along the bridge. We use Ap-A_n-$^{CP}A^m$-Y to indicate a sequence with an adenine tract of length *n*, a ^{CP}A at position *m* along the tract, and terminal base *Y* at the end of the tract (*Y* = G, I, or ^{CP}G). All eight nucleosides are well resolved by HPLC, allowing straightforward quantification of the ^{CP}G or ^{CP}A content per duplex.

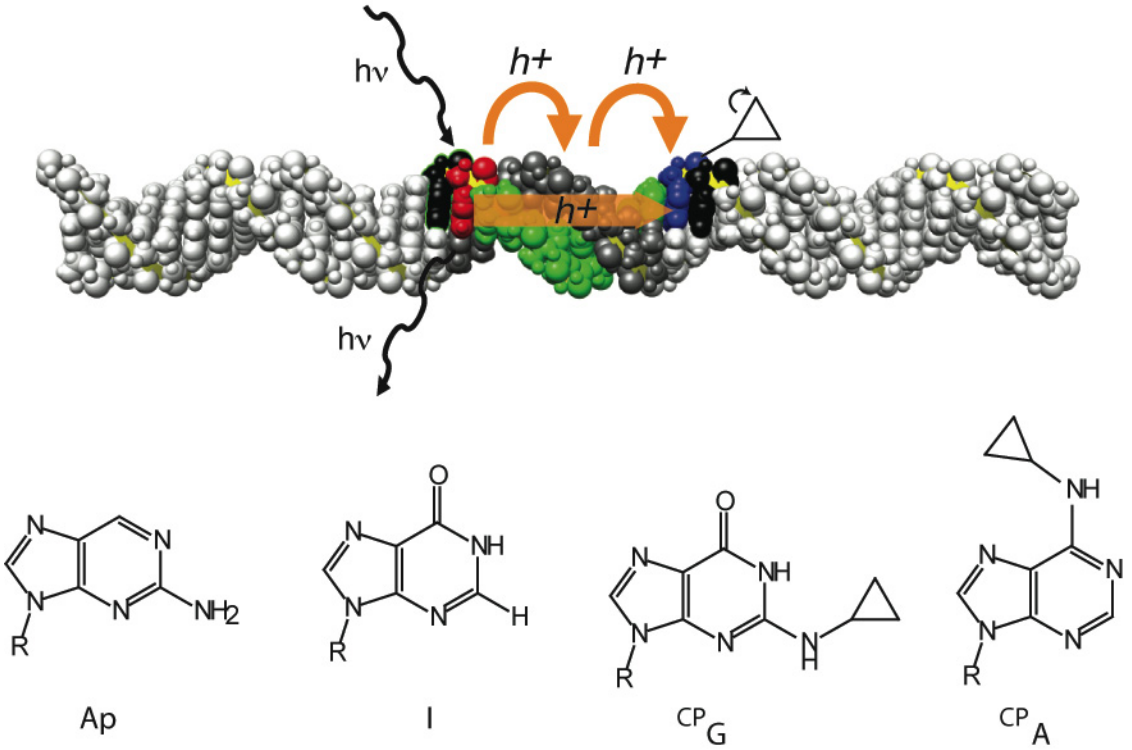

Figure 3.1. Pathways for single-step and multi-step CT in this work. 2-aminopurine (Ap) is selectively excited, and relaxes to a ground excited state that is competent for oxidizing guanine (blue) through the adenine bridge or oxidizing adenine (green) directly. A hole on adenine can then hop to the guanine. These CT processes are in competition with emission; hence emission yield is attenuated by charge transport. Structures of the four unnatural bases employed are provided.

3.3.2. DNA-MEDIATED OXIDATIVE DECOMPOSITION OF ^{CP}G BY Ap*

Upon irradiation, facile decomposition is observed for ^{CP}G, indicating oxidation of the guanine by photoexcited Ap (**Table 3.2**). For short donor-acceptor separation (n = 0–3), little ring-opening occurs, because charge recombination between the aminopurine radical anion and guanine cation radical is competitive with radical trapping at the ^{CP}G.[19,25] For four intervening adenines, the quantum yield peaks at about 1%, followed by a slow decay for longer sequences. The peak value is comparable to the quantum yield (1.7%) of emission from Ap-$(A)_n$-I sequences,[14] and the profile is similar to that which has previously been observed for oxidation of ^{CP}G by Ap.[19]

3.3.3. DETERMINATION OF SINGLE-STEP CT YIELDS FROM FLUORESCENCE QUENCHING YIELDS

Our values of single-step CT yield come from steady-state fluorescence quenching experiments with Ap.[19,29] The fluorescence of Ap in DNA is strongly quenched versus the free nucleoside, even if there is no guanine in the assembly. The presence of a nearby guanine leads to further quenching of fluorescence by a CT mechanism.[29-32] Adenine oxidation by Ap*, while favorable, is far slower than guanine oxidation, as is reduction of cytosine and thymidine by Ap*.[32,33] If the CT quenching by guanine competed with all other relaxation mechanisms, this would imply near quantitative CT between photoexcited Ap and guanine, inconsistent with transient absorption spectroscopy studies on the Ap excited state that find the decays of photoexcited Ap$(A)_3$I and Ap$(A)_3$G in duplex DNA to be indistinguishable,[32] and with

Table 3.2. Quantum yields of decomposition for CP-modified bases

Sequence	Quantum Yield of Decomposition
Ap-A_0-^{CP}G	0.00008 ± 0.00010[a]
Ap-A_1-^{CP}G	0.00002 ± 0.00008
Ap-A_2-^{CP}G	0.00029 ± 0.00016
Ap-A_3-^{CP}G	0.00344 ± 0.00009
Ap-A_4-^{CP}G	0.0086 ± 0.0002
Ap-A_5-^{CP}G	0.0068 ± 0.0005
Ap-A_6-^{CP}G	0.0026 ± 0.0005
Ap-A_7-^{CP}G	0.0017 ± 0.0003
Ap-A_8-^{CP}G	0.00099 ± 0.00003
Ap-A_9-^{CP}G	0.0013 ± 0.0001
Ap-A_{11}-^{CP}G	0.00049 ± 0.00006
Ap-A_{12}-^{CP}G	0.0007 ± 0.0001
Ap-A_7-$^{CP}A^4$	0.0096
Ap-A_7-$^{CP}A^7$	0.00096
LC-A_7-$^{CP}A^7$	0.000066
Ap-A_5-$^{CP}A^3$	0.0019 ± 0.0002
Ap-A_5-$^{CP}A^3$-G	0.0020 ± 0.0002
Ap-A_5-$^{CP}A^3$-^{CP}G	0.0017 ± 0.0002 (^{CP}A)
Ap-A_5-$^{CP}A^3$-^{CP}G	0.0011 ± 0.0003 (^{CP}G)
Ap-A_5-$^{CP}A^2$	0 ± 0.0002
Ap-A_5-$^{CP}A^4$	0.0061 ± 0.0002
Ap-A_5-$^{CP}A^5$	0.0021 ± 0.0002
Ap-A_6-$^{CP}A^3$	0.0022 ± 0.0002
Ap-A_6-$^{CP}A^3$-G	0.0020 ± 0.0001
Ap-A_6-$^{CP}A^3$-^{CP}G	0.0023 ± 0.0002 (^{CP}A)
Ap-A_6-$^{CP}A^3$-^{CP}G	0.0004 ± 0.0003 (^{CP}G)

a. Errors are reported as 90% s.e.m.

the relatively low overall quantum yield of ^{CP}G decomposition. Recent measurements of the time-resolved fluorescence and transient absorption of aminopurine constructs have determined that the hot excited state of aminopurine is quenched prior to vibrational relaxation ($\leq$ 200 fs).[34] This was ascribed to direct CT, but might also involve stacking interactions allowing barrierless conversion to the dark $n\pi^*$ state,[35] which is only 0.4 eV above the relaxed $\pi\pi^*$ state.[36] Furthermore, the temperature dependence of the Ap^* picosecond decay components supports the presence of two different populations of assemblies. Those in an initially CT-active state proceed to rapid CT, while CT for those in a less active configuration is conformationally gated.[37] This explains the similar picosecond decay kinetics of photoexcited $Ap(A)_3I$ and $Ap(A)_3G$ despite the difference in steady-state fluorescence quenching; the populations undergoing CT may not be in direct competition.

In summary, it appears that CT from Ap^* to guanine for assemblies that are initially in CT-active states competes only with emission. If single-step CT to guanine is in competition with other relaxation mechanisms as well, then this model will underestimate the quantum yield. For the above description of the excited state dynamics (**Figure 3.2**), the quantum yield of CT from the relaxed, CT-active state corresponds to the difference in emission quantum yields between assemblies that contain redox-active guanine and those that contain redox-inactive inosine. We can compare these values to our measurements for total CT yield from ^{CP}G decomposition.

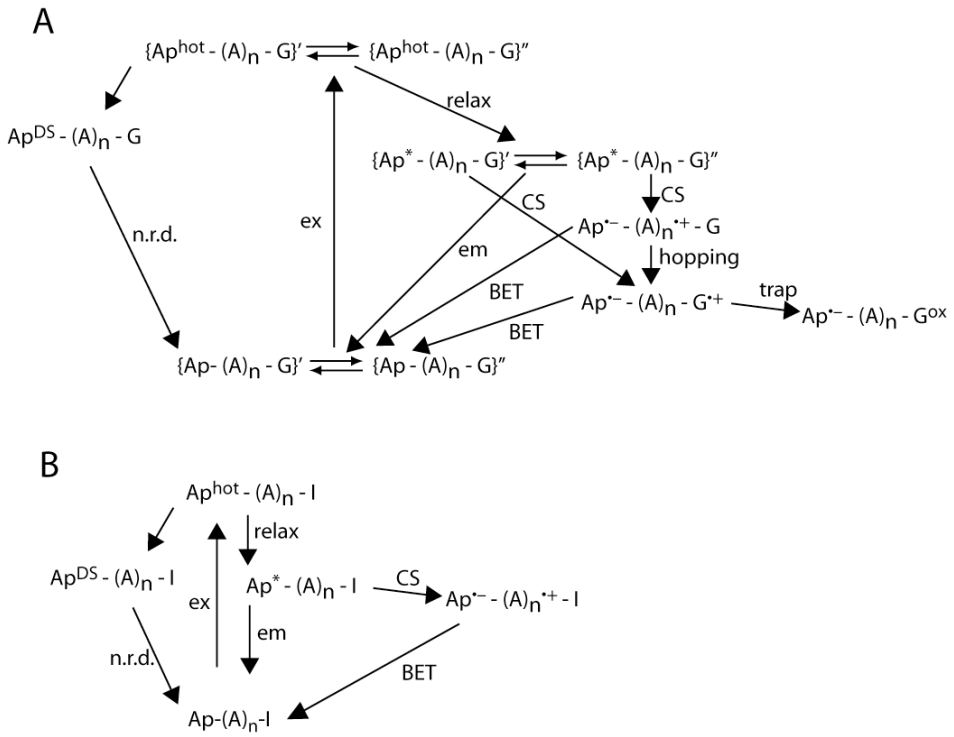

Figure 3.2. Excited-state dynamics of aminopurine in DNA. All duplexes are initially excited (ex) to a hot state (Ap^{hot}), which can either decay through a non-radiative pathway (n.r.d.) through a dark state (DS), or relax to the persistent excited state (Ap^{*}). For guanine-containing duplexes (**A**), some assemblies are in a CT-active state with respect to guanine at the time of excitation (single prime), while others are not (double prime). Assemblies that are not in a CT-active state with respect to guanine, or that contain inosine instead of guanine (**B**), can undergo either emission (em) or charge separation (CS) to generate the adenine cation radical, which regenerates the ground state upon back electron transfer (BET). If a guanine is present, the hole on adenine can hop to guanine. Assemblies that are in a CT-active state with respect to guanine can undergo either emission or charge separation to guanine. Guanine cation radical then decays by either ring-opening (in the ^{CP}G constructs) or BET. Relative heights are arbitrary.

3.3.4. COMPARISON OF SINGLE-STEP AND TOTAL CT YIELDS

It is not surprising that most CT in photoexcited Ap-A_n-^{CP}G is multi-step for n = 4–6 (**Figure 3.3**). Aminopurine is competent to oxidize adenine directly, generating a hole that can migrate across the adenine tract to guanine. Unexpectedly, the distance dependence for the total CT is steeper than the coherent component, such that all CT is coherent for n = 7, 8. This represents the first case of coherent CT overtaking incoherent CT at longer distances.

Furthermore, the changing contributions of the two mechanisms could not have been determined by solely measuring the total CT yield. The distance dependence for n > 4 is fit equally well by geometric or exponential decay (**Figure 3.4**); generally, fits of CT rates to these two decays tend to be equivalent for realistic bridge lengths.[38] In fact, the distance dependence of the total yield is similar to that observed for total CT between stilbenes in photoexcited stilbene-capped DNA hairpins, which are incompetent for coherent CT over more than a couple of base pairs.[39] The geometric dependence gives an η of 2.6, corresponding to a small bias towards migration away from the ^{CP}G,[40] probably due to coulombic attraction to the aminopurine anion radical.[41]

The yields of coherent CT determined using the model of **Figure 3.2** are the least generous possible, i.e. CT to guanine is only in competition with emission. If CT to guanine competes with CT to adenine, or with the pre-relaxation dynamics, then the coherent CT yield is necessarily higher than the values we use for the analysis here. Similarly, if charge injection from the hot aminopurine state can lead to ring-opening, our decomposition yield is an overestimate for the total CT yield from the relaxed excited

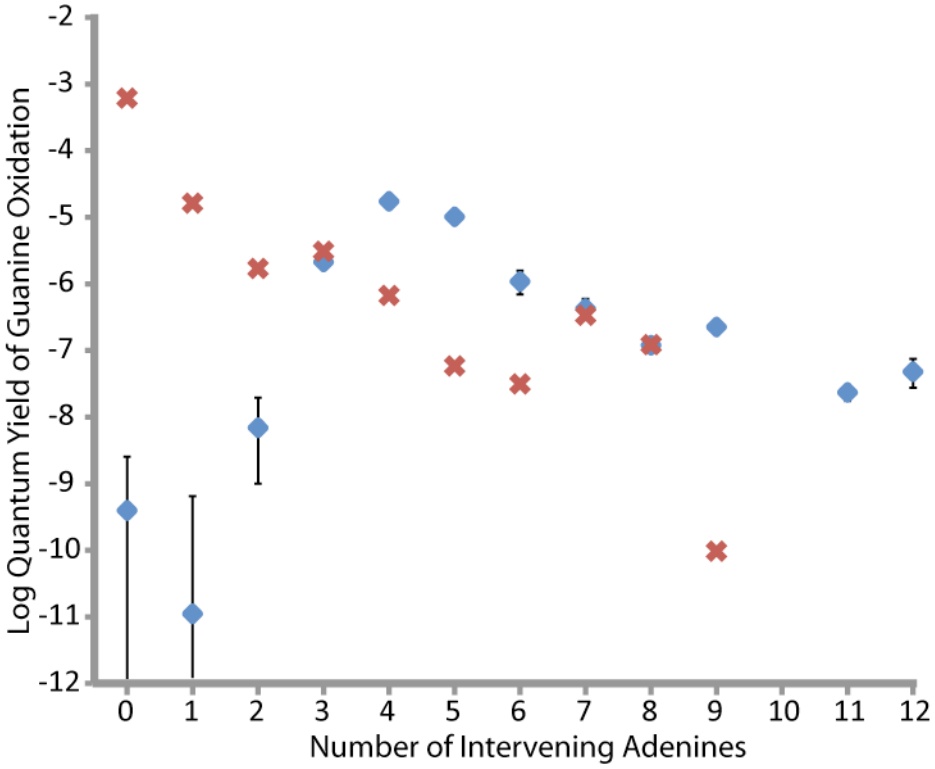

Figure 3.3. CT quantum yields as a function of bridge length for the Ap-A_n-^{CP}G series (blue diamonds), as determined by ring-opening of ^{CP}G, on a natural log scale. Duplexes (10 mM) were irradiated at ambient temperature for 30 sec at 325 nm in 5 mM sodium phosphate, 50 mM NaCl, pH 7.0 as described in the text. The experiments were repeated at least nine times, with the results averaged and the error expressed as 90% confidence intervals of the mean. On the same plot, fluorescence quenching quantum yields for the analogous duplexes are shown for comparison (red x's, data from reference 14).

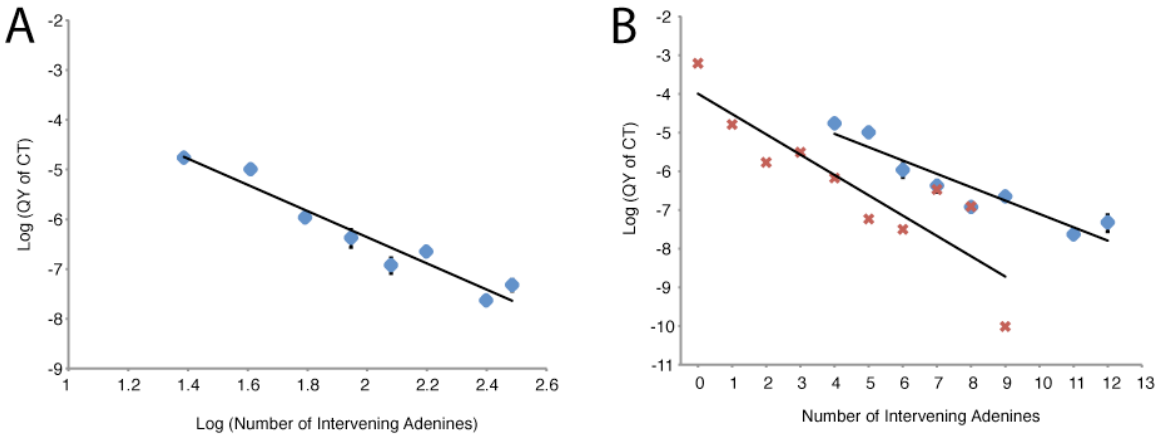

Figure 3.4. Fits of distance-dependent CT yields for the Ap-A_n-^{CP}G series on a log (**A**) and semilog (**B**) scale. Conditions are as in **Figure 3.3**. For the total CT yield (blue diamonds), the data is equally well-fit by geometric and exponential decay with distance. The decay constant from fitting to geometric decay, η, is 2.6. The decay constant from fitting to exponential decay is 0.3 per base (0.1 $Å^{-1}$). The single-step CT yields (red x's) do not fit well to an exponential distance dependence, due to the periodicity.

state. Hence, our values for coherent yield are lower bounds, while our values for total yield are upper bounds. Total CT is necessarily greater than its coherent component. In this context, the equivalence of the CT yields for coherent and total transport at n = 7, 8 validates the model for the excited-state dynamics.

3.3.5. DNA-MEDIATED OXIDATIVE DECOMPOSITION OF ^{CP}A BY Ap*

To directly measure oxidation of the bridge, we inserted ^{CP}A, an unnatural adenine analogue, into the adenine tract. The potential of Ap* is barely adequate for adenine oxidation, but we find rapid decomposition of ^{CP}A upon irradiation of Ap-containing duplexes (**Figure 3.5**). As ^{CP}A is moved along the 5-adenine tract, there is the same initial increase in yield due to charge recombination competing with trapping (**Table 3.2**).

We would expect that ^{CP}A in the adenine tract would interfere with incoherent oxidation of ^{CP}G. Far less ^{CP}G decomposition is observed for Ap-A_5-$^{CP}A^3$-^{CP}G and Ap-A_6-$^{CP}A^3$-^{CP}G than the respective assemblies without ^{CP}A, Ap-A_5-^{CP}G and Ap-A_6-^{CP}G. For both bridge lengths, the quantum yield of ^{CP}G decomposition when incoherent transport is blocked is similar to the quantum yield of emission quenching by guanine. This is consistent with our assignment of the emission quenching yield as the yield of coherent CT to guanine.

There is evidence for delocalization from the yield of ^{CP}A decomposition. Significantly less ^{CP}A decomposition is observed for Ap-A_5-$^{CP}A^3$-^{CP}G than for Ap-A_6-$^{CP}A^3$-^{CP}G, where the only difference is the number of adenines between ^{CP}A and

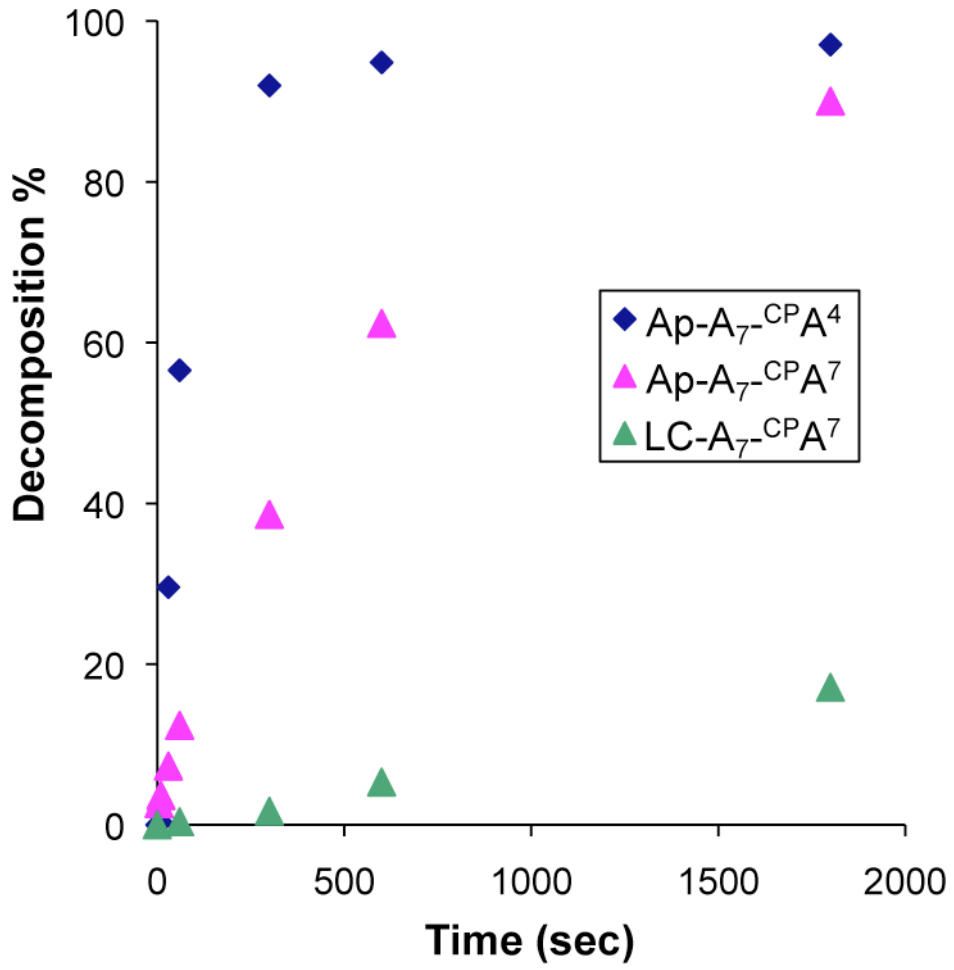

Figure 3.5. Time courses of ^{CP}A decomposition by irradiation of Ap–A_7-$^{CP}A^4$ (blue diamonds), AQ–A_7-$^{CP}A^7$ (purple triangles), and LC–A_7–$^{CP}A^7$ (green triangles). The decomposition in each case follows first-order kinetics. 10 μM duplexes were irradiated at 325 nm. Conditions are as provided in Methods.

^{CP}G. For two, but not three intervening adenines, ^{CP}G is competent to compete with ^{CP}A for the radical. This sensitivity to a distal trap could be due to polaron formation or transient delocalization along the adenine tract. We have previously observed similar behavior for oxidation of the higher-potential ^{CP}C near ^{CP}G, although in that case competition was not apparent for more than a single intervening adenine.[17]

Intriguingly, ^{CP}A decomposition is insensitive to whether the distant base is an inosine or guanine. When there is no guanine at the end of the adenine tract, the coherent CT pathway that leads to fluorescence quenching is eliminated. If coherent and incoherent CT are in competition, this should lead to an increase in the yield of charge injection to the adenine tract, but such increase in injection is not observed. Hence, incoherent and coherent CT must be proceeding from different populations, as in **Figure 3.2**.

We also observe sensitivity to the length of the adenine tract; Ap-A_5-^{CP}A^4 and Ap-A_7-^{CP}A^4 differ only in the length of the adenine tract, yet the quantum yield of ^{CP}A decomposition increases by 50% for the latter assembly. The longer adenine tract has more runs of 3–4 AT base pairs that include the ^{CP}A, and hence can accommodate more low-potential delocalized orbitals. Again, both a self-trapped polaron following injection and transient delocalization prior to injection are consistent with this interpretation.

3.4. CONCLUSIONS

We have performed direct comparison of the absolute yields of coherent and incoherent CT in the same DNA assemblies, demonstrating that coherent CT dominates the incoherent channel at a donor-bridge separation of 2.7 nm, but not for shorter adenine

tracts. The change of mechanism could not be determined from analyzing only the distance dependence of the total yield, which is fit equally well by exponential (superexchange) and geometric (hopping) decays. The transition from multi-step to single-step transport, opposite to that typically found across molecular bridges, is due to a shallower distance dependence for coherent CT versus incoherent hopping. The steeper decay for hopping might be due to coulomb attraction within the radical ion pair intermediate, while the shallow decay of coherent CT indicates that the distance dependence does not reflect the drop in bridge-mediated electronic coupling, but rather represents the conformational dynamics for forming a CT-active state. Coherent and incoherent CT do not appear to be in competition, implying that CT-active states favor the former and CT-inactive states favor the latter.

Over a long adenine tract that can accommodate delocalized domains, long-distance single-step CT dominates the overall transport. Models of DNA-mediated CT must consider the contribution of long-range transfer, subject to sequence-dependent conformational dynamics.

3.5. REFERENCES:

1) Chen, F.; Hihath, J.; Huang, Z.; Li, X.; Tao, N.J. *Annu. Rev. Phys. Chem.* **2007**, *58*, 535.

2) Davis, W.B.; Ratner, M.A.; Wasielewski, M.R. *J. Am. Chem. Soc.* **2001**, *123*, 7877.

3) Weiss, E.A.; Ratner, M.A.; Wasielewski, M.R. *Top. Curr. Chem.* **2005**, *257*, 103.

4) Newton, M.D.; Smalley, J.F. *Phys. Chem. Chem. Phys.* **2007**, *9*, 555.

5) Berlin, Y.A.; Grozema, F.C.; Siebbeles, L.D.A.; Ratner, M.A. *J. Phys. Chem. C* **2008**, *112*, 10988.

6) Weiss, E.A.; Tauber, M.H.; Kelley, R.J.; Ahrens, M.J.; Ratner, M.A.; Wasielewski, M.R. *J. Am. Chem. Soc.* **2005**, *127*, 11842.

7) Goldsmith, R.H.; Sinks, L.E.; Kelley, R.F.; Betzen, L.J.; Liu, W.; Weiss, E.A.; Ratner, M.A.; Wasielewski, M.R. *Proc. Natl. Acad. Sci. U.S.A.* **2005**, *102*, 3540.

8) Murphy, C.J.; Arkin, M.R.; Jenkins, Y.; Ghatlia, N.D.; Bossmann, S.H.; Turro, N.J.; Barton, J.K. *Science* **1993**, *262*, 1025.

9) Lewis, F.D.; Liu, J.; Weigle, W.; Rettig, W.; Kurnikov, I.V.; Beratan, D.N. *Proc. Natl. Acad. Sci. U.S.A.* **2002**, *99*, 12536.

10) Drummond, T.G.; Hill, M.G.; Barton, J.K. *Nat. Biotechnol.* **2003**, *21*, 1192.

11) Takada, T.; Fujitsuka, M.; Majima, T. *Proc. Natl. Acad. Sci. U.S.A.* **2007**, *104*, 11179.

12) Merino, E.J.; Boal, A.K.; Barton, J.K. *Curr. Op. Chem. Biol.* **2008**, *12*, 229.

13) Genereux, J.C.; Barton, J.K. *Chem. Rev.* **2009**, *in press*.

14) O'Neill, M. A.; Barton, J. K. *J. Am. Chem. Soc.* **2004**, *126*, 11471.

15) Adhikary, A.; Kumar, A.; Khanduri, D.; Sevilla, M.D. *J. Am. Chem. Soc.* **2008**, *130*, 10282.

16) Conwell, E. M.; Bloch, S. M. *J. Phys Chem. B* **2006**, *110*, 5801.

17) Shao, F.; Augustyn, K. E.; Barton, J. K. *J. Am. Chem. Soc.* **2005**, *127*, 17445.

18) O'Neill, M. A.; Barton, J. K. *J. Am. Chem. Soc.* **2004**, *126*, 13234.

19) Genereux, J.C.; Augustyn, K.E.; Davis, M.L.; Shao, F.; Barton, J.K. *J. Am. Chem. Soc.* **2008**, *130*, 15150.

20) Hall, D.B.; Holmlin, R.E.; Barton, J.K. *Nature* **1996**, *382*, 731.

21) Liu, C.-S.; Hernandez, R.; Schuster, G.B. *J. Am. Chem. Soc.* **2004**, *126*, 2877.

22) Williams, T. T.; Dohno, C.; Stemp, E. D. A.; Barton, J. K. *J. Am. Chem. Soc.* **2004**, *126*, 8148-8158.

23) Shafirovich, V.; Dourandin, A.; Huang, W.; Geacintov, N.E. *J. Biol. Chem.* **2001**, *276*, 24621.

24) Nakatani, K.; Dohno, C.; Saito, I. *J. Am. Chem. Soc.* **2001**, *123*, 9681.

25) O'Neill, M. A.; Dohno, C.; Barton, J. K. *J. Am. Chem. Soc.* **2004**, *126*, 1316.

26) Augustyn, K. E.; Genereux, J. C.; Barton, J. K. *Angew. Chem. Int. Ed.* **2007**, *46*, 5731.

27) Hatchard, C. G.; Parker, C. A. *Proc. R. Soc. Lon. Ser. A* **1956**, *235*, 518.

28) O'Neill, M.A.; Barton, J.K. *Proc. Natl. Acad. Sci. U.S.A.* **2002**, *99*, 16543.

29) Kelley, S. O.; Barton, J. K. *Science* **1999**, *283*, 375.

30) Somsen, O.J.G.; Keukens, L.B.; de Keijzer, M.N.; van Hoek, A.; van Amerongen, H. *ChemPhysChem* **2005**, *6*, 1622.

31) Manoj, P.; Min, C.-K.; Aravindakumar, C.T.; Joo, T. *Chem. Phys.* **2008**, *352*, 333.

32) Wan, C.; Fiebig, T.; Schiemann, O.; Barton, J.K.; Zewail, A.H. *Proc. Natl. Acad. Sci. U.S.A.* **2000**, *97*, 14052.

33) Fiebig, T.; Wan, C.; Zewail, A.H. *ChemPhysChem* **2002**, *3*, 781.

34) Wan, C.; Xia, T.; Becker, H.-C.; Zewail, A.H. *Chem. Phys. Lett.* **2005**, *412*, 158.

35) Hardman, S.J.O.; Thompson, K.C. *Biochemistry* **2006**, *45*, 9145.

36) Perun, S.; Sobolewski, A.L.; Domcke, W. *Mol. Phys.* **2006**, *104*, 1113.

37) O'Neill, M. A.; Becker, H. C.; Wan, C.; Barton, J. K.; Zewail, A. H., *Angew. Chem. Int. Ed.* **2003**, *42*, 5896-5900.

38) Goldsmith, R.H.; DeLeon, O.; Wilson, T.M.; Finklestein-Shapiro, D.; Ratner, M.A.; Wasielewski, M.R. *J. Phys. Chem. A* **2008**, *112*, 4410.

39) Lewis, F.D.; Zhu, H.; Daublain, P.; Cohen, B.; Wasielewski, M.R. *Angwe. Chem. Int. Ed.* **2006**, *45*, 7982.

40) Jortner, J; Bixon, M.; Langenbacher, T.; Michel-Beyerle, M.E. *Proc. Natl. Acad. Sci. USA* **1998**, *95*, 12759.

41) Grozema, F.C.; Tonzani, S.; Berlin, Y.A.; Schatz, G.C.; Siebbeles, L.D.A.; Ratner, M.A. *J. Am. Chem. Soc.* **2008**, *130*, 5157.

Chapter 4:

Modeling Redox Signaling between DNA Repair Proteins for Efficient Lesion Detection[†§]

[†] partially adapted from Boal, A.K.; Genereux, J.C.; Sontz, P.A.; Gralnick, J.A.; Newman, D.K.; Barton, J.K. *Proc. Natl. Acad. Sci. U.S.A.* **2009**, *106*, 15237.

[§] Dr. Amie Boal planned, performed, and analyzed all *in vivo* and mutation experiments and provided EndoIII and Pamela Sontz planned, performed, and analyzed the AFM experiments. Prof. Jeff Gralnick performed strain construction and assisted in designing *E. coli* experiments.

4.1. INTRODUCTION

Base excision repair (BER) proteins, from bacteria to humans, are challenged with combing the genome for DNA base lesions to maintain the integrity of our genetic material.[1,2] This challenge is remarkable given the low copy number of these proteins and that they must discriminate among small differences between modified and natural bases. For MutY, a BER protein in *E.coli* with a human homologue, there are 20 proteins in the *E.coli* cell[3] to interrogate 4.6 million bases; the ratio of binding affinities for the target lesion, an 8-oxoguanine:adenine mismatch, versus well-matched native base pairs is ≤ 1000.[4] Endonuclease III (EndoIII) recognizes a less prevalent lesion, hydroxylated pyrimidines, with equally low specificity; the copy number of EndoIII within *E.coli* is ~500.[1] How these glycosylases fix their substrate lesions, once found, has been well characterized[1,2], as are the structures of MutY and EndoIII bound to DNA.[5,6] Yet how these lesions are efficiently detected before excision is not established.

Location of damaged bases in the genome is likely the rate-limiting step in BER within the cell and, hence, a critical step in maintaining genomic integrity.[7] Current models for genome scanning to detect lesions involve protein sliding along the DNA, squeezing the backbone, slipping bases out to allow for interrogation, or finding transiently opened sites.[8,9] However, given the low copy number of these proteins and their need to sift through the genome to find often subtle base lesions, the time required for this search is long.

Many of these BER proteins contain [4Fe4S] clusters, common redox cofactors in proteins.[1,2] Increasingly, iron-sulfur clusters are found associated with varied DNA-binding proteins and located far from the enzymatic active site with no apparent function. For BER proteins, [4Fe4S] clusters were first thought to play a structural role. When not bound to DNA, these proteins are found in the

$[4Fe4S]^{2+}$ state and are not easily oxidized or reduced under physiological conditions.[10] However, for MutY and EndoIII, we have demonstrated using DNA-modified electrodes that DNA binding shifts the 3+/2+ cluster potential into a physiological range, ~100 mV vs. NHE for each BER enzyme;[11,12] DNA binding stabilizes the protein in the +3 form.

Given the sensitivity of DNA-mediated charge transport (CT) to mismatched and damaged bases, we have proposed that DNA repair glycosylases containing a redox-active [4Fe4S] cluster including EndoIII and MutY, use DNA CT as the first step in substrate detection by signaling one another to search cooperatively for damage in the genome.[11,12] DNA-mediated CT can proceed over long molecular distances on a short timescale.[13] Oxidative damage to DNA has been demonstrated with oxidants covalently tethered and spatially separated from damage sites at distances of >200 Å with negligible loss in efficiency.[14] Reductive CT has been shown to have an equally shallow distance dependence both in electrochemical studies[15] and in assemblies in solution.[16] Previous studies established that CT through DNA is possible in biological environments that include nucleosomes[17] and cell nuclei.[18] DNA CT is, however, extremely sensitive to perturbations in the intervening base-pair stack, such as DNA mismatches and lesions.[19,20] As an example, a single molecule of DNA covalently attached within a nanotube device can conduct charge perpendicular to the π-stack similarly to graphite, but the resistance increases 300-fold with a single base mismatch.[21] DNA-mediated electrochemistry has therefore been utilized in the development of sensors for mutational analysis[20] and protein binding.[22]

Given that this chemistry occurs at a distance and is modulated by the structural integrity of the base-pair stack, these reactions may be useful within the cell for long-range signaling to proteins. In that context, we have previously established the long-range oxidation of the DNA-bound BER enzymes in spectroscopic studies monitoring oxidation of the [4Fe4S] clusters by

guanine radicals in the duplex.[23] Importantly, we have also shown the injection of an electron into the base pair stack from the DNA-bound BER enzymes, with the electron trapped by a well-coupled modified base in the duplex.[24] Both with respect to hole injection into the DNA-bound proteins and electron injection into the DNA from the DNA-bound proteins, EndoIII and MutY behave equivalently, as expected given their similar DNA-bound redox potentials and structures. Here we explore whether it is reasonable to expect DNA-mediated CT to provide a means to facilitate the detection of damage *in vivo*, and then compare these predictions to some experimental data from *E. coli* and single-molecule AFM experiments.

4.2. METHODS AND RESULTS

4.2.1. DNA-BINDING AFFINITY OF ENDOIII

There are three properties that determine a protein's diffusive properties in a DNA environment: the one- and three- dimensional diffusion constants, and the nonspecific binding affinity for DNA.[8,25] Measurements have been performed for the nonspecific affinity of MutY and of EndoIII,[9,26] but these preceded the discovery that the electrochemical potential of iron-sulfur clusters in these proteins varies by 200 mV between the DNA-bound and free forms of the proteins.[27] Thus, measured affinities were for a mixture of oxidized and reduced protein. Hence, we measured binding affinities using EndoIII in the presence and absence of 3 mM DTT, to better estimate the individual nonspecific binding affinities of the two forms of the protein.

The binding buffer was 20 mM $NaPO_4$, 100 mM NaCl, 10% glycerol, 0.1 ug/uL bovine serum albumin. The gels were BioRad 10% TBE gels ran in 0.5X TBE at 4 ^oC. Protein was prepared at a concentration of 80 μM or 8 μM, and serial dilutions in factors of three were used to prepare the other protein concentrations. The labeled strand was of sequence

5'-CTGTAACGGGAGCTCGTGGCTCCATGATCG-3'. This strand and its complement were synthesized on an ABI DNA synthesizer using standard phosphoramidite chemistry, purified twice by reversed-phase HPLC and characterized by mass-spectrometry and UV-vis. Labeling was performed at the 5'-end with [^{32}P] γ-ATP using polynucleotide kinase, followed by isolation with Micro Bio-Spin 6 columns (BioRad). EndoIII was acquired from Dr. Amie Boal and stored at -80 ^{o}C. Samples were eluted through a 20% denaturing polyacrylamide gel for 1.5 hours at 90 W and imaged on a Storm 820 phosphoimager (Molecular Dynamics/ GE Healthcare). DNA bands were quantified by phosphoimagery using Image Quant 5.2 (Molecular Dynamics). In the absence of DTT, the dissociation constant was found to be 60 ± 10 nM. The presence of DTT increased the dissociation constant by about a factor of 5; the binding was weak enough such that greater than 80% DNA bound to protein would have required a higher concentration of EndoIII than was available. Interestingly, these results bracket the published[26] dissociation constant of 250 ± 100 nM for MutY with this DNA in 1 mM DTT.

The electrochemistry tells us that the dissociation constant (K_D) is between 2000 and 50000 times greater for the reduced versus the fully oxidized protein. Although we do not know the fraction of oxidized protein under ambient conditions, 60 nM serves as an upper bound for K_D^{ox}. We will use this highest possible value for K_D^{ox} and the corresponding lowest value for K_D^{red}, 120 μM, as they are those that are most favorable to the models that do not invoke CT signaling, and least favorable to the model for CT signaling. More accurate values will only increase the predicted improvement of CT signaling versus non-CT signaling models.

4.2.2. GENOME SCANNING CALCULATIONS WITHOUT CT SIGNALING

Protein diffusion to a cognate site on dilute, short DNA strands *in vitro* occurs faster than predicted by the Debye-Smoluchowski equation.[8] This is due to facilitation by the non-cognate DNA: protein weakly associates with non-specific regions of the DNA, and then slides in one dimension to the recognition sequence. *In vivo*, where the concentration of DNA is in the millimolar regime, the challenge of site recognition is different.[25,28] Rather than the non-specific DNA serving as a means to funnel the protein to the recognition site, it acts as a competitor that slows protein translocation. To overcome this challenge, the protein must frequently dissociate from non-specific DNA so that it can sample other portions of the genome, and hence avoid highly redundant sliding on sequences far from the target.

In this context, fast target location requires weak non-specific interactions, fast sliding along the DNA when association occurs, and strong specificity for protein recognition of cognate versus non-cognate DNA.[29] The physical challenge of achieving all of these conditions for the same protein has been widely discussed,[29-31] and many studies have demonstrated that fastest target location is achieved when the non-specific dissociation constant is equal to the concentration of base pairs.[28,32] For a transcription factor that does have the above properties, LacI, real-time single-molecule visualization of its translocation and target recognition within the cell is consistent with this model of efficient facilitated diffusion.[33]

DNA base excision repair proteins do not meet all of the conditions for fast target detection. The non-specific binding constants of oxidized and reduced EndoIII are about 40 nM and 40 μM respectively; the values for MutY appear similar.[26] The specificities are reported as ≤ 1000 for both EndoIII and for MutY.[4,26] There is evidence that the human oxoG:C-targeting base-repair enzyme hOGG1 can slide rapidly on stretched DNA.[34] Surprisingly, the one-

dimensional diffusion constant[35] is at the hydrodynamic limit. It is unclear whether this is consistent with the necessity of displacing bound water and ions, and how such rapid motion can allow specific recognition between the protein and its cognate lesion. We will not neglect the problem of extensive bound protein present in the cell,[36] which should substantially retard the maximum allowable sliding length.[31] Although this effect may help transcription factors with a defined cognate site and weak non-specific binding,[37] the presence of roadblocks should substantially slow search by repair proteins.

The simplest approach to calculating the rate of target recognition for MutY using facilitated diffusion is that described in the original derivation:[8]

$$T_{Search} = \ln\left(\frac{1}{1-P}\right)\left(\frac{2C_p\sqrt{D_1 K_D k_a}}{L}\right)^{-1}$$

$$k_a = 4\pi D_3 r_{DNA}$$

The protein diffusion constant, D_3, is determined from the Stokes-Einstein equation using the 10 cP viscosity of *E. coli* cytoplasm[38] and the measured Stokes radius of EndoIII (r_p).[39] A further adjustment must be made to consider the specificity; rapid dissociation will compete with catalysis. This is incorporated as

$$T_{repair} = T_{Search}\left(\frac{k_{cat}}{k_{cat} + \frac{k_d}{s}\left(\frac{s + l_s}{s}\right)}\right)^{-1}$$

$$l_s \equiv \sqrt{\frac{D_1}{k_d}}$$

where k_{cat} is the catalytic rate,[4] s is the specificity,[26] l_s is the sliding length, and D_1 is the one-dimensional diffusion constant.

This approach yields a respectable time of 96 seconds for a 90% chance of discovery and repair of a lesion by oxidized MutY. The challenge of this approach, however, is that it assumes that protein dissociation is followed by immediate reassociation to any other site on the genome *with equal probability*.[8,25,40] This derivation, while acceptable for short DNA strands in dilute solution, each containing a target site, is not appropriate in the context of genomic DNA, unless the protein has extremely weak non-specific affinity. It has been demonstrated by simulation that, for the genomic density present inside *E. coli*, a protein that dissociates from a single site is 87% likely to return to within a single sliding length of the original site.[25] When this factor, which represents only the most proximal dissociation-reassociation events, is considered, the search time increases to 230 seconds for the oxidized proteins. On a slightly larger scale, bacterial DNA adopts a solenoid-like structure, and the genome of *E. coli* is organized into discrete structural domains of 10 to 100 kb.[41] It is reasonable to expect that dissociation-reassociation events will feature substantial autocorrelation with respect to individual domains at each size-scale.

Furthermore, it has been shown that for *E. coli*, the average gap between bound structural proteins is about 10 to 80 bp.[42] This is adequate for the highly specific transcription factors such as LacI, which has a sliding length of < 85 bp,[33] and that might be able to ratchet other proteins off the edges of its cognate site, driven by recognition of part of the cognate site. For repair proteins, recognition is of a single base, and a lesion beneath a structural roadblock will only be found if the protein moves aside. Taking the most generous value of 80 bp, which is still much smaller than the 4400 bp sliding length without roadblocks, the search time for the oxidized protein becomes 430 minutes, much longer than the *E. coli* doubling rate. Hence, it is clear that target location by the base excision repair protein MutY is not explained by a straightforward diffusive mechanism.

4.2.3. GENOME SCANNING CALCULATIONS WITH CT SIGNALING

We have proposed that BER proteins bearing [4Fe4S] clusters exploit DNA-mediated CT as a fast, sensitive method to detect damage (**Figure 4.1**). This redox signaling model is initiated when one 2+ protein (donor) binds DNA (b, e), promoting electron transfer from the donor protein to a distal protein (acceptor) (c, f), already bound in the 3+ state. The newly oxidized donor protein remains DNA-bound while the reduced acceptor diffuses away (d, f). Integral to this model is a differential DNA affinity for the $[4Fe4S]^{3+}$ and $[4Fe4S]^{2+}$ forms of the protein. We have demonstrated this differential affinity by measuring a -200 mV potential shift associated with DNA binding that corresponds thermodynamically to ≥1000-fold difference in DNA affinity between the oxidized and reduced proteins.[27]

Importantly, the DNA-mediated CT reaction between two repair proteins can be considered a scan of the integrity of the intervening DNA, since DNA-mediated CT can only proceed through a well-stacked duplex. As illustrated in **Figure 4.1** (g), when the repair protein, already oxidized, is bound near a base lesion, DNA-mediated CT does not provide a pathway for reduction and subsequent protein dissociation. The protein instead remains bound to the duplex so that, on a slower timescale, the protein can processively diffuse to the target site; now, however, sliding is needed only across a small region and the low target specificity of the protein is sufficient for recognition.[4,37,43,44] Essentially, then, our proposal for base lesion detection utilizing DNA CT yields a redistribution of the BER enzymes onto local regions of the genome that contain lesions. Critical to this mechanism is DNA-mediated signaling among proteins bound at long range so that the proteins, despite their low abundance, cooperate with one another in localizing onto target sites. Simulations of MutY search using a similar mechanism have shown encouraging accumulation at lesion sites when CT is allowed.[45,46] These simulations allow direct electron

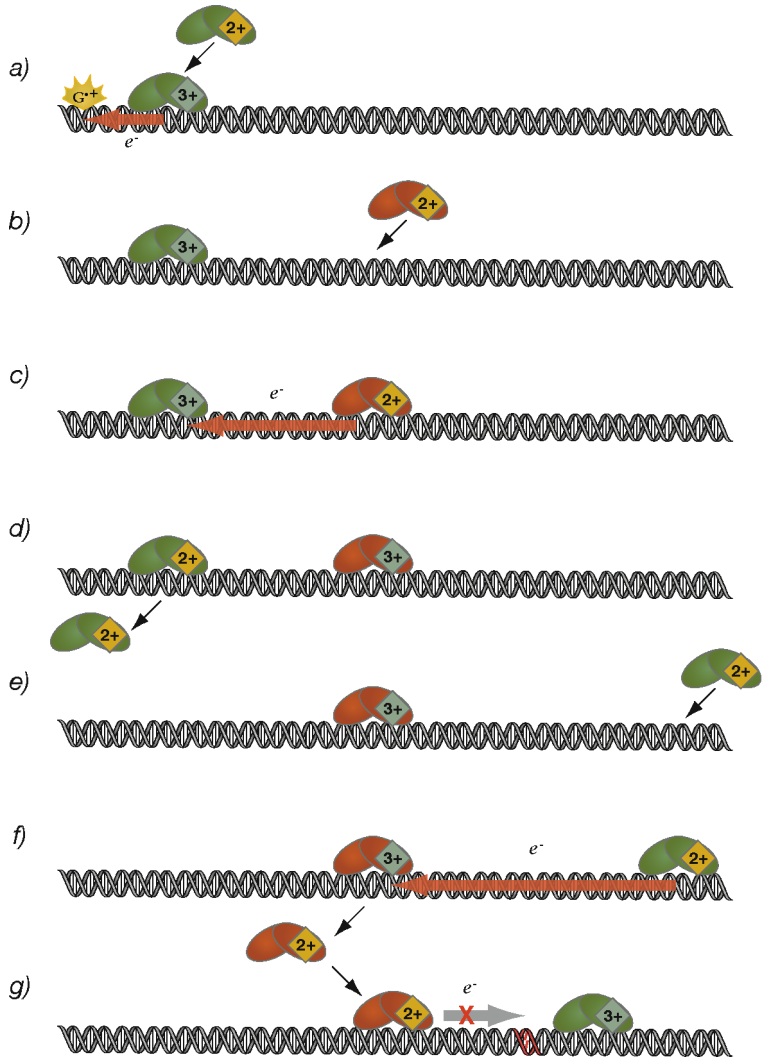

Figure 4.1. A model for DNA-mediated CT in DNA repair. In this model, DNA repair proteins, containing $[4Fe4S]^{2+}$ clusters, for example EndoIII (green) and MutY (orange), bind DNA, activating them towards oxidation to the $[4Fe4S]^{3+}$ state. The sequence of events is as follows: Guanine radical formation can oxidize a repair protein in a DNA-mediated reaction, stabilizing the oxidized protein bound to DNA (*a*). A second protein binds in the vicinity of the first protein (*b, e*). CT to a distally bound protein can occur through the DNA π-stack if the intervening DNA is undamaged (*c, f*). The newly reduced protein has a diminished affinity for DNA and diffuses away (*d*). If, instead, a lesion site is present between the proteins (*g*), the DNA-mediated CT step is inhibited and the oxidized protein remains bound to DNA. In this search mechanism the sum of the DNA-mediated electron transfer steps between proteins constitutes a full search of the genome yielding a redistribution of low-abundance DNA repair proteins in the vicinity of lesions.

injection over very long distances with DNA occupation, and also rely on hole absorption from oxidized 8-oxoguanine, a species known to be highly unstable to oxidation. Since it is not clear whether this is mechanistically allowed, we will take a substantially different approach in this work, limiting our study to CT signaling between proteins, with the DNA only acting as a mediator.

To exploit DNA-mediated CT, some proteins must exist in the oxidized state. There are many oxidants in the cellular milieu, and the level of oxidative stress will govern the proportion of oxidized protein. Indeed, we have shown that these proteins[23] and others[47] can be oxidized by guanine radicals, the first genomic signal of oxidative stress,[48] via DNA-mediated CT. There is also computational support for this activation being facile.[49]

We can calculate the step time for three-dimensional diffusion of the reduced protein to the DNA from

$$T_{Search} = \ln\left(\frac{1}{1-P}\right)\left(k_{CT}\Theta C_p\right)^{-1}$$

where k_{CT} is the rate of search using CT signaling and the other parameters are as defined above. Each oxidized protein provides a separate nucleation site for CT scanning, but draws from the same reservoir of reduced protein to scan different portions of the genome; hence the number of proteins is multiplied by Θ, the fraction of protein that is oxidized. For diffusive search,

$$k_{CT} = 3D_{CT}\left(\frac{2}{L}\right)^2$$

$$D_{CT} = \left(\frac{N}{4}\right)^2 t_s^{-1}$$

where D_{CT} is the effective diffusion of holes using proteins as steps, L is the length of the genome, N is the maximum distance for CT signaling, and t_s is the time for colocalization between the

oxidized and reduced proteins (effectively, the step time). The step length is a quarter of N due to a factor of two from the average yield of self-exchange between the proteins, and another factor of two since the average step length in this case will be half of the maximum step length.

The step time can be found from a modified Debye-Smoluchowski equation for protein collision with a rod of DNA within the cell volume, where the length of the rod is twice the number of bases, N, over which DNA-mediated CT can proceed, since reduced protein can transfer an electron from either side:

$$k_{assoc} = \frac{V}{C_p(1-\Theta)t_s} = 4\pi\kappa f D_3\left(r_{DNA} + r_p\right) + D_a a^3\sqrt{\frac{r_{DNA} + r_p}{a}}$$

$$r_{DNA} = \frac{2(N + l_{s,red})}{2\ln\left(\frac{2(N + l_{s,red})}{R_{DNA}}\right)}$$

$$D_a = \frac{kT\ln\left(\frac{a}{R_{DNA}}\right)}{3\pi\eta a}$$

where V is the cell volume, $C_p(1-\Theta)$ is the number of reduced repair proteins in the volume, r_{DNA} is the DNA radius, r_p is the Stokes radius of the protein, D_a is the segmental diffusion constant, and k_{assoc} is the bimolecular rate constant for protein association with the DNA target within the cellular volume. Any contact of the reduced protein within the DNA rod allows electron transfer to the DNA-bound oxidized protein. We also allow the reduced protein to slide to within this region, although the sliding length for the weakly associated reduced protein is negligible. The Smoluchowski equation is constructed with two terms: one describes the ballistic 3-dimensional diffusion of the reduced protein to the DNA and the second[50] considers the gyrations of a rod with a persistence length of 150 base pairs and the ends fixed as part of the chromosome. The translational DNA diffusion is considered to be negligible. The electrostatic (f) and orientational

(κ) constants are taken as unity,[51] in keeping with the high ionic strength of the *in vivo* environment. The dissociation rate of the protein is not included in our model because charge equilibration should occur on a much faster timescale than dissociation of the reduced protein. This time, for reasonable parameters ranges, varies from 0.5 ms to 2 ms, which corresponds to a sliding length of between 50 and 100 base pairs. This is similar to the distance between bound structural protein on the DNA; CT signaling minimizes the redundancy of search by the oxidized protein between redox events. Note that we make no distinction between 5' to 3' versus 3' to 5' transport, although subtle differences have been observed.[52]

Scanning through sliding/jumping without a CT search represents a boundary condition, so that the total time is

$$T = (T_{CT}^{-1} + T_D^{-1})^{-1}$$

where T_D is the diffusion scanning time, calculated as in Section 4.2.2.

In our model, the DNA is essentially scanned by the electron with the repair proteins facilitating electron migration. Thus we calculate a genome scanning time for MutY in *E.coli* that is significantly more efficient through DNA CT. Since an injected charge equilibrates on the nanosecond timescale,[51] and protein diffusion occurs in micro- to milliseconds, the rate-limiting step in this process is the 3D diffusion of this reduced protein to within CT range of the oxidized DNA-bound protein.

Importantly, since this model involves cooperation among the repair proteins, we can utilize the *total* concentration of these proteins within the cell, rather than copy numbers for MutY or EndoIII individually. Thus MutY, present in 20 copies, benefits from 500 copies of EndoIII.[1] We do, however, neglect contributions from any other proteins that might participate in DNA-mediated signaling; other DNA-bound proteins containing iron-sulfur clusters exhibit similar

potentials, and CT reactions involving these proteins too would substantially speed the search process.

Our model relies on the fact that DNA-mediated interprotein CT is much faster than protein diffusion, and that the oxidized repair proteins have higher nonspecific DNA affinity than the reduced proteins; both assumptions have experimental support.[13,27] One advantage of DNA CT over other search mechanisms is that the electron travels *through* the DNA base pairs and no proteins need to be displaced.[17,53]

Figure 4.2 shows how the interrogation time varies as a function of *N*, the maximum distance over which DNA-mediated CT proceeds, and ox, the percentage of proteins oxidized. Remarkably, permitting DNA CT over 500 bp with 10% oxidized protein yields a conservative interrogation time of 30 minutes, while DNA CT over 500 bp with 20% oxidized protein yields an interrogation time of 17 minutes; permitting DNA CT over 1500 bp yields scan times of about a minute. These values are well within the one hour doubling time of normally growing *E. coli*. While we have not yet established the distance limits for DNA CT, we have demonstrated substantial oxidative damage in tethered DNA assemblies *in vitro* over 60 bp and in DNA within mitochondria over ~100 bp.[14,54]

The dependence of interrogation time on the percentage of proteins oxidized is also noteworthy (**Figure 4.3**). The scanning efficiency resembles a switch that is turned on at low levels of oxidation, when DNA repair is needed. Activation of this switch depends upon the redox buffering capacity of the cell and the level of oxidative stress. This local activation of MutY by oxidized DNA has been supported by theoretical calculation.[48] Furthermore, there might be other redox-active DNA repair proteins in *E. coli*. If other proteins can participate in

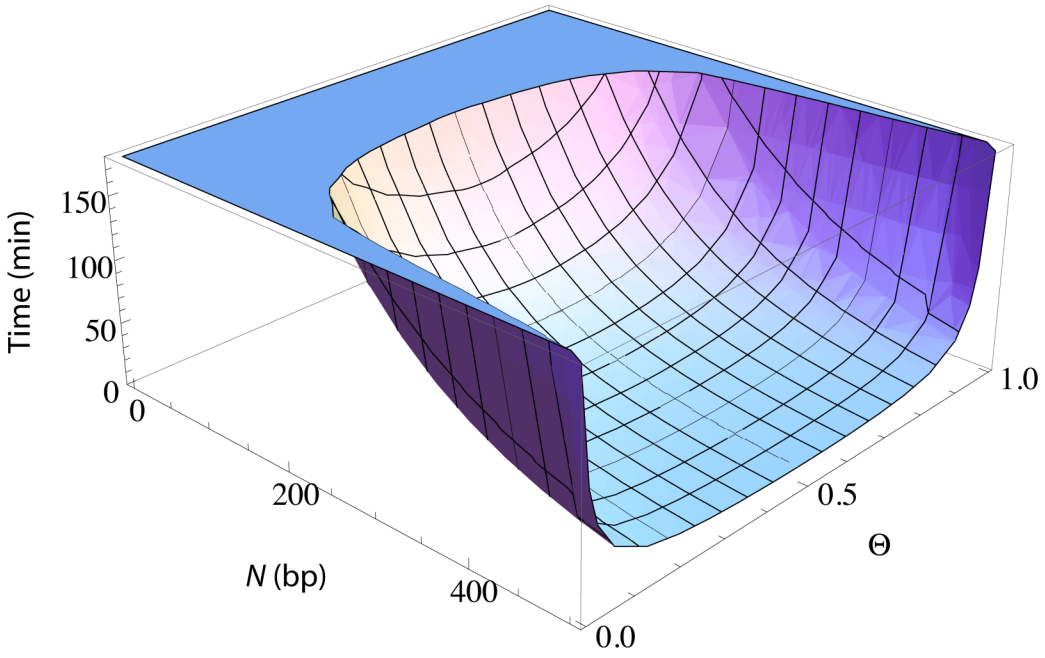

Figure 4.2. Scanning time as a function of maximum distance of DNA-mediated interprotein CT (N) and the fraction of repair proteins that are in the 3+ state (Θ) using the CT scanning model. At 10% oxidized protein with a maximum CT distance of 500 bp, the time required to interrogate the genome is ~5 minutes.

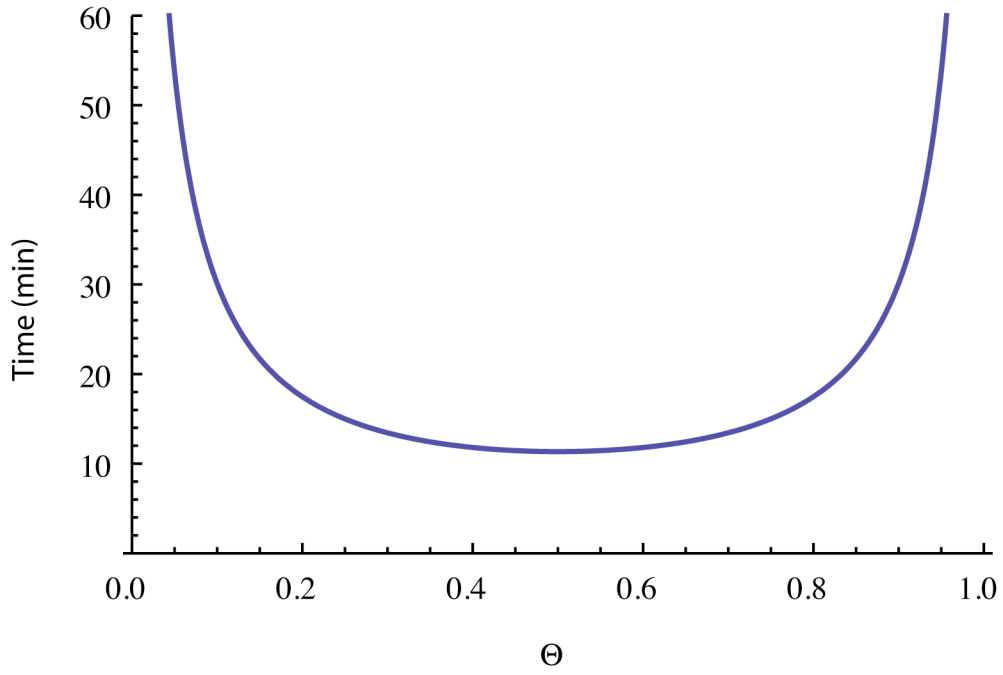

Figure 4.3. For N = 500, the search time using CT shows a sharp drop when a few proteins become oxidized. If all the protein is oxidized or reduced, then CT signaling is no longer possible.

helper function, search times would also rapidly decrease; the search rate increases with the square of searching protein.

We have not taken into account the effect of the reduced protein directly repairing damage. Besides our uncertainty in the reduced protein diffusion rate by an order of magnitude, a further concern is the fact that the specificity of the reduced protein has never been measured. For the weak binding of the reduced species, changes in specificity can change search time substantially. Experimentally determined specificities[4,26] have been measured using mutated protein and base analogues, and under conditions where even a small proportion of oxidized protein will determine the measurement. It has not been demonstrated whether the reduced protein has catalytic activity.

4.2.4. DISTRIBUTION OF ENDOIII BETWEEN TWO STRANDS OF DNA

The above mechanism suggests protein accumulation along a single DNA at a lesion site, which is the genomically relevant case. Recently, the Barton group has begun to explore EndoIII distribution between two different types of long strands: those with fully matched DNA, and those containing a single non-cognate lesion. The relative protein affinities are measured by AFM, with matched (2.2 kb, 1.6 kb) distinguished from mismatch-containing DNA (3.8 kb) on the basis of length. EndoIII accumulates on the mismatch-containing strand, in a manner dependent on the CT competence of the protein. In the context of the above model, one might not expect EndoIII to distinguish between these two types of DNA. After all, CT signaling does not affect the number of reduced and oxidized proteins on a given strand of DNA, it only changes their positions along the strand. How can a change in distribution along strands affect the distribution between strands?

A protein bound to genomic DNA has only one pathway for dissociation. On linear DNA, however, protein can dissociate by falling off, or by sliding off the ends.[55] How important these mechanisms are depends on the nature of the protein-DNA interaction, and the relative size of the strand length versus the sliding length. There is experimental evidence to support end-sliding as a dissociative mechanism for some proteins, but not for others. If end-sliding is an important component of the dissociation of EndoIII from linear DNA, then redistribution of the protein to a central lesion will increase the overall binding affinity of the protein to the DNA relative to the fully matched control.

The ratio of protein between the long and short strands is:

$$R_{L,S} = \frac{\#_L}{\#_S} = \frac{K_L}{K_S} = \frac{k_{a,L}}{k_{a,S}} \frac{k'_{d,S}}{k'_{d,L}}$$

where # is the number of proteins counted on a given strand of DNA, the subscripts *L* and *S* identify long and short DNA respectively, and k'_d represents the composite dissociation rate of protein from the DNA (including end-sliding). The rate of end-sliding is:

$$k_e(n) = \frac{D_1}{n^2} = \frac{k_d l_s^2}{n^2}$$

where *n* is the distance to the nearest end, if we assume that reflection at the ends is negligible and that the DNA is long enough that end-sliding is negligible for protein in the center of the DNA. The latter will clearly be the case for several thousand base-pair long DNA. In this case,

$$k'_d(n) = k_d\left(1 + \frac{l_s^2}{n^2}\right)$$

$$k'_d = 2k_d \sum_{1 \le n \le \frac{N}{2}} \phi_n \left(1 + \frac{l_s^2}{n^2}\right); \; \sum_n \phi_n = 1$$

where N is the length of the strand and ϕ_n is the protein distribution on the DNA. We can approximate ϕ_n as uniform along the DNA.

For the association constants,[8]

$$k_a = 4\pi D_3 r_g \left(1 - \frac{\tanh(\eta r_g)}{\eta r_g}\right)$$

$$r_g = \sqrt{\frac{Na}{3}}$$

where r_g is the radius of gyration, D_3 is the three-dimensional diffusion constant, a is the persistence length, and η is a parameter describing the geometry of the strand. That leaves a single parameter in the expression for $R_{L,S}$: the sliding length l_s.

For the case where all the protein is matched, and the sliding length is 22 bp, $R_{L,S}$ is expected to be about 1.8, which corresponds to a binding density ratio ($r \equiv R_L * N_S/N_L$) of 0.9. However, if a fraction φ of the protein is segregated in the middle of a long strand due to accumulation at a mismatch, then

$$k'_{d,MM} = 2k_d \sum_{1 \le n \le \frac{N}{2}} \phi_n \left(1 + \varphi \frac{l_s^2}{n^2}\right).$$

This provides a basis for justifying the preferential affinity of EndoIII for DNA containing a non-cognate mismatch over a strand that is fully matched.

4.3. EXPERIMENTAL VALIDATION OF CT SIGNALING

4.3.1. AFM MEASUREMENTS OF DISTRIBUTION OF ENDOIII BETWEEN DNA STRANDS

While we have earlier carried out studies establishing hole and electron injection across the protein/DNA interface,[22-24] our model also predicts that DNA/protein CT would promote the redistribution of repair proteins in the vicinity of base lesions or mismatches. We can assay for

this redistribution by AFM. A mixture of DNAs, both long (3.8 kilobase) DNA duplexes containing a single CA mismatch and short (2.2 and 1.6 kilobase) well-matched duplexes of the same total sequence were prepared;[56] the longer sequence was obtained by ligation of the two shorter sequences. This mixture of matched and mismatched DNA strands was incubated with EndoIII and examined using established AFM techniques[57] (**Figure 4.4**). Only clearly identifiable long or short strands were counted. Protein assignments were verified through analysis of their 4 nm heights in the images; without protein, features of this dimension are not observed and still larger heights indicate salt precipitates. Although a CA mismatch effectively inhibits DNA CT,[13] it is not a lesion that is preferentially bound by EndoIII; a gel shift assay on 21-mers with and without a central CA mismatch shows no detectable difference in EndoIII binding. Thus without DNA CT between bound EndoIII molecules, one might expect an equal density of proteins on the short and long strands.

We find that EndoIII shows a significant preference for the longer strands containing the CA mismatch. Examination of the number of proteins bound to 300 long strands and 465 short strands reveals a greater density of proteins bound to the long strand; r(long/short) is 1.6. If instead we examine the distribution of EndoIII on long versus short strands, where all strands are matched, we see a small preference for the short strands; the ratio of protein densities, r(long/short), is 0.9. When we calculate the strand preference based on DNA CT, this protein density ratio depends upon the DNA CT length and/or the length of the DNA over which protein can diffuse before dissociating. Using a signaling/sliding length of 90 base pairs, we calculate a protein density ratio of 1.6, that which we find, where half of the protein population is near the mismatch.

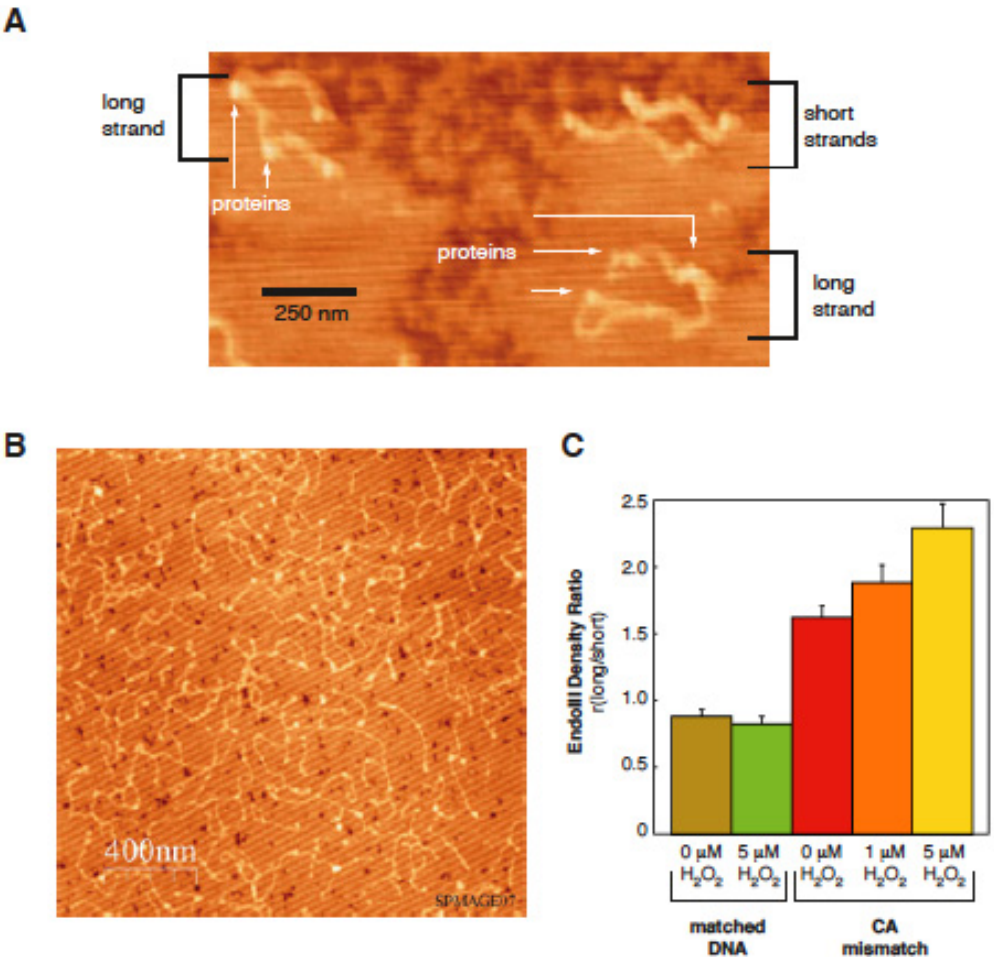

Figure 4.4. Measurements of repair protein distributions on DNA by AFM. A zoomed-in view (**A**) and a zoomed-out view (**B**) of representative AFM images of DNA strands incubated overnight with wild-type EndoIII. A higher density of proteins is apparent on the longer DNA strands containing the single base CA mismatch. Densities of 0.19 proteins bound per kilobase long strand and 0.12 proteins bound per kilobase short strand are observed, giving a density ratio (r(long/short)) of 1.6; the uncertantity is ≤ 10%. (**C**) Quantitation of protein density ratios. A CA mismatch is contained on the long strand except for the sample indicated by matched DNA, where both the long and the short strands are fully matched. EndoIII redistributes onto the strand with the CA mismatch and that preference is increased with increasing concentrations of peroxide.

AFM measurements as a function of oxidation of proteins bound to DNA, using H_2O_2 as oxidant, reveal an additional increase in the ratio of EndoIII bound to mismatch-containing strands. Examination of more than 250 long CA mismatch-containing strands and 300 shorter matched strands incubated with EndoIII and treated with 5 μM peroxide reveals a ratio of bound protein densities, r(long/short), of 2.4; when both long and short strands are matched, the ratio is 0.83.

These results are consistent with our model. DNA-mediated CT will drive the redistribution of repair proteins away from undamaged regions such that the proteins will cluster near damaged sites. As a result, we see the proteins redistribute preferentially onto the DNA strands containing the mismatch even though a CA mismatch is not a substrate for EndoIII. Moreover, as predicted by the model, the redistribution of EndoIII is more pronounced in the presence of oxidative stress.

4.3.2. TRANSVERSION ASSAYS IN *E. COLI* AND CT SIGNALING

This CT scanning model was tested *in vivo* by assaying for the cooperation among repair proteins facilitated by DNA-mediated signaling. If these proteins are able to help each other in their search for damage using DNA CT, knocking out the gene for EndoIII or reducing its capability to carry out CT should lead to a decrease in MutY activity *in vivo*. Assays for MutY and EndoIII activity inside *E. coli* cells have already been developed.[58] The assay for "helper function" used here employs engineered mutations in the *lacZ* gene to report the frequency of a particular base-pair substitution. The strain that serves as an assay for MutY activity, CC104, substitutes a cytosine for an adenine in the *lacZ* Glu 461 codon, which is essential for β-galactosidase activity. Since MutY prevents GC to TA transversions,[59] reversion of this original

mutation back to wild-type (wt) *lacZ* reflects a deficiency in MutY activity. Analogously, the CC102 strain[57] serves as an assay for EndoIII activity by monitoring GC to AT transitions.[60,61]

In the CC104 MutY activity reporter strain (**Table 4.1**), 20 ± 9 *lac*+ revertants are observed per 10^9 cells, while inactivation of *mutY* in CC104 (CC104 *mutY*-) causes the number of *lac*+ revertants to increase 15x (300 ± 33) as expected.[58,59] When the gene encoding EndoIII (*nth*) is inactivated in CC104 (CC104 *nth*-), the *lac*+ reversion frequency observed is 54 ± 5, more than a factor of two increase over CC104. Thus, loss of EndoIII does have a small but significant effect on MutY activity *in vivo*. This loss in activity is consistent with a loss in helper function by EndoIII, as predicted; the lower activity of MutY without EndoIII could reflect the lack of cooperative searching via DNA CT. An alternative explanation, however, is that MutY and EndoIII share some overlapping ability to repair lesions. In this case, the *lac*+ reversion frequency of the CC104 *mutY-/nth*- strain (270 ± 29) should be greater than that of CC104 *mutY*, but they are, within error, equivalent.

This *in vivo* relationship between EndoIII and MutY has been observed previously, although in different experimental contexts. Small increases in mutational frequency have been detected when *mutY* is inactivated in CC102,[58] as was also observed here, or when *nth* is inactivated in CC104.[61] In the latter case, it was proposed that this could be due to some intrinsic ability of EndoIII to repair oxidatively damaged guanine residues. Reported EndoIII repair activities do not prevent GC to TA transversion mutations[62] and, thus, are not relevant to the CC104 assay.

We can furthermore test directly whether the loss of MutY activity in the CC104 assay is the result of overlapping glycosylase activities by determining whether the number of *lac*+ revertants is still suppressed by an EndoIII mutant that is biochemically incompetent to carry out

Table 4.1. Assay for DNA repair in *E. coli* by MutY (CC104)

Strain	*Lac*+ Revertants[a,b]	Increase
	(*lac*$^+$ colonies/ 10^9 cells)	(x/CC104)
CC104[c]	20 ± 9	---
CC104 *nth-*	54 ± 5	2.7
CC104 *mutY-*	300 ± 33	15
CC104 *mutY-/nth-*	270 ± 29	13.5

a. *Lac*$^+$ revertants are reported as the average number of *lac*$^+$ colonies that arise per 10^9 cells plated on minimal lactose media.

b. These data represent a single set of experiments with 10 replicates per strain assayed concurrently. Values reported as the mean ± s.d.

c. CC104 strains reflect the rate of GC to TA transversion mutations and serve as a reporter for MutY activity in *E. coli*.

the glycosylase reaction. A mutant of EndoIII (D138A) that is known to be deficient in glycosylase activity[63] was introduced on a plasmid into both the CC102 and CC104 strains along with appropriate vector controls. Because this mutant cannot perform the base excision reaction, D138A fails to reduce the high reversion frequency observed with CC102 *nth*- . However, D138A is able to complement the CC104 *nth*- strain. Thus, the glycosylase activity of EndoIII is not required for its helper function to aid MutY in repairing lesions inside the cell. Nonetheless, it appears that EndoIII lacking D138 can bind DNA and contains an intact [4Fe4S] cluster.[63] Based upon our model, D138A should be competent to carry out DNA-mediated CT and thus serve as a helper to MutY, as we observe.

In our model, it is the ability to carry out DNA-mediated CT, not the glycosylase activity of EndoIII, that is critical to its helper function. Thus, perturbing the path for electron transfer to the DNA would interfere with this helper function. Aromatic tyrosine and tryptophan residues often facilitate long-range electron transfers in proteins,[64,65] and EndoIII contains many of these residues. In particular, Y82 is conserved in most EndoIII and MutY homologues,[66] and an analogous mutation (Y166S) in the human homologue of MutY is associated with cancer.[67] In the crystal structure, Y82 is located very close to the DNA backbone.[5] Y82A EndoIII was thus introduced on a plasmid into both reporter strains (CC102 and CC104) and their *nth* knockouts to explore whether this mutation attenuates helper function. Significantly, Y82A in the CC104 *nth*- strain shows an increase in mutation rate versus the CC104/Y82A and CC104/p controls (**Figure 4.5**). The number of *lac*+ revertants is found to increase by 53 ± 16% when comparing CC104 *nth*-/ Y82A to CC104/p. When comparing CC104 *nth*-/Y82A to CC104/Y82A, the number of *lac*+ revertants increases by 68 ± 13%. Similarly, for these trials, the ratio of the

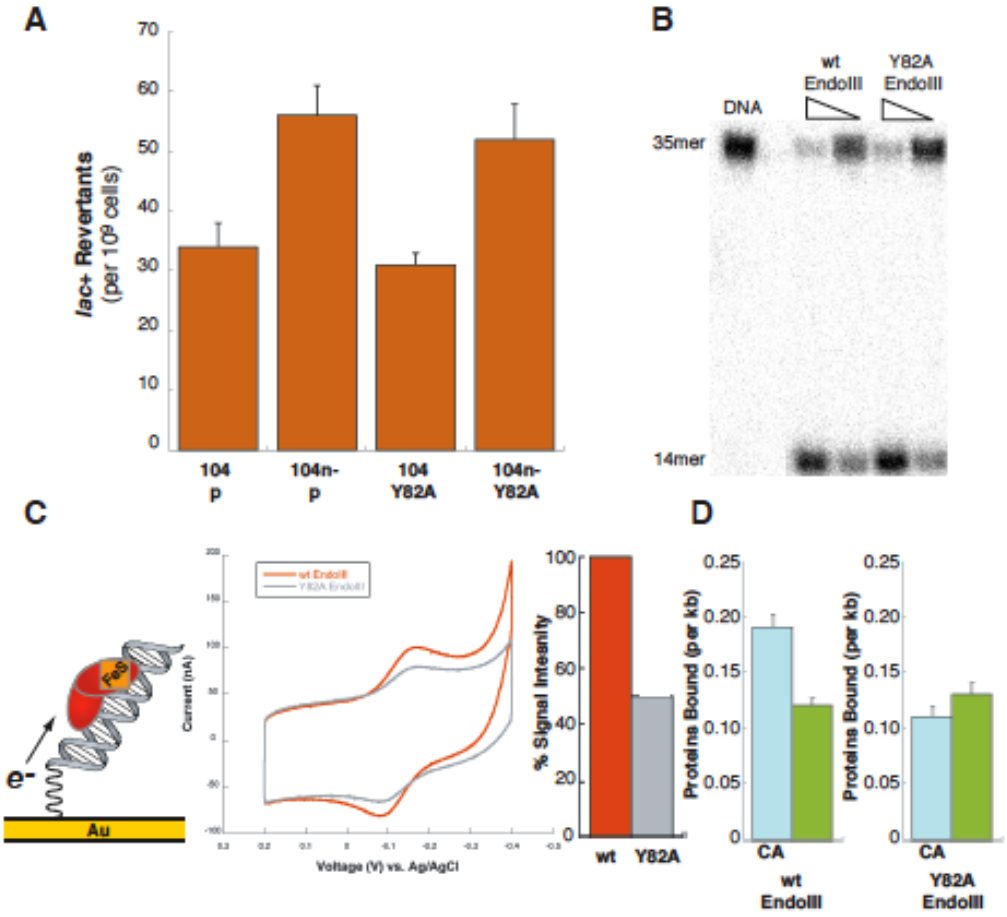

Figure 4.5. Y82A EndoIII, a mutant in DNA-mediated CT capability. (**A**) Bar graph showing *lac*+ revertants for CC104/p, CC104 *nth*-/p, CC104/Y82A and CC104 *nth*-/Y82A strains, where p denotes inclusion of an empty vector. *Lac*+ revertants are reported as the average number *lac*+ colonies that arise per 10^9 cells plated on minimal lactose media containing ampicillin. Data for the CC104 strains are shown based upon five sets of independent experiments, each containing 10 replicates per strain. (**B**) Autoradiogram after denaturing PAGE of ^{32}P-5'-TGTCAATAGCAAG**X**GGAGAAGT-CAATCGTGAGTCT-3' + complementary strand where X = 5-OH-dU base-paired with G. Protein samples (100 or 10 nM) were incubated with duplexes for 15 min at 37 °C and quenched with 1 M NaOH. Cleavage of the ^{32}P-labeled strand at the lesion site (**X**) by EndoIII results in formation of a 14mer. No significant difference in glycosylase activity (10% uncertainty) is observed between Y82A and wt EndoIII. (**C**) Cyclic voltammetry of Y82A EndoIII at a Au electrode modified with $SH(CH_2)_2CONH(CH_2)_6NHOCO$-5'-AGTACAGTCATCGCG-3' + complementary strand showing the reduction and reoxidation of the DNA-bound protein. DNA-modified surfaces were prepared, backfilled with mercaptohexanol, and wt or Y82A EndoIII was tested. Surfaces were then rinsed and the other protein analyzed on the same surface. Over several trials, the electrochemical signal associated with Y82A is 50 ± 13% smaller per [4Fe4S] cluster compared with wt EndoIII, reflecting poor electronic coupling of the mutant to the DNA-modified electrode. (**D**) Comparative densities for wt (left) and Y82A (right) EndoIII bound to matched versus mismatched (CA) strands measured by AFM. Although wt EndoIII preferentially redistributes onto the mismatched strand, Y82A shows no preference.

number of *lac*+ revertants for CC104 *nth*-/ p versus CC104/p is 165 ± 13%. These results clearly indicate that Y82A does not restore helper function.

It is noteworthy that inclusion of Y82A EndoIII in CC102 *nth*- leads to a diminished mutation rate, indicating that this mutant is competent for EndoIII activity inside the cell. Interestingly, the observation that Y82A complements CC102 *nth*-, but not CC104 *nth*-, is consistent with the conclusion that the glycosylase activity of EndoIII is not a source of helper function. Moreover the fact that Y82A complements CC102 *nth*- is understandable in the context of our model, because of the higher copy number of EndoIII in *E. coli* cells than MutY. In our model, without oxidative stress, we would predict that DNA CT is not essential for EndoIII repair activity inside the cell. We would therefore anticipate that the role of EndoIII in helping MutY search for lesions may be more important than the ability of EndoIII to find its own lesions. This distinction becomes more complex when considering that other DNA-binding proteins with iron-sulfur clusters might also participate in the signaling process.

To establish the biochemical characteristics of Y82A EndoIII, the protein was purified and its redox and glycosylase activities examined. Importantly, the mutant enzyme does contain the [4Fe4S] cluster, characterized by its distinctive absorbance spectrum. Y82A EndoIII also maintains glycosylase activity against a 5-OH-dU lesion in a ^{32}P-5'-endlabeled 35-mer duplex (**Figure 4.5**); the activity of the mutant in this assay is equal to that of wild type. Note that this experiment on a 35-mer duplex measures only the base excision reaction, not the search process. Similarly, in the *E. coli* EndoIII activity assay, where we expect that the search process is not rate-limiting, Y82A EndoIII activity is comparable to that of wild-type EndoIII. In contrast, D138A EndoIII, which instead inhibits the base excision reaction, fails to complement the *nth*

knockout in the EndoIII activity reporter strain but does complement the *nth* knockout in the MutY activity reporter strain, where lesion detection is limiting.

To test for DNA-bound redox activity, Y82A was examined on a Au electrode modified with thiol-terminated DNA duplexes. Significantly, in the cyclic voltammogram, the potential for the DNA-bound mutant resembles that of the wild type,[12] but the signal intensity is diminished (**Figure 4.5**). The protein concentrations are determined based on the 410 nm absorbance of the [4Fe4S] cluster; the smaller electrochemical signal observed with Y82A does not reflect a lower concentration of [4Fe4S] clusters. Over several trials, Y82A EndoIII exhibits a signal that is 50 ± 13% smaller than that for wt EndoIII (per [4Fe4S] cluster). This signal intensity provides a reliable measurement of reduction/oxidation of the DNA-bound protein. Since the glycosylase activity on the 35-mer is equal for the mutant and wild type, this diminished signal cannot reflect diminished binding of the mutant to the DNA. Instead this lowered signal intensity would be expected with an attenuated efficiency of CT from the cluster to DNA and reflects poor electronic coupling of the mutant with the DNA duplex. These results therefore indicate that Y82A EndoIII is defective in DNA-mediated signaling.

Significantly, and consistent with these results, examination of the distribution of Y82A on mismatched and matched strands by AFM shows no preference for the mismatched strand; we observe 0.11 proteins per kilobase long strand and 0.13 proteins per kilobase short strand (**Figure 4.5**). In fact, the ratio of protein densities on mismatched versus matched strands with Y82A, r(long/short) is 0.9, essentially equal to that of wild-type EndoIII bound to fully matched long versus short strands. Since the Y82A mutant, biochemically defective only in DNA CT, cannot redistribute to the vicinity of the lesion, DNA CT must play a role in finding the lesion both in the AFM experiment and in the helper function assay. These results together demonstrate

a distinct connection between DNA-mediated CT to the [4Fe4S] cluster, the detection of DNA defects, and the *in vivo* relationship observed between MutY and EndoIII.

4.4. DISCUSSION

These experiments indicate that MutY and EndoIII cooperate in their search for damage in the genome and redistribute in the vicinity of lesions consistent with CT scanning. This cooperation, or helper function, does not involve the glycosylase reaction. Based on their chromosomal arrangement, the expression of MutY and EndoIII, furthermore, do not appear to be linked.[68] There is also no chemical evidence that the proteins physically bind to one another, and their low abundance within the cell makes random associations improbable. This cooperation thus arises from a distance. Importantly, what does appear to be required for helper function is an intact [4Fe4S] cluster as well as an electroactive protein-DNA interface. Mutation of an aromatic amino acid residue near the DNA binding site, Y82A, leads to a decrease in CT efficiency *in vitro*, the inability of the protein to redistribute near lesions by AFM, and diminished helper function *in vivo*. These experiments thus establish a link between DNA-mediated CT and the cooperative search for damage by these repair proteins both *in vitro* and *in vivo*.

BER glycosylases are known to prevent mutations inside the cell, yet in most organisms, these enzymes are not required for normal growth and development.[2] Recently it was discovered that germline mutations in human BER homologues result in a genetic predisposition to cancer.[67] Specifically, the human homologue of *mutY* (*MUTYH*) is found mutated in a subset of patients predisposed to colorectal cancer. Many of the cancer-associated mutations in *MUTYH* are missense, or single amino acid, mutations. Though several of the most common mutants have

been characterized biochemically, it remains unclear exactly how these variants lead to disease. Given that initial detection of lesions is likely the rate-limiting step in BER,[7] it is possible that mutants with defects in protein-DNA CT would be associated with cancer. Indeed, many of these *MUTYH* missense mutations found in colorectal cancer patients result in loss or gain of aromatic residues near predicted protein-DNA interfaces.[67] Significantly, *MUTYH* contains two adjacent tyrosine residues (Y165 and Y166) that closely align with Y82 in *E. coli* EndoIII and inherited mutations in these *MUTYH* residues (Y165C and, less commonly, Y166S) are clinically relevant in cancer. These results thus provide tantalizing evidence for association between defects in lesion detection via DNA-mediated CT by BER enzymes and human disease.

Iron-sulfur clusters are becoming increasingly ubiquitous to proteins that repair, replicate, and transcribe DNA.[69,70] Recent characterizations of archaeal DNA primase, RNA polymerase, and nucleotide excision repair helicase (XPD) homologues reveal an iron-sulfur cluster required for normal enzyme function. Though the precise role of the cluster in these proteins is unclear, the cysteine residues ligating the cluster are conserved in eukaryotic homologues of these proteins. In archaeal XPD, moreover, the iron-sulfur cluster occupies a site far from the ATP hydrolysis domain but implicated in DNA binding.[69] It is interesting to consider whether in these proteins, as in BER enzymes, the iron-sulfur cluster is poised to send and receive redox signals mediated by the DNA helix, which may, in turn, modulate DNA binding affinity, enzyme activity, or protein structure. Such long-range signaling among proteins bound to DNA would make searching for lesions much more efficient and may generally provide a means of genome-wide communication to monitor cellular stresses.

DNA-mediated CT serves as a fast and efficient reaction that is exquisitely sensitive to lesions in the base-pair stack. This chemistry helps to explain how these repair glycosylases locate

their lesions efficiently in the cell, a key function since mutations in these enzymes in humans are implicated in colorectal cancer.[67] This mechanism furthermore provides a rationale for iron-sulfur clusters in DNA repair proteins. More generally, these experiments illustrate the importance of DNA-mediated CT in long-range signaling among proteins in low abundance that are bound to DNA. Other roles for DNA-mediated CT in biological signaling must now be considered.

4.5. REFERENCES

1. Demple B.; Harrison L. *Annu. Rev. Biochem.* **1994**, *63*, 915.

2. David S.S.; O'Shea V.L.; Kundu S. *Nature* **2007**, *447*, 941.

3. Bai, H.; Lu, A.-L., *J. Bacter.* **2007**, *189*, 902.

4. Francis A.W.; Helquist S.A.; Kool E.T.; David S.S. *J. Am. Chem. Soc.* **2003**, *125*, 16235.

5. Fromme J.C.; Verdine G.L. *EMBO J.* **2003**, *22*, 3461.

6. Fromme J.C.; Banerjee A.; Huang S.J.; Verdine G.L. *Nature* **2004**, *427*, 652.

7. Livingston A.L.; O'Shea V.L.; Kim T.; Kool E.T.; David S.S. *Nat. Chem. Biol.* **2008**, *4*, 51.

8. Berg O.G.; Winter R.B.; von Hippel P.H. *Biochemistry* **1981**, *20*, 6929.

9. Parker, J.B.; Bianchet, M.A.; Krosky, D.J.; Friedman, J.I.; Amzel, L.M.; Stivers, J. *Nature* **2007**, *449*, 433.

10. Cunningham R.P.; Asahara, H.; Bank, J.F.; Scholes, C.P.; Salerno. J.C.; Surerus, K.; Munck, E.; McCracken, J.; Peisach, J.; Emptage, M.H. *Biochemistry* **1989**, *28*, 4450

11. Boon E.M.; Livingston A.L.; Chmiel N.H.; David S.S.; Barton J.K. *Proc. Natl. Acad. Sci. U.S.A.* **2003**, *100*, 12543.

12. Boal, A.K.; Yavin, E.; Lukianova, O.A.; O'Shea, V.L.; David, S.S.; Barton, J.K. *Biochemistry* **2005**, *44*, 8397.

13. Wagenknecht, H. A., Ed. *Charge Transfer in DNA*; Wiley-VCH: Weinheim, **2005**.

14. Núñez M.E.; Hall D.B.; Barton J.K. *Chem. Biol.* **1999**, *6*, 85.

15. Kelley S.O.; Jackson N.M.; Hill, M.G.; Barton, J.K. *Angew. Chem. Int. Ed.* **1999**, *38*, 941.

16. Elias B.; Shao F.; Barton J.K. *.J Am. Chem. Soc.* **2008**, *130*, 1152.

17. Núñez M.E.; Noyes K.T.; Barton J.K. *Chem. Biol.* **2002**, *9*, 403.

18. Núñez M.E.; Holmquist G.P. Barton J.K. *Biochemistry* **2001**, *40*, 12465.

19. Boal A.K.; Barton J.K. *Bioconjugate Chem.* **2005**, *16*, 312.

20. Boon E.M.; Ceres D.M.; Drummond T.G.; Hill M.G.; Barton J.K. *Nat. Biotechnol.* **2000**,*18*, 1096.

21. Guo X.F.; Gorodetsky A.A.; Hone J.; Barton J.K.; Nuckolls C. *Nat. Nanotechnol.* **2008**, *3*, 163.

22. Boon E.M.; Salas J.E.; Barton, J.K. *Nat. Biotechnol.* **2002**, *20*, 282.

23. Yavin, E.; Boal, A.K.; Stemp, E.D.A.; Boon, E.M.; Livingston, A.L.; O'Shea, V.L.; David, S.S.; Barton, J.K. *Proc. Natl. Acad. Sci. U.S.A.* **2005**, *102*, 3546.

24. Yavin, E.; Stemp, E.D.A.; O'Shea, V.L.; David, S.S.; Barton, J.K. *Proc. Natl. Acad. Sci. U.S.A.* **2006**, *3610.*

25. Wunderlich Z.; Mirny L.A. *Nuc. Acids. Res.* **2008**, *36*, 3570.

26. Porello, S.L.; Williams, S.D.; Kuhn, H.; Michaels, M.L.; David, S.S. *J. Am. Chem. Soc.* **1996**, *118*, 10684.

27. Gorodetsky A.A.; Boal A.K.; Barton J.K. *J. Am. Chem. Soc.* **2006**, *128*, 12082.

28. Halford, S.E.; Marko, J.F. *Nuc. Acids Res.* **2004**, *32*, 3040.

29. Slutsky M.; Mirny L.A. *Biophys. J.* **2004**, *87*, 4021.

30. Bénichou, O.; Kafri, Y.; Sheinman, M.; Voituriez, R. *Phys. Rev. Lett.* **2009**, *103*, 138102.

31. Murugan, R. *Phys. Rev. E* **2009**, *79*, 061920.

32. Kolesov, G.; Wunderlich, Z.; Laikova, O.N.; Gelfand, M.S.; Mirny, L.A. *Proc. Natl. Acad. Sci. U.S.A.* **2007**, *104*, 13948.

33. Elf, J.; Li, G.-W.; Xie, X.S. *Science*, **2007**, *316*, 1191.

34. Blainey P.C.; van Oijen A.M.; Banerjee A.; Verdine G.L.; Xie X.S. *Proc. Natl. Acad. Sci. U.S.A.* **2006**, *103*, 5752.

35. This sliding is only pseudo-one dimensional, consisting of rotational motion around the twisted double helix. See Bagchi, B.; Blainey, P.C.; Xie, X.S. *J. Phys. Chem. B* **2008**, *112*, 6282.

36. Ali Azam, T.; Iwata, A.; Nishimura, A.; Ueda, S.; Ishihama, A. *J. Bacteriol.* **1999**, *181*, 6361.

37. Li, G.-W.; Berg, O.G.; Elf, J. *Nat. Phys.* **2009**, *5*, 294.

38. Mullineaux C.W.; Nenninger A.; Ray N.; Robinson C. *J. Bacteriol.* **2006**, *188*, 3442.

39. Asahara H.; Wistort P.M.; Bank J.F.; Bakerian R.H.; Cunningham R.P. *Biochemistry* **1989**, *28*, 4444.

40. Hu, T.; Grosberg, A.; Shklovskii, B. *Biophys. J.* **2006**, *90*, 2731.

41. Thanbichler M, Wang SC, Shapiro L (2005) The bacterial nucleoid: a highly organized and dynamic structure. *J Cell Biochem* 96:506-521.

42. Flyvbjerg, H.; Keatch, S.A.; Dryden, D.T.F *Nuc. Acids Res.* **2006**, *34* 1550.

43. O'Handley S.; Scholes C.P.; Cunningham R.P. *Biochemistry* **1995**, *34*, 2528.

44. Slutsky M.; Mirny L.A. *Biophys. J.* **2004**, *87*, 4021.

45. Fok, P.-W.; Guo, C.-L.; Chou, T. *J. Chem. Phys.* **2008**, *129*, 235101.

46. Fok, P.-W.; Chou, T. *Biophys. J.* **2009**, *96*, 2949.

47. Augustyn K.E.; Merino E.J.; Barton J.K. *Proc. Natl. Acad. Sci. U.S.A.* **2007**, *104*, 18907.

48. Burrows C.J.; Muller J.G. *Chem. Rev.* **1998**, *98*, 1109.

49. Lin, J.C.; Singh, R.R.; Cox, D.L. *Biophys. J.* **2008**, *95*, 3259.

50. Berg O.G. *Biopolymers* **1986**, *25*, 811.

51. Berg O.G.; von Hippel P.H. *Annu. Rev. Biophys. Chem* **1985**, *14*, 131.

52. O'Neill M.A.; Barton J.K. *Proc. Natl. Acad. Sci. U.S.A.* **2002**, *99*, 16543.

53. Núñez, M.E.; Noyes, K.T.; Gianolio, D.A.; McLaughlin, L.W.; Barton, J.K. *Biochemistry* **2000**, *39*, 6190.

54. Merino E.J.; Barton J.K. *Biochemistry* **2007**, *46*, 2805.

55. Surby, M.A.; Reich, N.O. *Biochemistry* **1996**, *35*, 2209.

56. Donahue W.F.; Turczyk B.M.; Jarrell, K.A. *Nucleic Acids Res.* **2002**, *30*, 95.

57. Chen L.; Haushalter K.A.; Lieber C.M.; Verdine G.L. *Chem. Biol.* **2002**, *9*, 345.

58. Cupples C.G.; Miller J.H. *Proc. Natl. Acad. Sci. U.S.A.* **1989**, *86*, 5345.

59. Nghiem Y.; Cabrera M.; Cupples C.G.; Miller J.H. *Proc. Natl. Acad. Sci. U.S.A.* **1988**, *85*, 2709.

60. Kreutzer D.A.; Essigmann J.M. *Proc Natl Acad Sci U.S.A.* **1998**, *95*, 3578.

61. Tano K.;, Iwamatsu Y.; Yasuhira S.; Utsumi H.; Takimoto K *J Radiat Res* **2001**, *42*, 409.

62. Thayer M.M.; Ahern H.; Xing D.; Cunningham R.P.; Tainer J.A. *EMBO J.* **1995**, *14*, 4108.

63. Kuo C.F.; McRee D.E.; Fisher C.L.; O'Handley S.F.; Cunningham R.P.; Tainer J.A. *Science* **1995**, *258*, 434.

64. Stubbe J.; Nocera D.G.; Yee C.S.; Chang M.C. *Chem. Rev.* **2003**, *103*, 2167.

65. Shih, C.; Museth, A.K.; Abrahamsson, M.; Blanco-Rodriguez, A.M.; Di Bilio, A.J.; Sudhamsu, J.; Crane, B.R.; Ronayne, K.L.; Towrie, M.; Vicek, A.; Richards, J.H.; Winkler, J.R.; Gray, H.B. *Science* **2008**, *320*, 1760.

66. Watanabe T.; Blaisdell J.O.; Wallace S.S.; Bond J.P. *J. Biol. Chem.* **2005**, *280*, 34378.

67. Cheadle J.P.; Sampson J.R. *DNA Repair* **2007**, *6*, 274.

68. Gifford C.M.; Wallace S.S. *Nuc. Acids. Res.* **2000**, *28*,762.

69. Fan, L.; Fuss, J.O.; Cheng, Q.J.; Arvai, A.S.; Hammel, M.; Roberts, V.A.; Cooper, P.K.; Tainer, J.A. *Cell* **2008**, *133*, 789.

70. Hirata, A.; Klein, B.J.; Murakami, K.S. *Nature* **2008**, *451*, 851.

Chapter 5:

Assaying Bridge Occupation in DNA-mediated Electrochemistry

5.1: INTRODUCTION

It has been proposed that DNA-mediated charge transport (CT) can be considered in two separate regimes.[1] In the first regime, charge that is injected at higher energy than the DNA bridge propagates by hopping between nucleotides. This process involves real occupation of the DNA. When the hole (electron) donor has inadequate potential to oxidize (reduce) the HOMO (LUMO) of the individual base pairs, then the bridge is only virtually occupied, and superexchange, with its consequently strong distance dependence, is the mechanism of CT. While there is now ample evidence that both types of CT occur in DNA,[2] this neat division based on the energy of the donor is not consistent with much of the existing evidence. Examples include the DNA-mediated long-range quenching of photoexcited Ru(II) or ethidium bromide intercalators by $[Rh(phi)_2(phen')]^{3+}$, and the transport of charge between stilbenes through a higher energy adenine tract.[3-5]

Over the previous decade, the Barton group has demonstrated that ground-state DNA-mediated CT can be achieved over long distances, with minimal loss of yield, in the context of DNA self-assembled monolayers on electrodes.[6] These systems are energetically analogous to DNA-mediated CT between proteins, which plays an essential role in lesion detection, and possibly other biological roles.[7] The DNA-mediated nature of this reaction has been demonstrated by the dependence of the yield and rate on structural parameters. CT rate decreases as the length of the alkyl surface linker increases, with a β of 1 $Å^{-1}$, indicating that CT is mediated by the covalent linker to the DNA.[8] Furthermore, probes designed to feature poor electronic conjugation to the DNA π-stack also show impaired CT yield.[9,10] Finally, as in other systems, structurally minimal perturbations that disrupt the DNA π-stack also attenuate DNA-mediated electrochemistry.[11-13] Importantly, if the electrochemical probes were instead dynamically

accessing the surface,[14] each of these conditions would have the *opposite* effect on CT rate and yield to that which is observed.

To summarize, three properties of DNA-mediated electrochemistry are particularly counter-intuitive with respect to theory.[6] First, probes are observed near their free potentials, covering a range of nearly a volt.[15] Second, DNA reduction has not been observed in this range in the absence of a probe. Third, none of the DNA bases are energetically within, or even near, the voltammetric range of electrochemical probes that have been applied.[16] These three properties are all inconsistent with direct oxidation of the DNA.

The incompatibility of the last property with a hopping mechanism can be demonstrated by considering the expected rate of charge injection. As demonstrated in Chapter 1, using extremely favorable parameters, the rate of injection from the electrode to an iron-sulfur cluster (0.1 V vs. NHE) is necessarily far below that of 0.002 s^{-1}. This is slower than the observed linker-limited rate of 30 s^{-1}, implying that hopping is not a reasonable mechanism for DNA-mediated electrochemistry due to the slow thermal population of the bridge.

However, in the absence of hopping, it is hard to explain the insensitivity of DNA-mediated electrochemistry to the length of the DNA.[11] The CT rate continues to be limited by tunneling through the linker even for a DNA bridge length of 11 nm.[17] For a modest β of 0.2 $Å^{-1}$,[18] the frequency factor would have to be a respectable 1 x 10^{11} s^{-1} to be consistent with experiment; however, this far from the bridge energies, β is by necessity much higher. Using the expression:

$$\beta = \frac{2}{a}\ln\left[\frac{\Delta\varepsilon}{2V} + \sqrt{1+\frac{\Delta\varepsilon^2}{4V^2}}\right] \qquad \textbf{(5.1)}$$

with a typical interbase coupling V of 0.05 V,[19] the energy gap $\Delta\varepsilon$ as 1 V, and a, the intersite separation as 3.4 Å yields a β of 1.8 Å^{-1}. For this β, a preexponential factor of 10^{87} s^{-1} is necessary to explain the experiment. This is unreasonable. Hence, for superexchange to be the dominant mechanism of DNA-mediated electrochemistry, very low β is necessary despite the distance between the donor and acceptor energies and the energy of the bridge states.

Although hopping and superexchange both seem unreasonable, there is no other mechanism that has been proposed for CT. To elucidate the nature of DNA-mediated electrochemistry, we consider the essential question of whether the DNA is, in fact, occupied and what the nature of these occupied intermediates might be. To answer this question, we perform electrochemistry on DNA containing a fast radical trap, analogous to those used in Chapters 2 and 3.

The *N*-cyclopropyl charge reporter has been used to demonstrate occupation of guanine, adenine and cytosine during DNA-mediated CT in solution. Particularly, N_4-cyclopropylcytosine (^{CP}C) is a fast reporter for DNA reduction.[20,21] This reporter can reveal analogous information about DNA-mediated electrochemistry. Herein, we develop and apply an assay for this chemical reaction in DNA films.

5.2. METHODS

5.2.1. DNA SYNTHESIS AND PREPARATION

DNA oligonucleotides were synthesized trityl-on using standard phosphoramidite chemistry on an ABI DNA synthesizer with Glen Research reagents. Redmond Red was incorporated on the 3' terminus by extension of the oligonucleotide on Redmond Red-labeled beads (Glen Research), using UltraMILD reagents (Pac-dG, iPr-Pac-dA, Ac-dC,

and phenylacetic anhydride capping mix (Glen Research). These strands were ultimately deprotected and cleaved from the resin by shaking the beads in 50 mM K_2CO_3 in dry methanol for several hours, then shaking in fresh solution for several hours. The aliquots of base solution were combined and lyophilized. ^{CP}C-modified oligonucleotides were prepared by incorporating the precursor base, 4-cyanoethylthio-uridine (Glen Research) as a phosphoramidite at the desired position, followed by deprotection of the cyanoethyl with 1 M DBU in dry acetonitrile for three hours. The oligonucleotides were subsequently incubated overnight in 6 M aqueous cyclopropylamine (Aldrich) at 60 ^{o}C. resulting in substitution, base deprotection, and simultaneous cleavage from the resin. The cleaved strands were dried *in vacuo* and purified by reversed-phase HPLC, detritylated by 80% acetic acid for 15 min, and repurified by reversed-phase HPLC. Oligonucleotides were characterized by MALDI-TOF mass spectrometry and UV-vis spectrophotometry.

For oligonucleotides containing a thiol linker, the strands were prepared without the terminal DMT group, and the linker added as previously described.[11] All duplex DNA was of the sequence:

CP-dsDNA: 5'- CGCGATGA^{CP}CTGTACT-3'

3'-RR-GCGCTACT GACATGA- OC(O)NH$(CH_2)_6$NHC(O)$(CH_2)_2$-5'-SH

where RR represents the Redmond Red. DNA was also prepared without the CP-modification, for use as a standard corresponding to the oxidation decomposition product.[22,23] Purified oligonucleotides were annealed together in degassed buffer at 100 μM, by heating to 90 ^{o}C for 5 minutes and slowly cooling to ambient temperature

over 90 minutes. Phosphate buffer (PB: 5 mM P_i, 50mM Na, pH 7.0) was used for all experiments.

5.2.2. Film Preparation and Electrochemistry

To assemble films, Au(111) surfaces on mica on glass, stored under N_2, were used (GE Healthcare). Upon removal from inert atmosphere, surfaces were immediately inserted into a cell, with a 7 mm diameter o-ring in direct contact with the surface. Into this cavity, 50 μM DNA, 100 mM $MgCl_2$ in PB was pipetted. Cells were stored under high humidity, in the dark, and at 4 ^oC for 20 to 50 hours. The solution was removed and saved for reuse, on the condition that HPLC analysis confirms its stability. All thiolated DNA was stored degassed and frozen, under Ar. Surfaces were washed with PB, 1 mM mercaptohexanol in 1% ethanol and PB was added, and the surface stored in the above conditions for 60 - 90 minutes. Surfaces were well washed, and then subjected to electrochemical assay with three-electrode configuration using a Ag/AgCl/(4% agarose in 3 M NaCl) reference electrode and Pt counterelectrode in a Faraday cage. Cyclic voltammetry (CV) (v = 100 mV/s) and chronocoulometry (CC) experiments were performed at ambient temperature on an electrochemical analyzer (CH Instruments, Austin, TX).

5.2.3. DNA Recovery and Analysis

A variety of recovery methods were attempted, with the best success achieved with mild heating of the gold surface to 70 ^oC, successive washes with PB at that temperature, fast cooling to 4 ^oC, immediate cold filtration (0.2 μm) of the collected washes, and immediate analysis by HPLC. HPLC was performed on a reversed-phase

analytical C18 column, with a 0.5 %/min gradient from 50 mM NH_4OAc to acetonitrile over the region of interest. The temperature of the buffers was controlled (55 ^oC) over the course of runs. High temperature was used to ensure dehybridization of double-stranded DNA should any be recovered from the film. For every set of experiments, standards for ^{CP}DNA, unmodified DNA, and deposition solution (i.e., double stranded, thiolated, DNA that was used to generate the monolayers) were also analyzed, as was a mercaptohexanol film assembled in the absence of DNA. Unless otherwise noted, all traces are at 260 nm, with the mercaptohexanol film subtracted to minimize background. Standards of the ^{CP}C-containing strand were consecutively run to provide calibration for quantification, although anomalously large peaks were occasionally observed. Quantification was not reliable below 2 pmol (5 pmol/cm^2). Online UV allows discrimination between DNA peaks and peaks due to other compounds.

5.3. RESULTS

5.3.1. HPLC ANALYSIS OF DNA RECOVERED FROM SELF-ASSEMBLED MONOLAYERS

DNA-modified films were generated on gold electrodes by self-assembly driven by covalent thiol on gold association. The DNA contains both the redox label Redmond Red,[17] to establish DNA-mediated CT, and the intervening fast radical trap ^{CP}C. By recovering the DNA after electrochemistry, and analyzing for ^{CP}C decomposition, we can determine some limits on the extent of charge occupation of the bridge. This experimental approach is illustrated in **Figure 5.1**.

The HPLC profile of the recovery solution from mercaptohexanol/Au monolayers shows four main features (**Figure 5.2**). These features were consistent across all films, prepared over many months. Feature A is the solvent front. Feature B is a small peak,

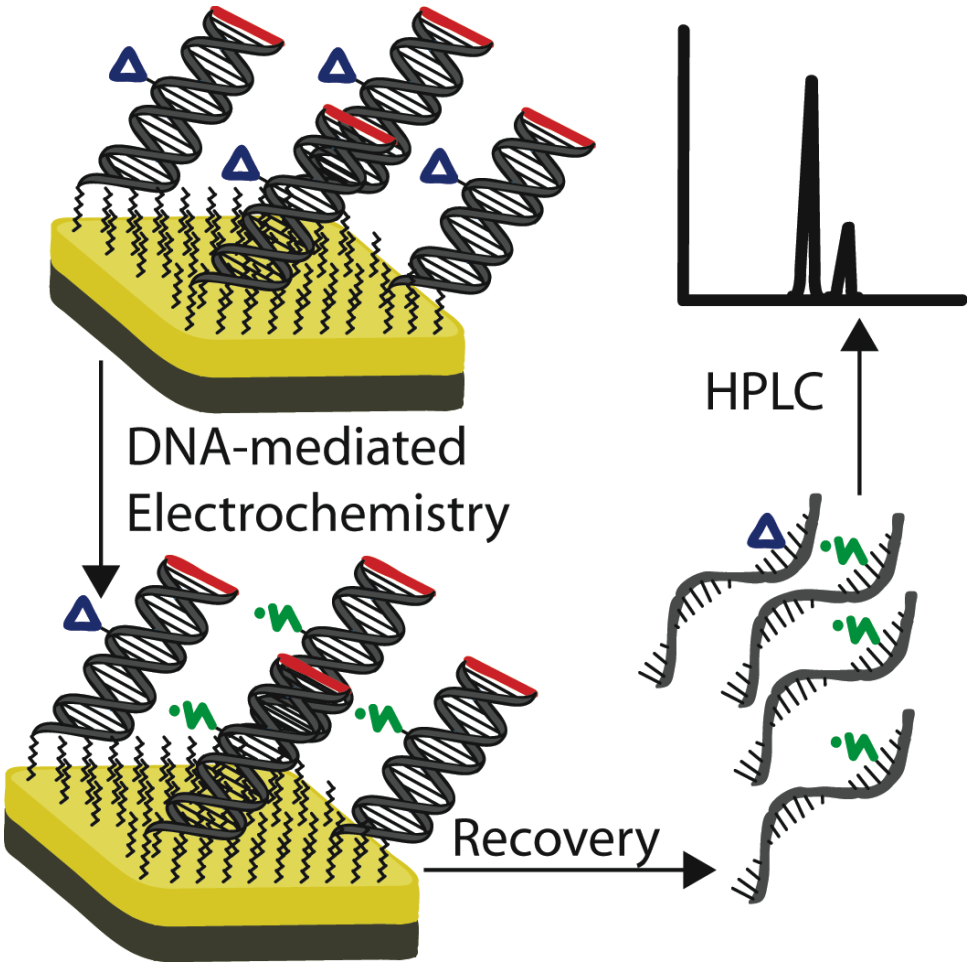

Figure 5.1. Experimental strategy for detecting ^{CP}C ring-opening during DNA-mediated electrochemistry. N_4-cyclopropylcytidine (^{CP}C, blue)- and Redmond Red (RR, red)-containing oligonucleotides were incorporated into a DNA-self assembled monolayer on gold, via the covalent gold-thiol bond. These films were backfilled with mercaptohexanol and subjected to electrochemical analysis. To determine whether this induced ring-opening (green), the relative amount of oligonucleotides containing the decomposition product cytosine and those containing ^{CP}C was quantified by HPLC.

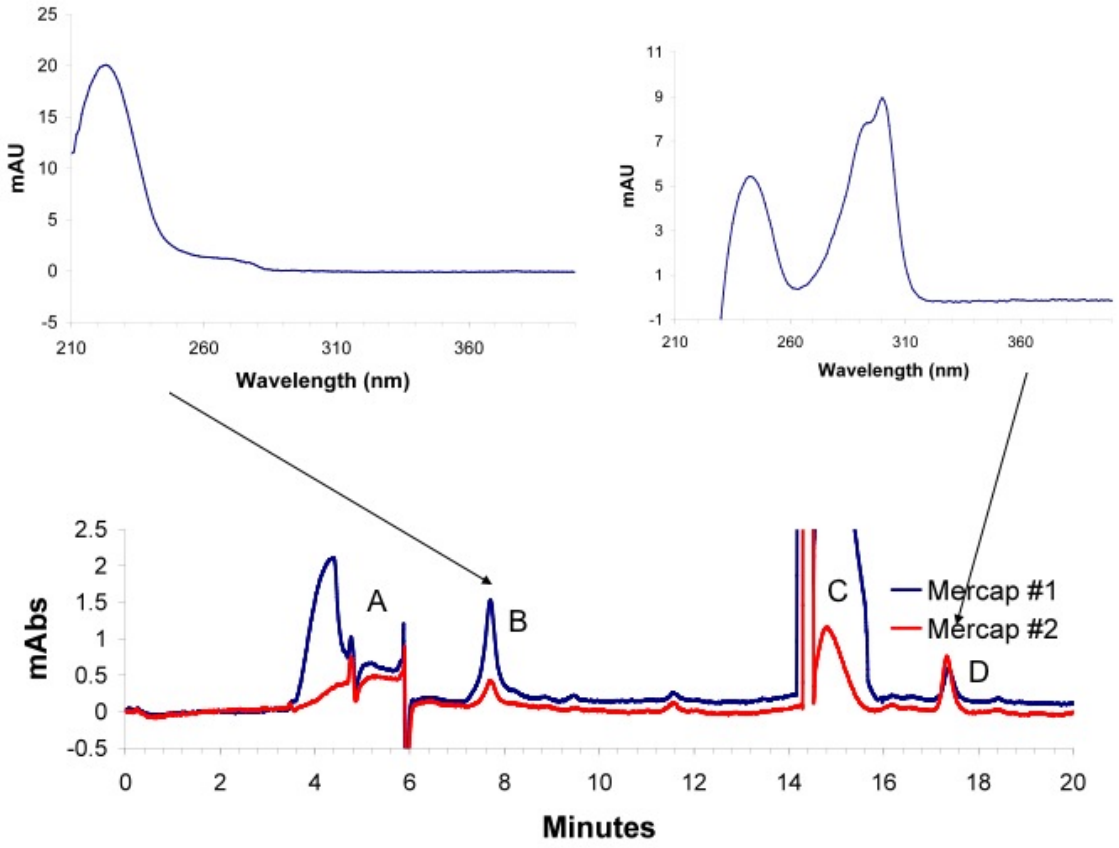

Figure 5.2. HPLC chromatogram (260 nm) of sample prepared by the recovery protocol from a mercaptohexanol self-assembled monolayer on gold. There are four main artifacts, none of which are DNA, observed in aliquots collected from the recovery protocol, as performed on mercaptohexanol films. The earliest (A) peak represents the injection front. The size of the largest (C) is strongly related to the time between recovery and analysis. The left inset indicates the UV-vis spectrum collected online for the pre-DNA elution peak (B), while the right inset is the UV-vis absorption spectrum for a late-eluting peak (D).

earlier than the DNA elution region, with a peak maximum below 220 nm. Feature C is centered far after the DNA elution region. This species absorbs across all wavelengths, indicating that the composition is most likely small particles. The size of this peak can vary from not present at all, to so large as to elute over ten minutes, obscuring the entire profile. This peak was found to depend on the recovery protocol; the cold filtration protocol described above suppresses this peak to negligible levels. Feature D is the latest eluting peak, far from the DNA elution region, and with absorbance maxima at 245 nm and 305 nm. None of these species was produced in adequate yield for mass spectrometric or chemical characterization.

If the recovery protocol is performed on a DNA-S/Au self-assembled monolayer that has been backfilled with mercaptohexanol below 1 mM, or for less than 1 hr, two new peaks appear, both with absorption profiles consistent with being oligonucleotides (data not shown). The first peak corresponds to the complementary (non-thiolated) strand. This assignment was confirmed by co-elution and mass spectrometry. The second peak is faster-eluting, and co-elutes with an impurity that appears in aliquots of the thiolated strand upon oxygen exposure, suggesting it is the sulfate product of the thiolated strand. This was confirmed by mass spectrometry.

To eliminate the sulfate peak, backfilling was extended to 1 hr, with 1 mM mercaptohexanol. This procedure was always successful, over several dozen experiments. One possibility is that more modest backfilling conditions were not successful in removing DNA that was loosely associated with the film.[24] Alternatively, the sulfate-nucleotide could represent a population that is in a different chemical or morphological environment. The former interpretation is consistent with recent work that demonstrates

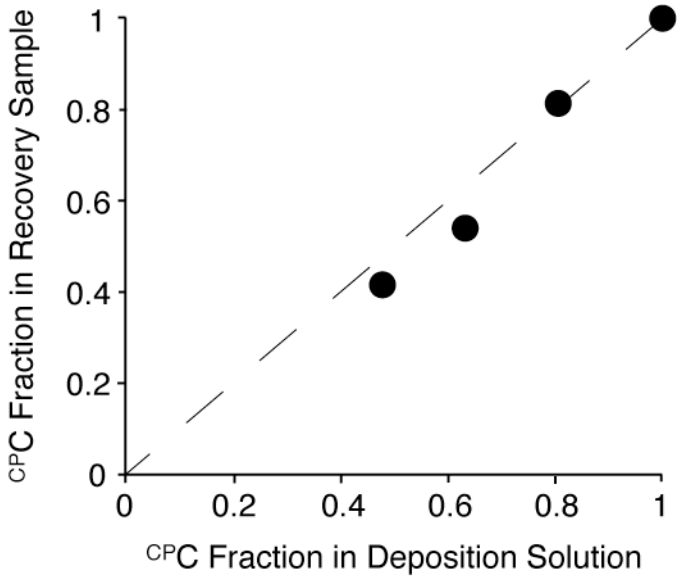

Figure 5.3. Analysis of ^{CP}C content in samples recovered from mixed monolayers. The fraction of ^{CP}C containing DNA, versus DNA containing the ring-opening product cytidine, in the recovery solution is similar to that in the deposition sample. There is little concentration, if any, of ring-opened product in the absence of electrochemical interrogation. The dashed line is unity, and traces at 290 nm were used for these samples.

ready association of non-covalently attached DNA with covalent DNA self-assembled monolayers on gold.

To further validate this technique mixed monolayers were assembled with varying fractions of ^{CP}C-containing and unmodified strands of the same sequence. The relative quantities of ^{CP}C-containing and unmodified strands can be determined by the peak areas by HPLC, as the strands are resolved by over a minute. The relative peak heights were strongly correlated with the monolayer composition (**Figure 5.3**), indicating that the recovery protocol neither induces ^{CP}C decomposition nor selectively enriches one type of oligonucleotide.

5.3.2. HPLC ANALYSIS OF ^{CP}C-DNA AFTER ELECTROCHEMISTRY

Having validated our protocol for recovery and HPLC analysis of ^{CP}C-containing DNA, we explored whether DNA-mediated electrochemistry could induce the ring-opening decomposition of ^{CP}C. Cyclic voltammagrams from electrochemistry on ^{CP}C-containing DNA monolayers did not reveal any novel features. Furthermore, applying cyclic voltammetry did not appear to affect the recovery profile from DNA monolayers.

Since single short pulses were inadequate to induce ring-opening, we explored the effects of both many short pulses and a few long pulses. Four separate films were subjected to pulse sequences of N * (0.5 s, + 60 mV; 0.5 s, -110 mV) for N = 500, 1000, 2000, 4000. Under these conditions, cyclic voltammetry before and after the pulse sequences reveals no loss of the faradaic signal associated with Redmond Red, implying that the film integrity has not been compromised (**Figures 5.4, 5.5** and **Table 5.1**). Furthermore, there is no obvious change in the chromatograms with more pulses.

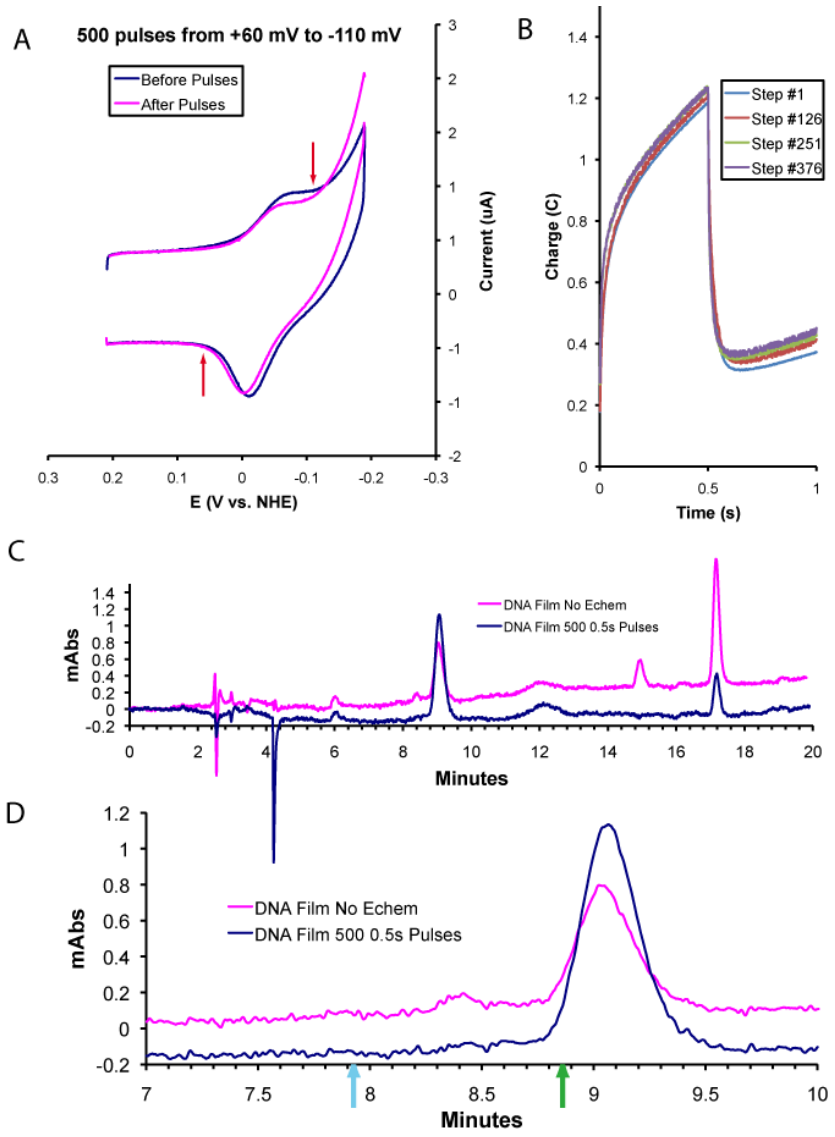

Figure 5.4. Analysis of ^{CP}C content after the pulse sequence 500 x (0.5 s, + 60 mV; 0.5 s, -110 mV). CV before and after the pulse sequence 500 x (0.5 s, + 60 mV; 0.5 s, -110 mV) (A) shows minimal effect of the pulse sequence on the film. Red arrows indicate the potentials switched between for this pulse sequence. Similarly, the CC traces (B) associated with the pulses do show significant change over the course of the pulse sequence. No new peaks are observed in the DNA elution region of the HPLC chromatogram (260 nm) (C, D). The elution times of the standards for DNA with (green arrow) and without (cyan arrow) the ^{CP}C modification are indicated.

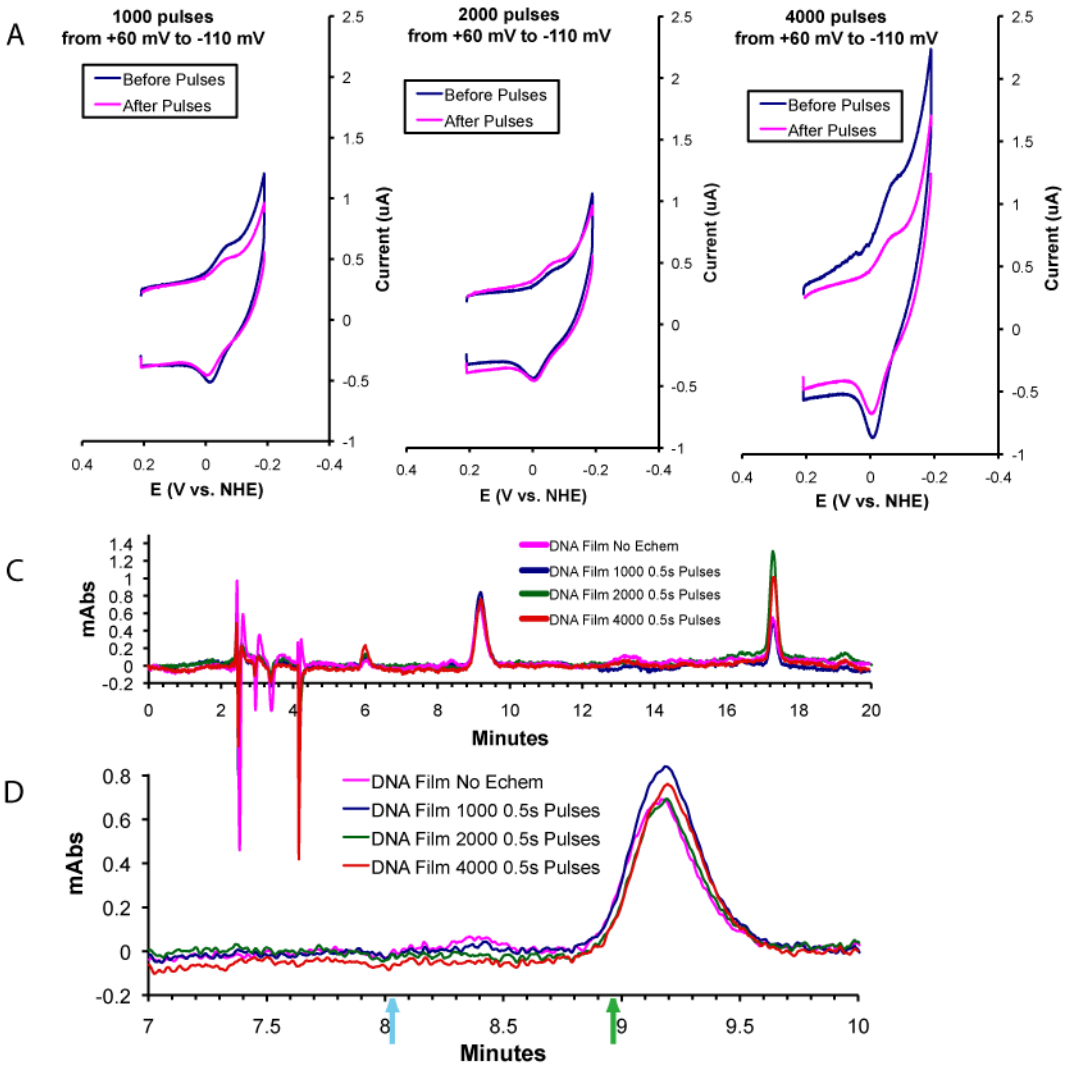

Figure 5.5. Analysis of ^{CP}C content after the pulse sequences *N* x (0.5 s, + 60 mV; 0.5 s, -110 mV). CV before and after the pulse sequences *N* x (0.5 s, + 60 mV; 0.5 s, -110 mV) (A), where *N* = 1000, 2000, 4000, show minimal effect of the pulse sequence on the film. No new peaks are observed in the DNA elution region of the HPLC chromatogram (260 nm) (C, D). The elution times of the standards for DNA with (green arrow) and without (cyan arrow) the ^{CP}C modification are indicated.

Table 5.1: Effect of pulse sequences on DNA monolayer coverage

Pulse Sequence	Quantification (in pmol/cm^2)		
	Before Pulses (by CV)	After Pulses (by CV)	Recovered (by stds)[a]
500 X 0.5 s, + 60 mV 0.5 s, -110 mV	27	27	n.d
1000 X 0.5 s, + 60 mV 0.5 s, -110 mV	10	8	12
2000 X 0.5 s, + 60 mV 0.5 s, -110 mV	11	10	10
4000 X 0.5 s, + 60 mV 0.5 s, -110 mV	23	14	11
1 X 1000 s, -110 mV	29	27	40
2 X 1000 s, -110 mV	10	6	8
4 X 1000 s, -110 mV	21	11	6
500 X 0.5 s, + 60 mV 0.5 s, -240 mV	10	11	10
1000 X 0.5 s, + 60 mV 0.5 s, -240 mV	16	15	30
2000 X 0.5 s, + 60 mV 0.5 s, -240 mV	16	11	10
500 X 0.5 s, + 60 mV 0.5 s, -340 mV	14	4	< 5
1000 X 0.5 s, + 60 mV 0.5 s, -340 mV	15	5	< 5
2000 X 0.5 s, + 60 mV 0.5 s, -340 mV	13	2	< 5

a) n.d. = not determined

Although previous work in our laboratory has found DNA films to be stable to electrochemical interrogation, the electrochemistry indicates that there is some superoxide generation at the electrode if the sample is not rigorously anaerobic, and hence it is not unreasonable to suspect that long pulse sequences might lead to some film degradation. The films were recovered and analyzed by HPLC. For each DNA film, substantial oligonucleotide is recovered, corresponding in elution to the ^{CP}C-containing strand. No evidence of the ring-opened product, or any other DNA, is observed.

Similar results were obtained for the pulse sequences N * (1000 s, -110 mV), where N = 1, 2, 4 (**Figure 5.6**), and for the pulse sequences N * (0.5 s, + 60 mV; 0.5 s, -240 mV) for N = 500, 1000, 2000 (**Figure 5.7**), although in the latter case, some degradation is observed for the longest pulse sequences. For the sequences N * (0.5 s, +60 mV; 0.5 s, -340 mV) for N = 500, 1000, 2000 (**Figure 5.8**), substantial degradation is observed (**Table 5.1**). As the cyclic voltammagrams and chronocoulometric traces both indicate substantial superoxide generation under these conditions, it is likely that the films themselves are decomposing. Strand cleavage should not be observable by our assay, as cleaved DNA would most likely be washed from the electrode during the initial washing steps of the recovery protocol. Nevertheless, the ring-opened product is not observed, despite detectable, though unquantifiable, levels of the intact deposited oligonucleotide being present.

There is a new peak under the most severe conditions (**Figures 5.7** and **5.8**), the UV-vis absorbance of which is consistent with it being an oligonucleotide, but the yield is too low for mass spectrometric analysis. Importantly, however, the height of this peak does not increase with increasing pulse number, indicating that it is not produced by electrochemistry; neither does the elution time correspond to that of the decomposition

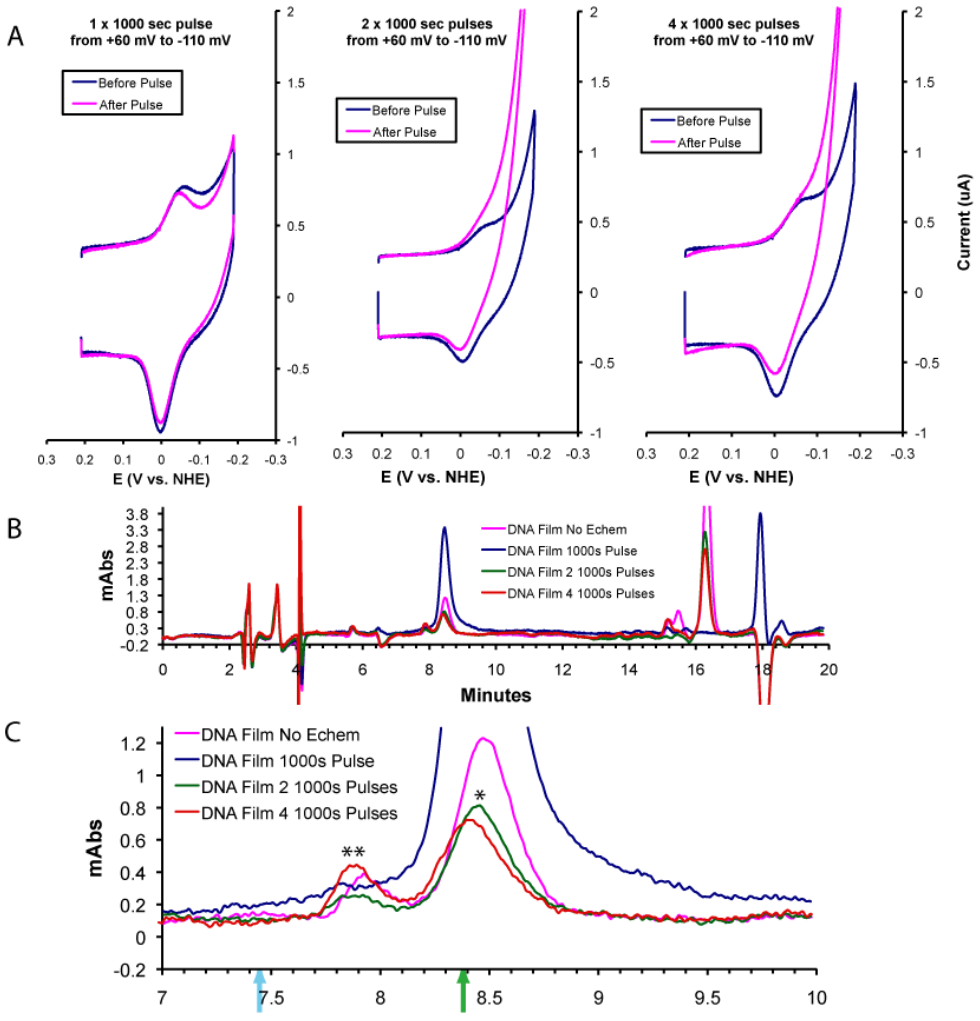

Figure 5.6. Analysis of ^{CP}C content after the pulse sequences *N* x (1000 s, -110 mV). CV before and after the pulse sequences *N* x (1000 s, -110 mV), where *N* = 1, 2, 4, show some effect of the pulse sequence on the film (A). The increase in background at high potentials is consistent with the generation of defects that allow increased access and consequent reduction of molecular oxygen. No new peaks emerge as a function of applied electrochemistry in the DNA elution region of the HPLC chromatogram (260 nm) (B, C). There is an uncharacterized peak (**), the area of which does not correlate with the applied electrochemistry, with UV-vis spectrum uncharacteristic of DNA, and present in the mercaptohexanol (no DNA) film. The elution times of the standards for DNA with (green arrow) and without (cyan arrow) the ^{CP}C modification are indicated.

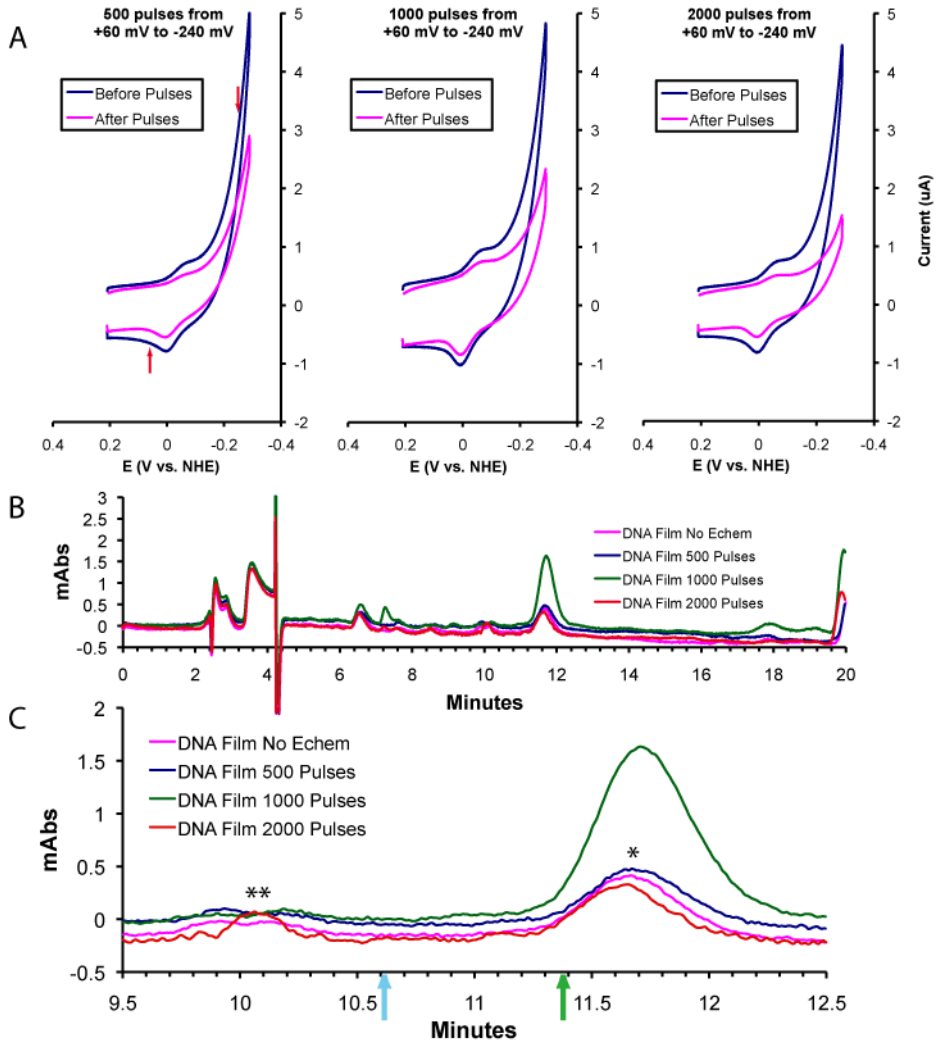

Figure 5.7. Analysis of ^{CP}C content after the pulse sequences *N* x (0.5 s, + 60 mV; 0.5 s, -240 mV). CV before and after the pulse sequences *N* x (0.5 s, + 60 mV; 0.5 s, -240 mV) (A), where *N* = 1000, 2000, 4000, show some effect of the pulse sequence on the film. The increase in background at high potentials is consistent with the generation of defects that allow increased access by and consequent reduction of molecular oxygen. No new peaks emerge as a function of applied electrochemistry in the DNA elution region of the HPLC chromatogram (260 nm) (B,C). There is an uncharacterized peak (**), the area of which does not correlate with the applied electrochemistry. The elution times of the standards for DNA with (green) and without (cyan) the ^{CP}C modification are indicated.

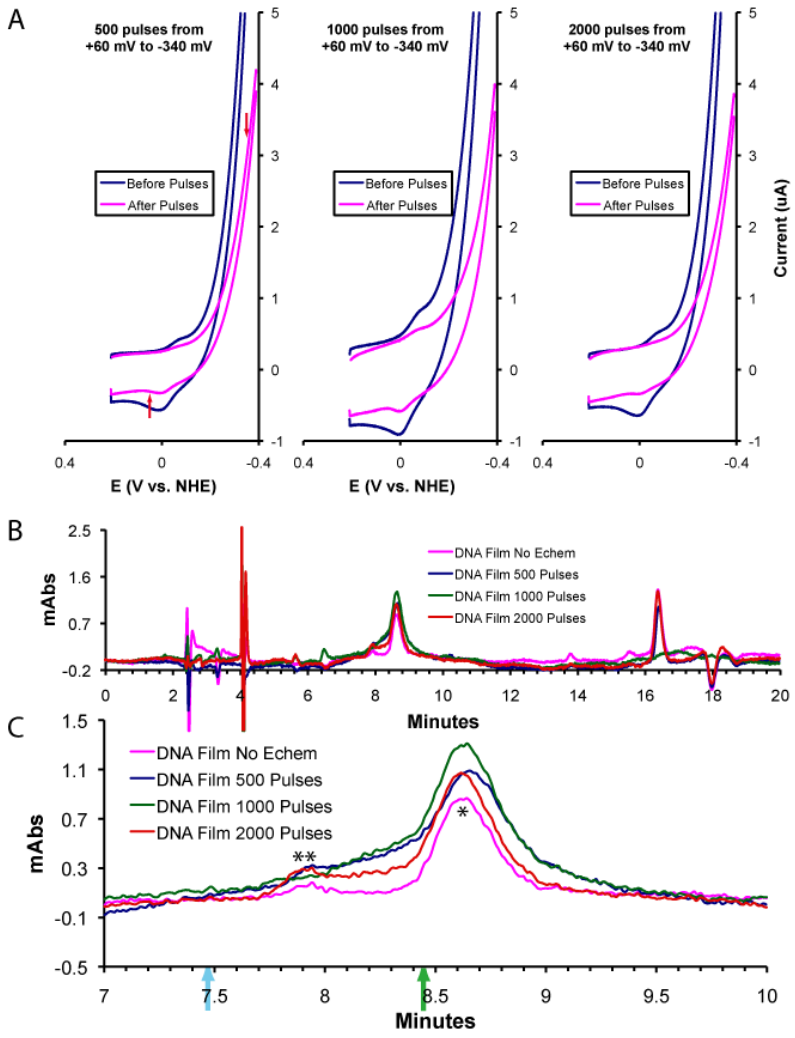

Figure 5.8. Analysis of ^{CP}C content after the pulse sequences *N* x (0.5 s, + 60 mV; 0.5 s, -340 mV). CV before and after the pulse sequences *N* x (0.5 s, + 60 mV; 0.5 s, -340 mV) (A), where *N* = 1000, 2000, 4000, show severe effect of the pulse sequence on the film. Besides the substantial increase in background, most of the faradaic signal associated with the Redmond Red is lost as the pulse sequence is extended. Although a new peak might emerge as a function of applied electrochemistry (**) in the DNA elution region of the HPLC chromatogram (260 nm) (B,C), it does not correspond to the decomposition standard. The elution times of the standards for DNA with (green) and without (cyan) the ^{CP}C modification are indicated.

standard. Hence, it is likely that this product corresponds to some other degradation process within the film, possibly due to superoxide reaction.

5.4. DISCUSSION

The electrochemistry, performed using the redox label Redmond Red with $E^{1/2}$ = -40 mV,[17] demonstrates the ability of DNA to mediate a charge at a potential far from the bases. How can we understand DNA-mediated electrochemistry that proceeds too far for superexchange, but at potentials incompatible with hopping? Decomposition of a radical trap on the bridge in response to DNA-mediated electrochemistry would demonstrate charge occupation of the bridge, and hence hopping as a mechanism for CT under these conditions. In contrast, superexchange involves only virtual occupation of the bridge, and hence would not lead to ^{CP}C decomposition. A lack of decomposition, as was observed here, is consistent with superexchange, and provides a strict limit on the time-scale of occupation if a hopping mechanism is in fact involved.

Consider the application of 4000 x (0.5 s, + 60 mV; 0.5 s, -240 mV) pulses (**Figure 5.7**). For low yields of decomposition:

$$Y = t_{EMF} f_{occ} k_{trap} \qquad (\mathbf{5.2})$$

where Y is the decomposition yield, t_{EMF} is the time of the applied potential, f_{occ} is the fraction of ^{CP}C occupied by the anion radical, and k_{trap} is the rate of trapping. Although k_{trap} has not been directly measured, we have demonstrated that it is greater than 1 x 10^9 s^{-1} for ^{CP}G;[25] we will use this value as a minimum. Our detection limit is certainly better than 5%. Hence, for the longest applied potential of 2000 total seconds, $f_{occ} < 2 \times 10^{-14}$. The presence of the redox probe is not a concern, since its potential is below the Fermi level and it is rapidly reduced. The reduced state will not compete for

transient occupation with the bridge. If transient states are indeed accessed, then they must satisfy the above constraint on f_{occ} since:

$$\int \frac{\phi(E)}{e^{(kT)^{-1}(E-E_{APP})}+1} dE = f_{occ} \qquad \textbf{(5.3)}$$

where $\phi(E)$ is the fraction of time that the LUMO of ^{CP}C has energy E and E_{APP} is -240 mV. For only two states, this corresponds to $\Delta G > 800$ mV, indicating that the equilibrium cytidine potential cannot be substantially above -1 V. The reduction potential of cytidine has been measured as about -2 V, so an equilibrium value far above that would have been surprising.

To evaluate the minimum potential for a transient state that is occupied on the time scale of DNA-mediated electrochemistry, we must know the coupling across the linker, which includes 14 methylenes. Then we can use the nonadiabatic CT relation:[28]

$$k_{CT} = \frac{k_B T\sqrt{\pi}}{\hbar\lambda} H_{DA}^2 \rho^{el} \int \frac{\exp\left\{-(E-\lambda+\eta)^2/(4\lambda k_B T)\right\}}{1+\exp(E/k_B T)} dE \qquad \textbf{(5.4)}$$

where H_{DA} is the donor-acceptor coupling, λ is the reorganization energy, ρ^{el} is the density of states on the electrode at the Fermi level,[29] and η is the overpotential, which is negative for endothermic injection. Over 14 methylenes, with $\beta \sim 1.1$ Å^{-1}, it would be surprising if the coupling is greater than 3×10^{-6} eV. Reorganization energies for CT in DNA have been estimated to range from 0.5 eV to 1 eV; for CT at an electrode the value will be approximately half, so here we will use the charitable value of 0.25 eV. If states on the DNA are in equilibrium, then

$$k_{obs} = f_{occ}\, k_{CT} \qquad \textbf{(5.5)}$$

This rate cannot satisfy the observed value of 30 s^{-1} for DNA-mediated electrochemistry,[8] subject to the constraint on f_{occ} determined above. For k_{CT} itself to be faster than 30 s^{-1},

the overpotential cannot be more than 120 mV above the potential of the probe. At that potential, the coupling between the DNA and the electrode must be at least 0.8 eV to both satisfy the constraint on DNA occupation and allow k_{obs} of 30 s^{-1}. Hence, hopping does not seem consistent with the present results.

On the other hand, these results are consistent with virtual occupation of the DNA bases, which does not lead to ring-opening. The challenge to this superexchange mechanism is the distance independence of the CT rate in DNA electrochemistry when the probe position is varied by 15 bases.[8] For a high energy barrier, the distance dependence of superexchange should be steep, but this is not experimentally observed. If low energy states are transiently formed to accommodate more facile superexchange, they will be subject to the same limitations of **Equation 5.3**. Furthermore, even for a low barrier where $V \sim \Delta\varepsilon$, the lower limit of β is about $0.7/a$ where a is the intersite distance on the bridge. For DNA base separation of 3.4 Å, and varying the probe position by 15 bases, this corresponds to a 3 x 10^5-fold drop in rate. For superexchange to be the mechanism of DNA-mediated electrochemistry, either the distance-dependence does not reflect a change in electronic coupling, or injection must be into a site fully delocalized on the DNA. The former case is true if the distance-dependence reflects conformational gating. This requires that CT be much faster than conformational gating even at long distances, and that the conformational gating occur faster than 30 s^{-1}. There are 14 methylenes in the linker between the DNA and the electrode. Taking β to be 0.2 $Å^{-1}$ in the DNA requires the rate through just the methylene linker to be 1 x 10^6 s^{-1}. To compare, the k^0 through 14 methylenes to ferrocene or pendant $[Ru(pyr)(NH3)_5]^{2+/3+}$ is about 1000 s^{-1}.[28] If we assume that 1000 s^{-1} is a reasonable value for oxidation of the probe at the first base, then for the rate over 15 bases to be below 30 s^{-1}, the β must be $\leq$ 0.07 $Å^{-1}$. This is

only reasonable if the sites that mediate superexchange are larger than a single base pair; for a low barrier, but still high enough to avoid hopping, the intersite distance must be at least three base pairs. Furthermore, if similar CT rates are observed over longer DNA bridges, the amount of delocalization that will be implied will be even greater. In summary, if superexchange is indeed the mechanism for DNA-mediated electrochemistry, there must be a transiently low barrier in the DNA, subject to the limits of **Equation 5.3**, and furthermore these states must be delocalized over several bases.

The above interpretation, however, is based on an absence of decomposition; if occupation does not lead to ^{CP}C decomposition in the monolayer, then **Equation 5.2** is not valid. It is possible that the environment around the ^{CP}C in films is not conducive to ring-opening, or that occupation at lower energy levels does not lead to trapping. A positive control would be necessary to demonstrate that we can perform ring-opening in films; current available modified bases are not within the electrochemical window of our system. This serves as an important caveat to the above analysis.

5.5 Conclusions

We have probed DNA-mediated electrochemistry in DNA-S/Au SAMs using a fast redox trap in the DNA bridge. To allow this measurement, we validated a protocol for oligonucleotide recovery analysis that allows us to observe and quantify the yield of chemical reactions in the monolayer. We do not observe any decomposition of the probe under conditions for which the monolayer is stable. If decomposition is an accurate proxy for cytidine occupation in monolayers, this result places a thermodynamic limitation on the energies and lifetimes of states that allow occupation of the DNA at applied potentials

far from the equilibrium potentials of the component nucleotides. It is hard to rationalize hopping with such a limit on DNA occupancy.

5.6. REFERENCES

(1) Jortner, J.; Bixon, M.; Langenbacher, T.; Michel-Beyerle, M.E. *Proc. Natl. Acad. Sci. U.S.A.* **1998**, *95*, 12759.

(2) Schuster, G. B., Ed. *Long-Range Charge Transfer in DNA, I and II;* Springer: New York, **2004**; Vols. 236, 237.

(3) Kelley, S.O.; Holmlin, R.E.; Stemp, E.D.A.; Barton, J. K. *J. Am. Chem. Soc.* **1997**, *199*, 9861.

(4) Murphy, C.J.; Arkin, M.R.; Jenkins, Y.; Ghatlia, N.D.; Bossmann, S.H.; Turro, N.J.; Barton, J.K. *Science* **1993**, *262*, 1025.

(5) Lewis, F.D.; Zhu, H.; Daublain, P.; Cohen, B.; Wasielewski, M.R. *Angew. Chem. Int. Ed.* **2006**, *45*, 7982.

(6) Treadway, C.R.; Hill, M.G.; Barton, J.K. *Chem. Phys.* **2002**, *281*, 409.

(7) Boal, A.K.; Genereux, J.C.; Sontz, P.A.; Gralnick, J.A.; Newman, D.K.; Barton, J.K. *Proc. Natl. Acad. Sci. U.S.A.* **2009**, *106*, 15237.

(8) Drummond, T.G.; Hill, M.G.; Barton, J.K. *Nat. Biotech.* **2003**, *21*, 1192.

(9) Inouye, M.; Ikeda, R.; Takase, M.; Tsuri, T.; Chiba, J. *Proc. Natl. Acad. Sci. U.S.A.* **2005**, *102*, 11606.

(10) Gorodetsky, A.A.; Green, O.; Yavin, E.; Barton, J.K. *Bioconjugate Chem.* **2007**, *18*, 1434.

(11) Kelley, S. O.; Jackson, N. M.; Hill, M. G.; Barton, J. K. *Angew. Chem., Int. Ed*. **1999**, *38*, 941.

(12) Boon, E. M.; Ceres, D. M.; Drummond, T. G.; Hill, M. G.; Barton J. K. *Nat. Biotech.* **2000**, *18*, 1096.

(13) Boal, A.K.; Barton, J.K. *Bioconjugate Chem.* **2005**, *16*, 312.

(14) Anne, A.; Demaille, C. *J. Am. Chem. Soc.* **2008**, *130*, 9822.

(15) Gorodetsky, A.A.; Buzzeo, M.C.; Barton, J.K. *Bioconjugate Chem.* **2008**, *19*, 2285.

(16) Steenken, S.; Telo, J.P.; Novais, H.M.; Candeias, L.P. *J. Am. Chem. Soc.* **1992**, *114*, 4701.

(17) Gorodetsky, A.A.; Dietrich, L.E.P.; Lee, P.E.; Demple, B.; Newman, D.K.; Barton, J.K. *Proc. Natl. Acad. Sci. U.S.A.* **2008**, *105*, 3684.

(18) Berlin, Y.A.; Grozema, F.C.; Siebbeles, L.D.A.; Ratner, M.A. *J. Phys. Chem. C* **2008**, *112*, 10988.

(19) Voityuk, A.A. *J. Chem. Phys.* **2008**, *128*, 115101.

(20) Elias, B.; Shao, F.; Barton, J. K. *J. Am. Chem. Soc.* **2008**, *130*, 1152.

(21) Elias, B.; Genereux, J.C.; Barton, J.K. *Angew. Chem. Int. Ed.* **2008**, *47*, 9067.

(22) Shao, F.; O'Neill, M. A.; Barton, J. K. *Proc. Natl. Acad. Sci. U.S.A.* **2004**, *101*, 17914.

(23) Shao, F.; Augustyn, K. E.; Barton, J. K. *J. Am. Chem. Soc.* **2005**, *127*, 17445.

(24) Murphy, J.N.; Chang, A.K.H.; Yu, H.-Z.; Bizzotto, D. *J. Am. Chem. Soc.* **2009**, *131*, 4042.

(25) Cf. footnote 22 in Chapter 2.

(26) Fiebig, T.; Wan, C.Z.; Zewail, A.H. *Chem. Phys. Chem.* **2002**, *3*, 781.

(27) Seidel, C.A.M.; Schulz, A.; Sauer, M.H.M. *J. Phys. Chem.* **1996**, *100*, 5541.

(28) Newton, M.D.; Smalley, J.F. *Phys. Chem. Chem. Phys.* **2007**, 9, 555.

(29) Traub, M.C.; Brunschwig, B.S.; Lewis, N.S. *J. Phys. Chem. B* **2007**, *111*, 6676.